molecular microbiology

Refining the pH response in Aspergillus nidulans: a modulatory triad involving PacX, a novel zinc binuclear cluster protein

Journal:	*Molecular Microbiology*
Manuscript ID:	MMI-2015-15295.R1
Manuscript Type:	Research Article
Date Submitted by the Author:	17-Aug-2015
Complete List of Authors:	Bussink, Henk-Jan; Imperial College London, Section of Microbiology Bignell, Elaine; Imperial College London, Section of Microbiology Munera-Huertas, Tatiana; Imperial College London, Section of Microbiology Lucena-Agell, Daniel; Centro de Investigaciones Biológicas CSIC, Department of Cellular and Molecular Biology Scazzocchio, Claudio; Imperial College London, Section of Microbiology Espeso, Eduardo; Centro de Investigaciones Biológicas CSIC, Department of Cellular and Molecular Biology Bertuzzi, Margherita; University of Manchester, Institute for Inflammation and Repair Rudnicka, Joanna; Imperial College London, Section of Microbiology Negrete-Urtasun, Susana; Imperial College London, Section of Microbiology Peñas-Parilla, Maria; Imperial College London, Section of Microbiology Rainbow, Lynne; Imperial College London, Section of Microbiology Penalva, Miguel; Centro de Investigaciones Biologicas CSIC, Department of Cellular and Molecular Biology Arst, Herb; Imperial College London, Section of Microbiology Tilburn, Joan; Imperial College London, Section of Microbiology
Key Words:	pH regulation, transcription, palF, autogenous regulation

Refining the pH response in *Aspergillus nidulans*: a modulatory triad involving PacX, a novel zinc binuclear cluster protein

Henk-Jan Bussink[1], Elaine M. Bignell[1,2], Tatiana Múnera-Huertas[1], Daniel Lucena-Agell[3], Claudio Scazzocchio[1,4], Eduardo A. Espeso[3], Margherita Bertuzzi[2], Joanna Rudnicka[1], Susana Negrete-Urtasun[1], Maria M. Peñas-Parilla[1], Lynne Rainbow[1], Miguel Á. Peñalva[3], Herbert N. Arst Jr.[1] and Joan Tilburn[1*]

[1] *Section of Microbiology, Imperial College London, Flowers Building, Armstrong Road, London SW7 2AZ, UK.*

[2] *Manchester Fungal Infection Group, Institute for Inflammation and Repair, University of Manchester, 46 Grafton Street, Manchester M13 9NT, UK.*

[3] *Department of Cellular and Molecular Biology, Centro de Investigaciones Biológicas CSIC, Ramiro de Maeztu 9, Madrid 28040, Spain.*

[4] *Institute for Integrative Biology of the Cell (I2BC), CEA, CNRS, Université Paris-Sud, Orsay, France.*

*Corresponding author

Joan Tilburn

Email j.tilburn@imperial.ac.uk, Telephone +1 240 271 4557

Running title: PacX and pH regulation refinement in *A. nidulans*

Key words: pH regulation, transcription, PacX, *Aspergillus nidulans*, zinc binuclear cluster, *palF* regulation.

Summary

The *Aspergillus nidulans* PacC transcription factor mediates gene regulation in response to alkaline ambient pH which, signalled by the Pal pathway, results in the processing of $PacC^{72}$ to $PacC^{27}$ via $PacC^{53}$. Here we investigate two levels at which the pH regulatory system is transcriptionally moderated by pH and identify and characterize a new component of the pH regulatory machinery, PacX. Transcript level analysis and over-expression studies demonstrate that repression of acid-expressed *palF*, specifying the Pal pathway arrestin, probably by $PacC^{27}$ and/or $PacC^{53}$, prevents an escalating alkaline pH response. Transcript analyses using a reporter and constitutively expressed *pacC* *trans*-alleles show that *pacC* preferential alkaline-expression results from derepression by depletion of the acid-prevalent $PacC^{72}$ form. We additionally show that *pacC* repression requires PacX. *pacX* mutations suppress PacC processing recalcitrant mutations, in part, through derepressed PacC levels resulting in traces of $PacC^{27}$ formed by pH-independent proteolysis. *pacX* was cloned by Impala transposon mutagenesis. PacX, with homologues within the Leotiomyceta, has an unusual structure with an amino-terminal coiled-coil and a carboxy-terminal zinc binuclear cluster. *pacX* mutations indicate the importance of these regions. One mutation, an unprecedented finding in *A. nidulans* genetics, resulted from an insertion of an endogenous Fot-1-like transposon.

Introduction

Fungi, ubiquitous in nature, occupy niches of wide ranging and fluctuating pH values. This is enabled by efficient pH homeostasis and a pH regulatory system which ensures the appropriate synthesis of molecules with respect to environmental pH. The system mediating this response was first recognized in *Aspergillus nidulans* (Caddick *et al.*, 1986). Homologous systems occur throughout the ascomycetes where they are known as the Pac/Pal system in the filamentous fungi (Caddick *et al.*, 1986; Tilburn *et al.*, 1995) and as the Rim system in yeasts (Su and Mitchell, 1993a, b; Lambert *et al.*, 1997; Ramon *et al.*, 1999; Davis *et al.*, 2000a, b). They also extend to the basidiomycetes (Aréchiga-Carvajal and Ruiz-Herrera, 2005; O'Meara *et al.*, 2010; Ost *et al.*, 2015).

The fungal pH responsive regulatory domain encompasses a very large number of genes including those involved in nutrient acquisition, ion homeostasis, alkali metal and pH tolerance, cell wall metabolism, exported metabolite production, female development, sporulation, dimorphic shift, tissue penetration and invasive growth (Lamb *et al.*, 2001; Lamb and Mitchell, 2003a; Bensen *et al.*, 2004; Eisendle *et al.*, 2004; Baek *et al.*, 2006; Ruiz and Ariño, 2007; Nobile *et al.*, 2008; Alkan *et al.*, 2013; Trushina *et al.*, 2013; Bertuzzi *et al.*, 2014; Chinnici *et al.*, 2014; O'Meara *et al.*, 2014). As many of these activities or attributes are crucial in a host environment, pH regulation is an important virulence determinant of fungal pathogenicity of animals, including humans, plants and fungi themselves (Davis, 2000a; Davis, 2003; Bignell *et al.*, 2005; Moreno-Mateos *et al.*, 2007; Nobile *et al.*, 2008; Zou *et al.*, 2010; Alkan *et al.*, 2013; Trushina *et al.*, 2013; Bertuzzi *et al.*, 2014; O'Meara *et al.*, 2014) and reviewed in (Peñalva *et al.*, 2008; Davis, 2009; Selvig and Alspaugh, 2011; Cornet and Gaillardin, 2014).

The mechanism of pH regulation has been studied largely in *A. nidulans* and *Saccharomyces cerevisiae* with additional contributions particularly from work in *Candida albicans* and *Yarrowia lipolytica*. The pH response is mediated by the three Cys2-His2 finger transcription factor, *A. nidulans* PacC (Tilburn *et al.*, 1995) or Rim101 in *S. cerevisiae* (Su and Mitchell, 1993b). Under acidic conditions the *A. nidulans* PacC full length form, $PacC^{72}$, is protease inaccessible due to intramolecular-interactions involving the C-terminal moiety (Espeso *et al.*, 2000). At neutral to alkaline ambient pH PacC undergoes two-step proteolysis. The first step, which occurs in response to pH signalling, removes approximately 180 C-terminal residues to yield $PacC^{53}$ (Díez *et al.*, 2002); the second, almost certainly mediated by the proteasome, removes a further ~240 residues to give the $PacC^{27}$ processed form, and is pH-independent (Hervás-Aguilar *et al.*, 2007). $PacC^{27}$ predominates in the nucleus (Mingot *et al.*, 2001), where it activates alkaline expressed genes, such as *ipnA* (isopenicillin-N synthase) (Espeso and Peñalva, 1996) and represses acid expressed genes (Tilburn *et al.*, 1995), such as *gabA* (GABA permease) (Espeso and Arst, 2000). However, $PacC^{72}$ and $PacC^{53}$ can bind a PacC DNA target site (Díez *et al.*, 2002) and, as they are not excluded from the nucleus (Mingot *et al.*, 2001; Davis, 2003; Fernández-Martínez, MAP, EAE, unpublished), might also participate in gene regulation.

pacC mutations which remove the $PacC^{72}$ C-terminus or otherwise disrupt its intramolecular-interactions result in an open, proteasome-accessible conformation leading to constitutive PacC processing and alkalinity mimicry (Orejas *et al.*, 1995; Tilburn *et al.*, 1995; Espeso *et al.*, 2000). Loss-of-function mutations in the *pal* (pH signal transduction) genes or *pacC* result in acidity mimicry (Arst *et al.*, 1994; Tilburn *et al.*, 1995; Fernández-Martínez *et al.*, 2003). It appears that traces of $PacC^{27}$ are produced independently of pH signal transduction from a minor proportion of protease accessible $PacC^{72}$ which exists in equilibrium with the majority of protease inaccessible $PacC^{72}$ (Peñalva and Arst

et al., 2004; Peñas *et al.*, 2007; Peñalva *et al.*, 2008). This possibly explains the less extreme phenotype of null *pal* compared to *null pacC* mutations, which result, additionally, in cryosensitivity and reduced growth and conidiation (Tilburn *et al.*, 1995; Fernández-Martínez *et al.*, 2003).

pH signalling occurs at the plasma membrane in *A. nidulans* (Galindo *et al.*, 2012; Lucena-Agell *et al.*, 2015) and *S. cerevisiae* (Obara and Kihara, 2014) where it involves dedicated Pal (Arst *et al.*, 1994) (or Rim) pH signal transduction components and the participation of certain endosomal sorting complex required for transport (ESCRT)-I, -II, and -III components (Xu *et al.*, 2004; Calcagno-Pizarelli *et al.*, 2011) reviewed by (Peñalva *et al.*, 2014). The plasma membrane sensor is PalH [Rim20 and Dgf16 in *S. cerevisiae* and *C. albicans* (Barwell *et al.*, 2005; Rothfels *et al.*, 2005)]. PalH localization is assisted by PalI (Calcagno-Pizarelli *et al.*, 2007) and stabilized by strong interactions between the PalH cytoplasmic tail and the arrestin PalF (Herranz *et al.*, 2005) (Rim8). PalF becomes phosphorylated and ubiquitylated in alkaline media (Herranz *et al.*, 2005) and the importance of this ubiquitylation, in *A. nidulans*, is demonstrated by the ability of genetically encoded ubiquitin attachment to PalF to signal constitutively (Hervás-Aguilar *et al.*, 2010). PalF recruits Vps23 of ESCRT-I (Herrador *et al.*, 2010; Galindo *et al.*, 2012), which is thought to recruit ESCRTII components. Vps32 of ESCRT-III participates in the incorporation of PalC (Galindo *et al.*, 2007) [probably YGR122w in yeast and named YlRim23 in *Y. lipolytica* (Blanchin-Roland, 2011)] which is required for inclusion of PalA (Galindo *et al.*, 2012) (Rim20). PalA binds PacC^{72} via two YPxL(I) motifs flanking the signalling protease (PalB) cleavage site (Vincent *et al.*, 2003). Finally the cysteine protease PalB (Denison *et al.*, 1995) (Rim13) is recruited through interaction of its MIT domain with Vps24 (Rodríguez-Galán *et al.*, 2009; Lucena-Agell *et al.*, 2015). The transient signalling foci are dissociated by Vps4 (Galindo *et al.*, 2012).

Mutations in *pacC* which prevent PacC signalling proteolysis affect the signalling proteolysis site (Díez *et al.*, 2002; Peñas *et al.*, 2007) or PalA binding sites (Vincent *et al.*, 2003) and are phenotypically identical to those in the *pal* signal transduction genes except that, unlike *pal*⁻ mutations which are recessive, they are co-dominant with the wild-type allele in diploids (see below).

The Pac/Pal system mediates a rapid and effective response to alkalinization, switching genes on or off as appropriate to ensure survival in these adverse conditions. However fungi also grow in acidic environments and normally prefer to do so. *A. nidulans* can grow in media of pH values as low as pH 2 (Dijkema *et al.*, 1986) and in a study of the influence of pH on the growth of toxigenic *Aspergillus*, *Penicillium* and *Fusarium* species, the majority of the 61 isolates were able to grow around pH 3-3.5 and some as low as pH ~2 (Wheeler *et al.*, 1991). To adapt to acidic conditions, fungi must be able to control, even switch off, the alkaline ambient pH response. Here we describe, for *A. nidulans,* a tripartite system whereby this is achieved which includes a new player in the pH response.

Results

New insights into the pacC/pal *pH regulatory response.*

pacC *autoregulation, revisited.*

pacC is an alkaline expressed gene. In wild-type strains *pacC* transcript levels are low under acidic conditions and relatively high under alkaline conditions (Tilburn *et al.*, 1995). In addition, they are low in acidity mimicking *pal*$^{-}$ and certain *pacC*$^{+/-}$ partial loss-of-function strains and relatively high in *pacC*^{c} constitutive, alkalinity mimicking mutants, irrespective of the growth pH (Tilburn *et al.*, 1995). This strongly suggested that *pacC* is positively regulated by PacC^{27}, in a similar manner to alkaline expressed structural genes, such as *ipnA* (Orejas *et al*., 1995; Tilburn *et al.*, 1995; Espeso and Peñalva, 1996).

However, the hypothesis of *pacC* positive autoregulation failed to explain a number of subsequently observed phenomena. Firstly, in contrast to *pal*$^{-}$ alleles which are recessive to the respective wild type alleles in diploids, *pacC* processing recalcitrant alleles *pacC*$^{+/-}$20205, *pacC*$^{+/-}$207, *pacC*$^{+/-}$209 and *pacC*$^{+/-}$210 are co-dominant with the wild type allele in diploids, a feature which enabled the isolation of *pacC*$^{+/-}$207, *pacC*$^{+/-}$209 and *pacC*$^{+/-}$210 as suppressors for GABA utilization in a homozygous *areA*^{r} (unable to use nitrogen sources other than ammonium) diploid (Arst *et al.*, 1994; Espeso and Arst, 2000; Díez *et al.*, 2002; Fernández-Martínez *et al.*, 2003; Vincent *et al.*, 2003). Secondly, and in agreement, there are reduced levels of expression of *pacC*^{c}700, a GFP tagged allele encoding PacC^{27}, in a diploid containing *pacC*$^{+/-}$209 as compared with that of a *pacC*700 haploid strain or of *pacC*700 in a diploid strain containing a *pacC* null allele, as detected by epifluorescence microscopy (Fig. S1A). Thirdly, there exists an apparently paradoxical phenomenon whereby the hypostasis of a *pal*$^{-}$ allele and the epistasis of a *pacC*^{c} allele can be inverted by ectopic over-expression of *pacC*$^{+}$ from a strong

heterologous [*alcA* (alcohol dehydrogenase)] promoter in a *pacC*^{c} *pal*$^{-}$ strain (Fig. S1B and JT, J Mingot, M Orejas, T Suárez, EAE, MAP, HNA, unpublished). All of these observations indicate that there is a negative function or activity associated with the PacC unprocessed form.

The testing of the original hypothesis directly was enabled by the isolation of the *pacC*$^{-}$6309 null allele, which differs from the wild type transcript in only three nucleotides and contains a chain termination mutation in the physiological start codon, such that it can specify at most PacC residues 1 through 4 by using an alternative start codon (Fernández-Martínez *et al.*, 2003). The northern blots in Fig. 1A show the results of pH shift experiments. In the wild-type strain *pacC* transcript levels are low under acidic conditions and rapidly rise upon alkalinization to peak approximately 15 min after shifting, falling to steady state levels after about 60 min. In contrast, in the *pacC*$^{-}$6309 null strain, *pacC* transcript levels are largely constant throughout and considerably elevated relative to those of the wild-type strain under acidic conditions. As PacC^{72} is the almost exclusive PacC form in acidic media, this strongly implicates PacC^{72} as a repressor of *pacC*.

To investigate the possibility of PacC^{72} repressor function further we used *pacC*$^{-}$6309 transcript as a reporter for *pacC* expression in the presence and absence of different *pacC* alleles in *trans,* expressed from a moderately strong constitutive promoter. Fig. 1B shows that *pacC*$^{-}$6309 transcript levels (lane 2) are unaffected by the expression of GFP::PacC5-251, which approximates PacC^{27}, (lane 1, merodiploid) but are undetectable in the presence of GFP::PacC5-678 under acidic conditions where PacC is almost exclusively in the PacC^{72} form (lane 3). In the same strain, after 45 min of exposure to alkaline medium, which results in very extensive processing of PacC^{72} (see Fig. 2), *pacC*$^{-}$6309 transcripts are restored to appreciable levels (lane 4). These results give further compelling evidence that PacC^{72} is a repressor of

pacC expression. Furthermore, PacC^{27}, originally hypothesized to be an activator of *pacC* expression (Orejas *et al*., 1995; Tilburn *et al.*, 1995), appears not to have an effect.

These data strongly suggest that *pacC* is negatively autoregulated by PacC^{72} and is alkaline-expressed due to derepression which occurs upon PacC^{72} processing in response to pH signalling. Thus, *pacC* processing recalcitrant alleles are negatively *trans*-acting in diploids with wild type or constitutive alleles because their gene product represses the heteroallelic promoter (Fig. S1A). In a similar way, in a haploid, a *pal*$^{-}$ allele becomes epistatic to a *pacC*^{c} allele when *pacC*$^{+}$ is ectopically over-expressed due to large amounts of PacC^{72} switching off expression of the *pal*-independent *pacC*^{c} allele (Fig. S1B).

Transcriptional regulation of palF *prevents a run-away alkaline pH response.*

Fig. 2 illustrates PacC processing. In response to alkalinization, PacC^{72} is processed via PacC^{53} to PacC^{27}. The response is very swift with PacC^{53} appearing after 4 min (Panel A) and, in fact, as early as 2.5 min (data not shown). After 30 to 60 min PacC^{72} has disappeared yet between 90 and 150 min PacC^{72} begins to accumulate again, indicating that PacC processing has become limited at the signalling proteolysis step (Fig. 2B). Therefore, the possibility of pH regulation of transcription of the pH regulatory *pal* genes and the consequences of their over-expression were explored. *palA*, *-B*, *-C*, *-H* and *-I* were found to be expressed largely independently of pH and/or the mutational status of other pH regulatory components, ie., *pacC* and *palF* (Denison *et al.*, 1995; Negrete-Urtasun *et al.*, 1997; Denison *et al.*, 1998; Negrete-Urtasun *et al.*, 1999). However, *palF* was found to be an acid expressed gene (Fig. 3A and B). *palF* transcript levels are highest under acidic conditions and in acidity mimicking mutants and relatively low under alkaline growth conditions and in alkalinity mimicking mutants (Fig. 3A). Moreover, on shifting from acidity to alkalinity, *palF* transcript levels rapidly fall very low between 30

and 120 min after transfer, being somewhat restored after 4 hours (Fig. 3B). This transcriptional behaviour resembles the temporal pattern of PacC processing and suggests that expression of *palF* might be rate-limiting in pH signal transduction. This is supported by over-expression studies (Fig. 3C and D) which show that *palF* expression from the strong, inducible *alcA* (alcohol dehydrogenase) promoter results in alkalinity mimicry, as indicated by reduced acid phosphatase expression on ethanol-containing, low phosphate medium, whereas there were no such phenotypic consequences of the over-expression of *palA*, *-B*, *-C*, *-H* or *-I* (data not shown). In addition, *palF* over-expression is sufficient to suppress the very leaky *palB*524 mutation (Peñas *et al.*, 2007), for acid phosphatase expression (Fig. 3D) and to rescue partially certain leaky mutations in *palH* and *palC* and *palI*32 (data not shown). [*palI*32 is a null allele which, like all *palI* mutations, has a less extreme phenotype than non-leaky mutations in the other *pal* signal transduction pathway genes (Denison *et al.*, 1998)]. *palF* over-expression from a modified *gpdA* (glyceraldehyde 3-phosphate dehydrogenase) promoter (*gpdA*^{mini}) (Pantazopoulou and Peñalva, 2009) also results in alkalinity mimicry as detected in petri dish assays [Fig. 3F and (Hervás-Aguilar *et al.*, 2010)]. Western blot analysis demonstrates that *gpdA*^{mini} driven *palF* over-expression results in elevated levels of PacC processing and largely overrides attenuation of pH signalling as manifested by the much reduced levels of PacC^{72} detectable 60 min and 120 min after shifting (Fig. 3E). The appreciable levels of PacC^{27} produced under acidic growth conditions (Fig. 3E) are indicative of pH signalling and suggest that, in agreement with the alkalinity mimicking phenotype, constitutive expression of PalF results in an inappropriate pH response.

These results suggest that the *A. nidulans* pH regulatory response is subject to negative feedback in a fashion similar to that involving *RIM8* of *C. albicans* and *S. cerevisiae* (Ramon *et al.*, 1999; Porta *et al.*, 1999; Lamb and Mitchell, 2003). These results also support some recent mathematical modelling

predictions which suggest the presence of a negative feedback loop in the PacC activation process (Ke *et al.*, 2013).

pacX*: a new gene involved in the pH regulatory response.*

Identification and genetic mapping of pacX*.*

The first identified *pacX* mutation, designated *pacX*1, was isolated, following UV mutagenesis of a *pacC*$^{+/-}$20205 (processing recalcitrant) strain, amongst numerous (largely intragenic) revertants selected for their ability to grow at pH 8.0. *pacX*1 which segregated as a single trait, independently of *pacC*, was localized further to chromosome VIII using parasexual genetics. In view of this localization and the *pacX*1 phenotype, which includes the partial restoration of alkaline phosphatase biosynthesis, it seemed possible that *pacX*1 is allelic to *suA*1*palB*7, a mutation linked to the *argC*3 translocation breakpoint on chromosome VIII, isolated and characterized by Dorn (1965), during his studies of the phosphatases of *A. nidulans*. Guided by these results, and those of Clutterbuck, (1993), *pacX*1 was mapped 8.3 and 16 map units respectively between the *argC*3 translocation breakpoint and *hisC*38. Allelism with *suA*1*palB*7 and *suD*2*palA*1, also isolated by Dorn (http://fgsc.net/Archive/nid.html), was confirmed by further genetic analysis (data not shown) and determination of mutant sequence changes (see below).

Characterization of the pacX *mutant phenotype: by-passing pH signal transduction*

*pacX*1 was found to suppress loss-of-function mutations in each of the *pal* pH signal transduction genes, specifically, *palA*1, *palB*7, *palC*4, *palF*15, *palH*17 and *palI*30. Phenotype testing of the *pacX*1 *palA*$^{-}$, -*B*$^{-}$, -*C*$^{-}$, -*F*$^{-}$, -*H*$^{-}$ and -*I*$^{-}$, *pacX*1 *pacC*$^{+/-}$20205 (Fig. 4), *pacX*1 *pacC*$^{+/-}$207, *pacX*1 *pacC*$^{+/-}$209 and *pacX*1

pacC$^{+/-}$210 (data not shown) double mutants showed that, in addition to partial restoration of growth at pH 8.0 and alkaline phosphatase biosynthesis, *pacX*1 reduces the derepressed levels of acid phosphatase to levels intermediate between those of the *pal*$^{-}$, *pacC*$^{+/-}$20205, *pacC*$^{+/-}$207, *pacC*$^{+/-}$209 and *pacC*$^{+/-}$210 strains and those of wild type strains and *pacX*1 not only abolishes molybdate sensitivity, it results in moderate molybdate resistance relative to wild type strains and similar to that observed in *pacC*^{c} constitutive strains. *pacX*1 single mutants are alkalinity mimicking, molybdate resistant and have somewhat elevated levels of alkaline phosphatase and reduced levels of acid phosphatase (hence the *pac* designation) (Fig 4). In addition, they have slightly reduced conidiation, at pH 6.5 and they are resistant to lithium toxicity. Thus, in Petri dish tests, *pacX*1 single mutants resemble weak *pacC*^{c} constitutive mutants.

The range of pacC *alleles phenotypically modified by* pacX^{-} *mutations.*

Numerous *pacX* mutations have been selected as suppressors of *pal*$^{-}$ or *pacC*$^{+/-}$ processing recalcitrant mutations (Table 1). All extant *pacX* mutations have the same phenotype and *pacX* mutant sequence changes clearly show that these are loss-of-function (see, for *example*, *pacX*3503 and *pacX*20, Table 1). The range of *pacC* alleles affected by *pacX*$^{-}$ mutations was further explored by phenotype testing of a variety of *pacC* alleles in combination with *pacX*$^{-}$ mutations. The results (Table 2) demonstrate that *pacX*$^{-}$ mutations are unable to suppress *pacC*$^{-}$ null mutations and severe *pacC* truncation alleles. However, *pacX*$^{-}$ mutations enhance the toxicity of the over-expressed *alcA*^{p}::PacC5-252 allele, which approximates the PacC processed form. In addition, *pacX*1 is additive with the weak constitutive mutations *pacC*^{c}234, *pacC*^{c}39 and *pacC*^{c}20042; that is, the *pacC*^{c} *pacX*1 double mutants are more alkalinity mimicking than the *pacC*^{c} single mutants (Table 2 and data not shown). The epistasis of *pacC*$^{-}$

alleles to *pacX*$^-$ alleles strongly suggests that PacC acts downstream of, or is more directly involved than PacX in the pH regulatory response.

Whilst it appears that a *pacX*$^-$ phenotypic manifestation requires the PacC processed form to be largely functional, not all conforming alleles are affected. For example, the alkalinity mimicry of *pacC*$^{c/-}$20000 (5-251 + 5) is enhanced, with respect to morphology, by *pacX*$^-$, but *pacC*$^{c/-}$20601 (5-260) (Mingot *et al.*, 1999), which contains the intact processed form and has a similar phenotype, appears to be unaffected. *pacC*^{c}69 (L340S) and *pacC*^{c}50 (5-266) (Tilburn *et al.*, 1995; Mingot *et al.*, 1999; Espeso *et al.*, 2000) do not appear to be phenotypically enhanced by *pacX*1, possibly because increased alkalinity mimicry in these strong constitutive backgrounds requires sensitivity beyond that of Petri dish tests. Lack of suppression of acidity mimicking mutants *pacC*$^{+/-}$230 (PacC5-238fs) and *pacC*$^{+/-}$206 (PacC5-310fs) (Mingot *et al.*, 1999) which are both suppressed by mutations affecting the proteasomal degradative pathway (JT and HNA, unpublished) suggests that the effects of *pacX*1 are insufficient to offset this process. Possibly for similar reasons, *pacC*$^{+/-}$7601 (5-379fs) (Tilburn *et al.*, 1995), which contains a long frame-shifted tail, is also unaffected. *pacC*504 (*pacC*5) M5I (5-523) (Tilburn *et al.*, 1995), is a muted *pacC*^{c}5 allele due to mutation removing the preferred translation start site and lack of additivity (data not shown) suggests that *pacX*1 is insufficient to compensate for this. Hypostasis (data not shown) of *pacX*3 to *pacC*700 *pacC*$^{+/-}$70001 which prevents PacC^{27} nuclear import (Fernández-Martínez *et al.*, 2003) implies that suppression by *pacX*3 requires appropriate localization of PacC^{27}.

Molecular effects of pacX$^-$ *mutations*.

pacX$^-$ mutations result in derepression of *pacC* expression. Northern blots in Fig. 5A demonstrate that, after growth in neutral media, *pacX*1, *pacC*$^{+/-}$20205 *pacX*1 and *palB*7 *pacX*1 strains all have elevated

pacC transcript levels, relative to the respective *pacX*$^{+}$ strains, similar to those in the *pacC*^{c}14 strain. In a pH shift experiment (Fig. 5B), the *pacX*20 strain has constant *pacC* transcript levels, independent of growth pH and similar to those obtained in the wild-type strain in response to alkalinization. Thus *pacX*$^{-}$ mutants resemble *pacC*$^{-}$ null (Fig. 1A) and *pacC*^{c} (Fig. 5A and data not shown) mutations in having derepressed *pacC* transcript levels.

The effects of *pacX*1 on *pacC* transcript levels are reflected in PacC DNA binding activity detected in EMSAs where there are considerably increased amounts of the lower mobility complex containing PacC^{72} and/or PacC^{53} from protein extracts of a *pacX*1 strain relative to those from a wild type strain from neutral grown mycelia (Fig. S2). The relatively modest increase in the amount of the higher mobility complex, containing PacC^{27}, from the *pacX*1 strain indicates that *pacX*1 does not override the *palF* transcriptional negative feedback loop (Fig. S2A). In *pal*$^{-}$ or *pacC*$^{+/-}$20205 *pacX*1 double mutants, which are phenotypically pH independent, there are increased amounts of both the lower and higher mobility complexes relative to those in the *pal*$^{-}$ or *pacC*$^{+/-}$20205 single mutants (Fig. S2B and C).

Western blot analyses of shift experiments in Fig. 5C, where all three PacC forms can be distinguished, confirm that the increased amounts of complexes detected in EMSAs from the *pacX*$^{-}$ strains are due to increased amounts of protein, rather than improved binding efficiencies. In addition they demonstrate that prior to the 120 minute time point all PacC forms, where present, are considerably elevated in the *pacX*20 strain relative to those in the wild type. After 120 min PacC levels in the *pacX*20 strain have fallen and both the relative proportions and the amounts of the three PacC forms are very similar in both strains.

PacC^{72} levels are also highly elevated in the *palB*38 *pacX*20 strain relative to those in the (null) *palB*38 single mutant and similar to those obtained in the *pacX*20 single mutant under acidic conditions (Fig. 5C). On shifting to alkalinity, levels of PacC^{72} remain fairly constant in both *palB*38 strains and appreciable amounts of PacC^{27} and partial degradation products in the *palB*38 *pacX*20 strain are detectable throughout. These bands are attributable to C-terminal, processive, Pal-independent proteolysis of the minor proportion of PacC^{72} having an 'open', and proteasome accessible, conformation which exists in equilibrium with the much more numerous PacC^{72} molecules which are 'closed' and proteasome resistant (Espeso *et al.*, 2000; Díez *et al.*, 2002; Hervás-Aguilar *et al.*, 2007; Peñas *et al.*, 2007; Peñalva *et al.*, 2008).

Cloning the pacX *gene by transposon mediated mutagenesis.*

Extensive attempts to rescue the *pacX*1 mutant phenotype by co-transformation of an *argB*2 *pacX*1 *palA*1 strain with plasmid pILJ16 carrying *argB*$^+$ (Johnstone *et al.*, 1985) and chromosome VIII allocated Lorist or pWE15 derived cosmids (Brody *et al.*, 1991) selecting for *argB*$^+$ and testing for the *palA*1 alkaline sensitivity phenotype on pH 8.0 medium were unsuccessful. A subsequent PCR analysis suggested that *pacX* may be absent from these libraries. Transposon mediated mutagenesis was chosen as an alternative cloning strategy because of the ease with which a *pacX*$^-$ mutation could be selected. This took advantage of available strains carrying the modified Impala transposon from *Fusarium oxysporum* tagged with the *yA* gene, required for green pigmentation of conidia, inserted in the promoter of the *niaD* gene thus resulting in the inability to utilize nitrate (Li Destri Nicosia *et al.*, 2001). A *yAΔ*::*Ncpyr4*, *pabaA*1, *niaD*::*impala*::*yA*$^+$, *pacC*$^{+/-}$20205 strain was constructed and transposition was found to occur at a frequency of ~10^{-5}. Conidia of this strain were spread on pH 7.5

medium with nitrate as sole nitrogen source to select simultaneously for *pacX*⁻ mutations and restoration of the *niaD*⁺ genotype by excision of the Impala transposon. Out of an estimated 600,000 transposition events one colony was obtained. The mutant (BG2) was found, by diploid analysis, to contain the insertion on linkage group VIII. This location and the phenotype of BG2 strongly suggested that the insertion had occurred in *pacX,* as subsequently confirmed (see below). *pacX* genomic and cDNAs sequences were determined as described in **Experimental Procedures**.

PacX sequence

The *pacX* sequence specifies a 661 residue protein. A zinc binuclear cluster DNA binding motif is located towards the carboxy-terminus between residues 445 and 472 and a region predicted to form a coiled-coil structure occurs in the region of residues 178 to 224 (Fig. 6 and Fig. S3). In BLAST searches of the databases the region containing the putative DNA binding domain and the amino-terminus extending to residue 228 are the most highly conserved (see below), indicating their functional importance (Fig. 6, Fig. S3 and Fig. S4). Different algorithms all predict a nuclear localization for PacX; ngLOC (17.6 % nuclear 14.5% cytoplasmic), PSORT II (73.9% nuclear) with cNLS mapper predicting highly probable monopartite (TPGKRPRSDSGEF, residues 10 to 22, score 6.5) or bipartite (ETPGKRPRSDSGEFPPIASKVPKT, 9 to 32, score 9.0) NLSs. An NES (nuclear export sequence) is predicted with high probability by NetNES between residues 179 and 191 (Fig. 6).

The coiled-coil prediction for *A. nidulans* PacX is 1 and therefore very strong (Fig. S3). The distancing of the coiled-coil region from the zinc binuclear cluster is somewhat conserved amongst PacX homologues (Fig. 6 and Fig. S3). Coiled-coils are putative oligomerization domains and the role of the coiled-coil is supported by the partial dominance of *pacX1 vis a vis pacX*⁺ (Fig. S5). *pacX*1 results in a

frame-shift after residue 301 (Table 2), thus conserving the coiled-coil element but deleting the Zn cluster. A number of point mutations map within the putative coiled-coil element (Fig. S3, S4 and Table1).

The PacX putative DNA binding domain (Fig. 6) conforms to the consensus sequence of zinc binuclear cluster motifs (Todd and Andrianopoulos, 1997; MacPherson *et al.*, 2006) characteristic of, even if not completely exclusive to, fungi (Scazzocchio, 2015). Zinc binuclear cluster DNA binding motifs are almost universally at the amino-terminus of cognate transcription factors (MacPherson *et al.*, 2006); however that of PacX is towards the carboxy-terminus, which resembles *S. cerevisiae* Ume6p (Strich *et al.*, 1994) and *C. albicans* Czf1p [(Whiteway *et al.*, 1992) reviewed by (MacPherson *et al.*, 2006)]. Infrequent but not unique to PacX and its orthologues are the two Pro residues N terminal to the first Cys, and the absence of a Pro residue one or two residues N-terminal to the fourth cysteine (Fig. S4). The dimerization element is usually in Zn-cluster proteins a few residues C-terminal to the DNA binding motif, and it is typically shorter than the one seen in PacX, such as 15 residues for Gal4, 19 residues for Ppr1 (Marmorstein *et al*., 1992; Marmorstein and Harrison, 1994) with the maximal length predicted for such a C-terminal coiled-coil dimerization domain being 25 residues (Schjerling and Holmberg, 1996). This contrasts with the 46 residue-long putative coiled-coil, 221 residues amino-terminal to the first Cys of the Zn cluster extant in PacX. It could be proposed that while the function of the standard dimerization domain found in Zn binuclear clusters is to permit the recognition of DNA inverted, everted or direct repeats separated by a few base pairs [e.g. 11 in Gal4, 6 in Ppr1 and UaY (Marmorstein *et al*., 1992; Marmorstein and Harrison, 1994; Suarez *et al*., 1995)], the probable dimerization of PacX may serve an altogether different function.

Phylogenetic analysis

Searching with blastp using the PacX protein sequence as *in silico* probe of the 431 fungal genomes available in the Joint Genetics Institute database on the 30th of January 2015 showed PacX homlogues to be present in the Pezizomycotina and not in any other fungal taxon, but being absent from the two sequenced genomes of the Orbiliomycetes and the seven sequenced genomes of the Pezizomycetes, basal classes of the Pezizomycotina. Absence from these and other ascomycete taxons (Saccharomycotina and Taphrynnopmycotina) was confirmed with a tblastn search. Searching the NCBI protein data base, excluding the Pezizomycotina failed to reveal any homologues with either blastp or tblastn. Although within the Eurotiomycetes the sequence is very conserved, the phylogenetic tree (Fig. S6) and the alignment (Fig. 6 and Fig. S4) demonstrate that there is much divergence within the Pezizomycotina. Within the Sordariales the sequence even within the zinc binuclear cluster is divergent, as shown by the *Neurospora crassa* sequence in the alignment (Fig. 6). Within the Dothidiomycetes the sequences diverge even more and form two clusters roughly corresponding to the Pleosporales and Capnodiales with one outgroup (see legend to Fig. S6 for details), secondary loss has occurred in several species, mainly within the Sordariales, including *Magnaporthe grisea* and *Podospora anserina* (confirmed by tblastn).

Mutant sequence changes

44 mutant sequence changes confirm the identity of the gene (Table 1). Clustering of missense mutations exclusively to within the amino-terminus and the predicted coiled coil region itself and the zinc binuclear cluster or immediately adjacent to it underscores the functional importance of these regions (Fig. S4). The results of comparing PacX to the consensus derived from an alignment of 177

PacX homologues using the ConSurf algorithms (http://consurf.tau.ac.il/) for the identification of functional regions in a protein are presented in Fig. S4, and the predictions for mutated residues are summarized in Table 1. All of the missense mutations affect conserved residues or residues which occur in conserved regions (Fig. S4). Three out of four mutations in the coiled-coil *pacX*3505(R209P),, *pacX*22(R216P) and *pacX*9(R221P) are basic to non polar. Theses are changes of Arg to Pro, a residue which breaks α-helices. However the coils/pcoils algorithm (http://toolkit.tuebingen.mpg.de/pcoils) only revealed in each case minor changes for the probability or length of the predicted coiled-coil. All mutations within this region [which includes *pacX*11(A223G)] change conserved residues which are predicted to be exposed and functional and may affect a specific interaction of PacX. The majority of truncating mutations remove conserved regions of the protein. Even more extreme truncations, *pacX*3503 and *pacX*20, terminate the protein at residues 12 and 44, respectively, thus removing almost all of the protein, confirming that these classically obtained *pacX* alleles are complete loss-of-function (Table 1). The absence of mutations and poor conservation in the C-terminus suggested that this region might be dispensable. This was confirmed with an engineered allele expressing PacX residues 1 to 499 from the *alcA* promoter (*alcA*^{p}::PacX1-499) and integrated at *pyroA*, which was found to be as functional as the full length protein expressed from the same promoter (*alcA*^{p}::PacX1-661) at the same integration site. *pacX*3507 which terminates the protein after Ser506 and therefore retains the functional region has a long (41 residue) out-of-frame tail which might destabilize the protein or interfere with its activity and thus cause the loss-of-function phenotype.

pacX mutations also include the intergenic duplication in *pacX*24 and the Impala transposition into the *pacX* promoter of *pacX*12. In addition, *pacX*18 was found to be an insertion identical to the Fot1-like transposon in chromosome VIII defined by AN0826 (encoding the transposase). Surprisingly, sizing

of the region of AN0826 amplified using external primers shows the transposon to be retained at its resident locus in the mutant strain (see Supplementary Data).

PacX nuclear localization

The PacX sequence, which contains putative nuclear localization signals and a putative zinc binuclear cluster DNA binding domain, strongly suggested that PacX functions in the nucleus. PacX localization was investigated by live epifluorescence microscopy of a strain expressing PacX::GFP and HhoA::mCherry (histone 1). Fig. 7 shows that PacX::GFP is localized within the nuclei where it forms one strongly fluorescent, discrete spot per nucleus. Shifting from acidity to alkalinity for one hour had no effect on PacX::GFP localization which therefore appears to be pH independent (Fig. 7). PacX localization resembles that of the proline degradation pathway-specific zinc binuclear cluster transcription factor PrnA which has proline-independent, sub-nuclear localization (Pokorska *et al.*, 2000).

Discussion

PacX is a protein of unusual domain structure, with a conspicuous coiled-coil helix amino-terminal to a typical carboxy-terminal fungal Zn cluster. The pH signalling pathway, including the central transcription factor PacC/Rim101 is conserved throughout the ascomycetes and , to a certain extent, in the basidiomycetes and has been studied in ascomycetous yeasts and basidiomycetes (Penalva *et al*., 2008; Penalva *et al*., 2014; Davis, 2009; Selvig and Alspough, 2011; Blanchin-Roland, 2013; Cornet and Gaillardin, 2014; Obara and Kihara, 2014; Herrador *et al*., 2015; Ost *et al*., 2015, and references therein) (in addition to *A. nidulans* and other filamentous ascomycetes). However, the additional putative transcription factor PacX is an evolutionary novelty. It occurs only in the pezizomycotina and within the limits of the paucity of sequences available, particularly in the orbiliomycetes, it seems to have appeared after the divergence of the other classes of the Pezizomycotina (Leotiomyceta) from the Pezizomycetes and the Orbiliomycetes. Recent studies, including those combining fossil and molecular, data differ as to whether the Pezizomycetes or the Orbiliomycetes constitute the most basal group of the Pezizomycotina (Schoch *et al.*, 2009; Prieto and Wedin, 2013; Beimforde *et al.*, 2014). However these studies agree that the Leotiomyceta have diverged from the other two classes most probably in the Silurian era (~430 Mya). Thus the appearance of PacX correlates with a major phylogenetic split, which may coincide with the establishment of biotic interactions with vascular plants (Prieto and Wedin, 2013).

The characterization of mutations in *pacX* has pin-pointed the crucial functional regions, which correlate with those conserved throughout the Leotiomyceta. One mutation however is quite unique: In more than 60 years of *A. nidulans* genetics, this is the first and only reported mutation resulting from

an insertion of an endogenous transposon. What is even more surprising, is that the *Fot-1* like element defined by AN0826 did not transpose by a mechanism of cut and paste, characteristic of the transposons of this class, including the heterologous transposition of the *Fusarium oxysporum Fot1* transposon in *A. nidulans* [(Li Destri Nicosia *et al.*, 2001) and refs therein]. but rather by a copy and paste mechanism (see Supplementary Data).

Proposed role(s) of PacX together with negative autoregulation of *pacC* and the negative feedback acting on *palF* are incorporated in a model for the control of the alkaline pH response, which is shown in Fig. 8. PacC^{72} exists predominantly in a closed proteasome inaccessible conformation in equilibrium with a small fraction of molecules assuming a less favourable open, proteasome-accessible conformation, thus providing a substrate for the Pal independent bypass. In the absence of pH signal transduction, PacC^{72} is largely unprocessed (Figs. 2 and 5C) and, with the participation of PacX, represses its own transcription, as demonstrated by the increased *pacC* transcript levels obtained in *pacC* null or *pacX* null strains (Figs. 1A and 5B). This would reduce substrate-driven flux through the Pal independent pathway. However, over-expression of *pacC* by itself produces no detectable phenotype and over-expressing *pacC* alleles expressed from the *alcA* or *gpdA*^{mini} promoter are hypostatic to *pal*$^{-}$ mutations [Fig. 9 and Mingot *et al.*(2001) and JT, América Hervás-Aguilar, HNA and MAP, unpublished]. In contrast, *pacX*$^{-}$ mutations result in alkalinity mimicry, and they are able to suppress *pal*$^{-}$ and processing recalcitrant *pacC*$^{+/-}$ mutations. Moreover they are able to suppress *pal*$^{-}$ mutations even when *pacC* is expressed from the heterologous *alcA* (Fig. 9) and *gpdA*^{mini} (data not shown) promoters, i.e. independent of *pacC* derepression. In addition, *pacX*$^{-}$ mutations augment aspects of the phenotypes of *alcA*^{p}::PacC5-250 and *pacC*$^{c/-}$20000 (PacC5-251), alleles which specify truncated proteins that approximate PacC^{27} and do not require further processing (Table 2). These effects strongly suggest

that PacX inhibits PacC^{27} activities in a manner separate from and in addition to its negative effects on *pacC* transcription. PacX mediated inhibition of PacC^{27} activities also potentially explains why the very small amounts of PacC^{27} present in *pacX*$^{-}$ *pal*$^{-}$ strains (Fig. 5C) are able to suppress the *pal*$^{-}$ phenotype to such an appreciable extent (Fig. 4). The alkalinity mimicking phenotype of *pacX*$^{-}$ mutations which result in elevated alkaline phosphatase (*palD*) and reduced acid phosphatase (*pacA*) levels demonstrates that PacX affects both activator and repressor functions of PacC^{27} and that it is required for normal responses to acidity and neutrality.

The onset of PacC processing occurs less than 4 minutes after exposure to alkalinity (Fig. 2A) and this rapid response would be facilitated by the pool of PalF accumulated under acidic conditions, due to *palF* being acid expressed (Fig. 3A and B). After approximately 1.5 to 2 hours steady state conditions are established and PacC^{72} begins to accumulate again (Fig. 2B), indicating that the signalling proteolysis has become limiting and that the signal has become attenuated. Work presented here, wherein over-expression of *palF* from a heterologous promoter largely prevents accumulation of PacC^{72} in alkaline media strongly suggests that repression of *palF* transcription, directly or indirectly, by PacC^{53} or PacC^{27} plays a major role in this attenuation. It appears that there is a relatively modest fall in PalF protein levels as compared with the fall in *palF* transcript levels, in response to alkalinization. This suggests that attenuation is not a function of absolute PalF amounts but rather that of the rate of *de novo* PalF synthesis. Low rates of PalF synthesis might inhibit Pal signalling, for example, by limiting the rate of the crucial PalF ubiquitylation. Other modifications might be affected. In addition to ubiquitylation, *A. nidulans* PalF is phosphorylated in an alkaline pH dependent fashion (Herranz *et al.*, 2005). Interestingly CK1-mediated phosphorylation of *S. cerevisiae* Rim8 has recently been reported to prevent Rim signalling (Herrador *et al.*, 2015). Thus attenuation might be achieved by limiting the rate

of *de novo*, unphosphorylated, pathway-activating PalF. An even more tempting scenario would be that the degree of signalling is a balance between the levels of ubiquitylated and phosphorylated PalF. In this situation the effects of small changes in *de novo* synthesized PalF would be additive and could well account for the quite profound effects observed on over-expression of PalF (Fig. 3E and F).

Thus control of the alkaline pH response ensures that both the response to alkalinization is Pal signal transduction dependent and an escalating alkaline pH response is prevented by attenuation of pH signalling by negative feedback via repression of *palF* transcription by $PacC^{53}$ and/or $PacC^{27}$. It is tempting to speculate that the absence of PacX in yeasts correlates with the absence of pH signal independent activation of the pH responsive transcription factor. In *S. cerevisiae* Rim101 processing occurs in one step and is entirely Rim signal transduction dependent (Li and Mitchell, 1997; Lamb *et al.*, 2001; Xu and Mitchell, 2001). In *C. albicans*, although Rim signal dependent Rim101 C-terminal processing occurs in both acidic and alkaline media to different extents, it is thought that the alkaline active 74-kDa form is the product of a single Rim13-mediated proteolysis (Li *et al.*, 2004; Xu *et al.*, 2004). However, in *Y. lipolytica* it has been suggested that Rim101 might be processed similarly to *A. nidulans* PacC (Lambert *et al*., 1997; Blanchin-Roland, 2013).

pH regulation of the *palF* homologues *RIM8* in *S. cerevisiae* and *C. albicans*, which are also preferentially expressed in acidic media, has been reported (Ramon *et al.*, 1999; Porta *et al.*, 1999a; Lamb and Mitchell, 2003b), suggesting that negative feedback limiting the arrestin component of the pathway might be a general feature of the pH response. However, in contrast to PalF, where ubiquitylation is strictly pH- and PalH-dependent and pivotal in the response, *S. cerevisiae* Rim8 ubiquitylation appears to be pH independent and takes place in a double *rim20Δ dfg16Δ* mutant

background, lacking both PalH homologues. However, the role of Rim8 ubiquitylation in Rim signalling becomes clear if the Vps23-Rim8 interaction is debilitated by mutation of a SPX motif in the latter (Herrador *et al.*, 2010). *C. albicans* Rim8 undergoes hyperphosphorylation, instead of ubiquitylation, in a manner linked to Rim101 processing (Gomez-Raja and Davis, 2012).

Many *pacC/RIM101* homologues, like *A. nidulans pacC* [(Tilburn *et al.*, 1995) and Figs. 1 and 5B], are preferentially expressed under neutral to alkaline conditions. These include those of: *Beauveria bassiana* (Zhou *et al*., 2014) *C. albicans* (Bensen *et al.*, 2004), *Fusarium oxysporum* (Caracuel *et al.*, 2003), *Magnaporthe oryzae* (Landraud *et al.*, 2013), *Metarhizium robertsii* (Huang *et al.*, 2015),*Trichoderma harzianum* (Moreno-Mateos *et al.*, 2007), *Trichoderma virens* (Trushina *et al.*, 2013), *Wangiella* (*Exophial*) *dermatitidis* (Wang and Szaniszlo, 2009) *Y. lipolytica* (Lambert *et al*., 1997) but not, curiously, *S. cerevisiae* (Lamb *et al.*, 2001; Serrano *et al.*, 2002; Lamb and Mitchell, 2003b; Viladevall *et al.*, 2004). This suggests that autoregulation might be a common feature but the absence of reporter studies precludes determining whether this would be positive or negative.

The mechanism(s) of PacX action is/are not clear but what appears to be dual functionality could be achieved by a single mechanism. For instance, if $PacC^{72}$ and $PacC^{27}$ were to compete for nuclear import and/or DNA binding, PacX antagonism of $PacC^{27}$ could fulfil both functions. This might involve protein-protein interactions between PacX and PacC, possibly via the PacX coiled-coil domain and/or direct DNA binding of PacX through the zinc binuclear cluster. PacX localization, which is almost exclusively nuclear, supports a mechanism occurring within the nucleus.

Investigations into *pacC* and *palF* promoter occupancy, the possibility of PacC and PacX interaction, PacX sub-nuclear localization and post-transcriptional regulation of PalF are topics for future research.

Experimental Procedures

A. nidulans *strains, phenotype analysis, genetic techniques and growth media*

A. nidulans strains carried previously described markers, in general use*; s*tandard media, phenotype testing and genetic techniques were used (Caddick *et al.*, 1986; Clutterbuck, 1993; Arst *et al.*, 1994; Tilburn *et al.*, 1995), and references therein). LiCl and MoO_4^{2-} plates were prepared by the addition of lithium chloride or sodium molybdate solution to appropriately supplemented minimal medium (Cove, 1966) containing 1% D-glucose and 5 mM ammonium tartrate, to the desired concentration (100 - 500 mM LiCl and 25 mM MoO4). Neomycin containing plates were prepared by the addition of neomycin sulphate powder to 1 or 0.5 mg ml^{-1} to molten minimal medium minus glucose, containing 1% D-glucose or 1% ethanol (added after autoclaving), respectively and 5 mM ammonium tartrate. pH 8.0 medium followed (Cove, 1976). Dropout media were prepared from fully supplemented yeast Dropout medium (Clontech) containing additional supplements appropriate for the auxotrophies of the strains, 5 or 10 mM urea as nitrogen source and 1% D-glucose, added after autoclaving. Acidic dropout medium and MFA (Penas *et al*., 2007), which contained 5 mM ammonium tartrate as nitrogen source, were was buffered with 50 mM citrate to give pH 4.3 and alkaline dropout medium and MFA were buffered with 100 mM HEPES to give ~pH 8.3. MFA was also buffered to give pH 5.6 with 100mM NaH_2PO_4 (plus 100 mM NaCl); pH 6.8 with 50 mM NaH_2PO_4 and 50 mM Na_2HPO_4 (plus 50 mM NaCl) and pH 7.9 with 100 mM Na_2HPO_4. To obtain conidiospores for transposon mutagenesis strain 2431A (see below *Transposon mutagenesis*) was grown on minimal media (see above) with 10 mM $NaNO_2$ as sole nitrogen source, buffered to pH 6.5 with 50 mM MES. To select simultaneously for growth on nitrate as sole nitrogen source and for loss-of-function in *pacX* we used pH 7.5 medium, minimal

medium (see above, (Cove, 1966) buffered to pH 7.5 by addition of 50 mM phosphate buffer (made from stock solutions 500 mM Na_2HPO_4 and 500 mM NaH_2PO_4), containing 10 mM $NaNO_3$ as sole nitrogen source and 10 x PABA (40 µg. ml^{-1}. 4-aminobenzoic acid).

Construction of strains

Plasmid pALC-*argB* (*Bgl*II) (Mingot *et al.*, 1999) was used for the construction of *pacC* and *pal* over-expression cassettes containing cDNA of *pacC* and one of each of the *pal* signal transduction genes (Denison *et al.*, 1995; Tilburn *et al.*, 1995; Maccheroni *et al.*, 1997; Negrete-Urtasun *et al.*, 1997; Denison *et al.*, 1998; Negrete-Urtasun *et al.*, 1999) under *alcA*^{p} (alcohol dehydrogenase promoter) control. This plasmid contains a functional *alcA*^{p}, containing a transcription start site, separated from the *trpC* terminator by a polylinker, and a mutant *argB* gene to direct integration to *argB* by repair of the *argB*2 allele. *pal* over-expressing strains were constructed by DNA mediated transformation (Tilburn *et al.*, 1995) of double mutants, *argB*2 and appropriately *pal*$^{-}$ for the corresponding over-expressed gene, with selection for *argB*$^{+}$ transformants, screening for the *pal*$^{+}$ phenotype and Southern blot analysis to identify appropriate single copy integrants. Appropriate *pal*$^{+}$ transformants were subsequently crossed to obtain *pal* over-expressing strains in otherwise *pal*$^{+}$ genetic backgrounds. *alcA* driven PacC5-678 over-expressing strains were obtained by transformation of strain MAD397 *yA*2 *argB*2 *palA*1 *pacC*Δ::*Ncpyr4 pantoB*100 with p[*alcA*^{p}::PacC5-678], as described by Mingot *et al.* (1999), to give transformant *yA*2 *palA*1 *argB*:: *alcA*^{p}::PacC5-678 *pacC*Δ::*Ncpyr4 pantoB*100 (MAD0415) which was crossed to HB85 *pabaA*1 (*yA*2 *or yA*Δ::*Ncpyr4*) *argB*2 *pacX*20 to give strains (9-1) (*yA*2 or *yA*Δ*Ncpyr*4) (*pyrG*89?) *argB*::*alcA*^{p}::PacC5-678 *palA*1 *pacC*Δ*Ncpyr4,* (9-21) *paba*A1 (*yA*2 or *yA*Δ::*Ncpyr4*)

(*pyrG*89?) *argB*::*alcA*^{p}::PacC5-678 *palA*1 *pacC*Δ::*Ncpyr4* *pacX*20 and (9-17) *paba*A1 (*yA*2 or *yA*Δ::*Ncpyr4*) (*pyrG*89?) *alcA*^{p}::PacC5-678 *pacC*Δ::*Ncpyr4* *pantoB*100 (Fig. 9).

The *pacX* gene was 3' tagged with GFP and S-tag using spacer-GFP/S-tag-Af*pyrG* cassettes (Yang *et al.*, 2004) and introduced by gene replacement into a *nkuA*Δ::bar recipient strain (KUG4). KUG4 *pyrG*89 *pyroA*4 *niiA*4 *nkuA*Δ::bar was constructed by crossing to a strain *nkuA*Δ::bar *niiA*4 *biA*1 *pyroA*4 (kindly provided by Prof Michael Hynes). The S-tagged *pacX* allele was denoted *pacX*35. Strain ALO2 *pacX*::GFP::AfpyrG (*pyrG*89?) *pyroA*4 HhoA::mCherry *niiA*4 *nkuA*::bar was obtained by crossing transformant A1 *pyrG*89 *pyroA*4 *niiA*4 *nkuA*Δ::bar *pacX*::GFP::Af*pyrG* with strain LO1421 containing HhoA::mCherry (kindly provided by Prof Berl Oakley).

Strains *pabaA*1 *yA*2 *gpdA*^{mini}::GFP-PacC(5-678)::*pyroA* *pacC*Δ::*Ncpyr4* (MAD1713) and *pabaA*1 *yA*2 *gpdA*^{mini}::GFP-PacC(5-251)::*pyroA* *pacC*Δ::*Ncpyr4* (MAD1710) were obtained by transformation of a *pabaA*1 *yA*2 *pacC*Δ::*Ncpyr4* *pyroA*4 recipient strain with plasmids p1673 and p1666, respectively, and identification of transformed clones carrying single-copy integration events at *pyroA* by Southern blotting. p1673 and p1666 encode GFP-PacC(5-678) and GFP-PacC(5-251) fusion proteins, respectively. Coding regions were obtained as *Hin*dIII-*Eco*RI fragments by PCR, using templates described in (Mingot *et al.*, 1999), and introduced into the multiple cloning site of pgpd003 (Pantazopoulou and Peñalva, 2009), downstream of the *gpdA*^{mini} promoter. Strains J2422 *yA*2 *gpdA*^{mini}::GFP::PacC5-678::*pyroA*$^{+}$ *pacC*$^{-}$6309 (*pacC*63) *pantoB*100 and J2427 *gpdA*^{mini}::GFP::PacC5-251::*pyroA*$^{+}$ *pacC*$^{-}$6309 (*pacC*63) were derived by crossing MAD1713 and 1710 respectively to J2384 *areA*^{r}5 *pyroA*4 *pacC*$^{-}$6309 (*pacC*^{c}63) *pantoB*100 and the *pacC*$^{-}$6309 allele was detected amongst the progeny by PCR. TM280 *pabaA*1 *gpdA*^{mini}::PalF::GFP::*pyroA* *palF*15 was obtained by transformation of recipient strain TM261 *pabaA*1

*pyroA*4 *palF*15 with pTM9015. pTM9015 was derived from p1673 by QuikChange mutagenesis (Agilent Technologies Inc.) using primers p1673-EcoRI-Fw and p1673-EcoRI-Rv (Table S1) to introduce an *Eco*R1 site into which *palF* cDNA was inserted in place of *pacC*.

The construction of endogenously expressed MYC3-tagged PacC (allele name *pacC*900) is described by Peñas *et al.* (2007) and endogenously HA3-tagged PalF (allele name *palF*500) or HA3-tagged PalF expressed from $gpdA^{mini}$ promoter are described by Hervás-Aguilar *et al.* (2010). Strain MAD2352, *wA*4 *pyroA*4 *inoB*2 *palF::HA3::pyrGfum pyrG*89 *nkuA*Δ::bar *pacC*900 was obtained by transformation of MAD1732 (Hervás-Aguilar *et al.*, 2010). MAD4500, *yA*2 *pabaA*1 *pantoB*100 *pyroA*4::[*pyroA**-$gpdA^{mini}$::*palF*::HA_3] *pacC*900 $nkuA^{+}$ was derived by crossing MAD3319 *yA*2 *pabaA*1 *pantoB*100 and MAD3007 *pantoB*100::[*pantoB**::$gpdA^{mini}$::*palH*::myc3] *pyroA*4::[*pyroA**::$gpdA^{mini}$::*palF*::HA3] *pacC*900 Δ*nkuA*::*bar*?).

Northern Blots

Growth conditions for Northern blot analyses are given in the appropriate Figure legends. RNA was extracted as described by Tilburn *et al.* (1995) or by a modified Drosophila procedure http://www.koko.gov.my/CocoaBioTech/RNA%20Isolation23.html#procedure, as follows. Lyophilized mycelium was ground in a 2 ml tube with a glass rod and mixed with 800 µl of GHCl solution (5 mM DTT, 7.5 M guanidium hydrochloride (Sigma), 25 mM sodium acetate, pH 7.0, 0.5% N-lauryl sarcosinate) and shaken vigorously with an equal volume of phenol:chloroform:isoamylalcohol (25:24:1) or acidic (pH 4.5) phenol:chloroform:isoamylalcohol (125:24:1). After centrifugation the RNA was precipitated from 400 µl of the aqueous phase with 16 µl of 1M acetic acid and 400 µl of ethanol with incubation at -80^{o}C for 1 - 2 hours. The RNA was pelleted by centrifugation and resuspended in

400 µl of GHCl solution and precipitated as before. The RNA was washed with 100% ethanol, then 75% ethanol, air dried and resuspended in RNAase free water and stored at -80^{o}C. Northern blotting followed Tilburn *et al.* (1995). Heat or UV fixed membranes were stained with methylene blue (Sambrook *et al*., 1989) and probed with appropriate radiolabelled (^{32}P) or digoxygenin (DIG) labelled (Roche) DNA fragments. *pacC* specific probes were prepared from PCR fragments obtained with primers (Table S1) TILREV and 1217FF or BIGFF (^{32}P labeled) or 850U and 1217FF (DIG labeled, Fig. 1B). Loading controls were established using a ^{32}P labelled ~650 bp *Nco*I-*Nco*I fragment from the *A. nidulans* actin gene (Fidel *et al.*, 1988) or methylene blue stained 18S rRNA, as indicated.

Western Blots

Mycelia were cultured and sampled essentially as described by Galindo *et al* (2012) except that 5 mM ammonium tartrate was used as nitrogen source and alkaline medium was buffered to pH 8.0 with 100 mM HEPES. Lyophilised mycelia were homogenised, using a 5 mM ceramic bead, following Hervás-Aguilar *et al.* (2010). Cell lysis followed a method adapted from an *S. cerevisiae* protocol (Stimpson *et al.*, 2006). 6 mg samples of powdered biomass were weighed and transferred to 2 ml microcentrifuge tubes. Proteins were solubilised in 1 ml tube^{-1} lysis solution (0.2 M NaOH, 0.2% (v/v) β-mercaptoethanol with vigorous vortexing. Proteins were precipitated with 7.5% trichloroacetic acid (TCA) and pelleted by centrifugation at 14,000 x g for 5 min at 4^{o}C. Pellets were solubilized in 100 µl Tris base, mixed with 200 µl of Laemmli buffer (Laemmli, 1970) and incubated at 100^{o}C for 2 min. Proteins (5 to 10 µl of each sample were resolved in 8% SDS-polyacrylamide gel, transferred to nitrocellulose membranes. For MYC_3::PacC and actin blots were reacted with either mouse monoclonal anti-c-myc (at 1/2,000 dilution) (Clone 9E10, Sigma-Aldrich) or mouse anti-actin

monoclonal antibody (1/4,000) (Clone 4, MP Biomedicals, LLC). Peroxidase conjugated goat anti-mouse IgG immunoglobulin (Jackson) at 1/5,000 and 1/8,000 respectively were used. PalF::HA_3 blots were reacted and developed as described by Hervás-Aguilar *et al.* (2010). Peroxidase activity was detected with Amersham Biosciences ECL.

Transposon mutagenesis

pacX was cloned by tagging it with the impala transposon form *Fusarium oxysporum* in a manner similar to that employed to tag the *azgA* (Cecchetto *et al.*, 2004) and *rrmA* (Olszewska *et al.*, 2007). Starting from strain CS2778 (Li Destri Nicosia *et al.*, 2001) which contains an impala yA^+ tagged element interrupting the *niaD* promoter we obtained strain 2431A, *yA*Δ::*Ncpyr*4, *pabaA*1, $niaD^p$*::impala::*yA^+ $pacC^{-/+}$20205 by crossing. The *impala* excision frequency in strain 2431A was determined to be of the order of 10^{-5}, similar to that reported for strain CS2778 (Li Destri Nicosia *et al.*, 2001). Strain 2431A is unable to grow on nitrate by virtue of the *impala* element inserted in the *niaD* promoter and it is unable to grow at pH 7.5 due to the presence of the $pacC^{-/+}$20205 mutations. Thus, a strain able to grow on nitrate at pH 7.5 should result from simultaneous excision of the *impala* element and its insertion in *pacX*, which would suppress the phenotype of $pacC^{-/+}$20205. Conidiospores of strain 2431A were obtained on minimal media with $NaNO_2$ as sole nitrogen source and plated by top layering on the appropriate selective media ($NaNO_3$ as sole nitrogen source, pH 7.5, see above). One putative strain (BG2) carrying a transposon insertion in *pacX* was selected as able to grow in this medium. Based on the excision frequency of strain 2431A and the number of viable conidiospores plated we calculated that ~600,000 $niaD^+$ colonies were generated in the experiment that yielded the putative *pacX* insertion.

Determining DNA sequence flanking the Impala insertion site.

Genomic DNA of strain BG2 was isolated and used as template to obtain DNA sequence flanking the impala insertion site by PCR using a single primer yA1 and cycling conditions as described by Karlyshev *et al.* (2000). The major fragment of ~0.9 kbp was gel purified and sequenced using oligo yA2. The fragment was re-amplified using primer yA1, digested with *Bam*HI (to obtain fragments having a single yA1 sequence), and the gel-purified major fragment of ~650 bp was sequenced using primer yA1. These sequencing reactions combined gave 708 bp of sequence flanking the insertion site. Primer sequences are given in Table S2.

Determining the pacX *genomic and cDNA sequences and* pacX *mutant sequence changes*

BLAST search of the (then unfinished) *A. fumigatus* genome database (Nierman *et al.*, 2005) suggested a possible *A. fumigatus* homologous gene having a C-terminal zinc binuclear cluster. A larger *A.nidulans pacX* fragment was PCR amplified using the *pacX*-specific primer XF2 and a degenerate primer ZNF2 based on the sequence of the zinc binuclear cluster of the putative *A. fumigatus* homologue. In the first 3 cycles an annealing temperature of 45^{o}C was employed, followed by 30 cycles at 55^{o}C; 20 pmoles of XF2 and 200 pmoles of ZNF2 were used per reaction. The resulting ~1.6 kbp fragment was gel purified and sequenced. A DNA fragment made by PCR using primers XF5 and XR5 was used to isolate *pacX* clones from a λ gt10 cDNA library (Osmani *et al.*, 1988). Two cDNA clones contained the entire *pacX* coding sequence and sequencing confirmed the presence of one intron. Nucleotide sequence of the 5' region of the *pacX* gene (upstream of the impala insertion and cDNA sequence) was obtained following an 'inverse' PCR strategy. Essentially, DNA of BAC clone 28C10 obtained from an *A. nidulans* BAC library prepared by Ralph Dean and obtained from

https://www.genome.clemson.edu/online_orders?&page=productGroup&service=bacrc&productGroup=96 was digested with various restriction enzymes, purified and treated with T4 DNA ligase to circularize fragments. The DNA was PCR amplified using two ("outward-facing') primers expected to give no product on linear DNA, XR6 and XF2, which resulted in~1.8 and ~2.8 kbp DNAs when BAC 28C10 DNA had been digested with *SacII* and *XhoI*, respectively. The PCR fragments were sequenced using XR1 and additional primers.

Genomic DNA of *pacX* mutants was PCR amplified using *pacX*-specific primers (e.g., XF2 and XR8) and the fragments were sequenced using additional gene specific primers. Mutations were, in most cases, confirmed on the opposite strand of a different PCR fragment.

Primer sequences are given in Table S1.

In silico analyses

PacX orthologues were searched in the JGI (http://genome.jgi-psf.org/programs/fungi/index.jsf) and NCBI databases (http://blast.ncbi.nlm.nih.gov/Blast.cgi). *A. nidulans Fot1*-like elements were searched in http://www.aspgd.org/ (Cerqueira *et al.*, 2014). Alignments were carried out with MAFFT version 7 5, http://mafft.cbrc.jp/alignment/server/ (Katoh and Standley, 2013), refinement with BMGE, http://mobyle.pasteur.fr/cgi-bin/portal.py#forms::BMGE (Criscuolo and Gribaldo, 2010), Maximum Likelihood Phylogeny with PhyMl, http://phylogeny.lirmm.fr/phylo_cgi/alacarte.cgi, (Dereeper *et al.*, 2008; Guindon *et al.*, 2010) calculating also approximate likelihood ratio tests (Anisimova and Gascuel, 2006). Tree drawing was done with Figtree (http://tree.bio.ed.ac.uk/software/figtree/). Coiled-coil prediction was carried out with http://toolkit.tuebingen.mpg.de/pcoils (Parry, 1982; Lupas *et al.*, 1991; Lupas, 1996). Conservation and putative functionality of individual PacX residues was calculated with

ConSurf, http://consurf.tau.ac.il/ (Ashkenazy *et al.*, 2010; Celniker *et al.*, 2013). Nuclear localization signals were searched with ngLCO http://genome.unmc.edu/ngLOC/index.html, (King and Guda, 2007) PSORT II, http://psort.hgc.jp/form2.html, (Nakao and Nakai, 2002), cNLS Mapper, http://nls-mapper.iab.keio.ac.jp/cgi-bin/NLS_Mapper_form.cgi, (Kosugi *et al.*, 2009) NetNes, http://www.cbs.dtu.dk/services/NetNES/ (La Cour *et al.*, 2004).

Microscopy and imaging techniques.

For PacX localization studies, the PacX::GFP HhoA::mCherry strain ALO2 was cultured at 28^{o}C in LabTek chambers (Rochester NY) containing WMM [watch minimal medium (Peñalva, 2005)], adjusted to acid or alkaline pH as described (Galindo *et al.*, 2007). Epifluorescence images were acquired with a Leica DMI6000 inverted optics microscope coupled to a Hamamatsu ORCA ERII camera, using Metamorph software (Molecular Devices) and SemrockBrightlinefilter sets for red and green fluorescence emission, essentially as described (Pantazopoulou and Peñalva, 2009; Pantazopoulou and Peñalva, 2011). Z-stacks of images were processed using the Metamorph 'unsharp' filter and, when needed, used to construct maximal intensity projections. Images were exported to Corel as TIFF maps.

Acknowledgements

This work was supported by the Wellcome Trust (Grants 067878 and 084660/Z/08/Z to HNA and JT), BBSRC studentships for JR and LR, Ministerio de Economía y Competitividad (Spain) Grants BIO2009-07281 and BIO2012-30965, and Comunidad de Madrid (grant S2010/BMD2414) to MAP and by grants to EMB from the Wellcome Trust (WT093596MA), the Medical Research Council (G0501164) and the BBSRC (BB/G009619/1). Daniel Lucena-Agell was holder of a FPI fellowship and work in EAE's laboratory is supported by grant BFU2012-33142 from the Spanish Ministerio de Economia y Competitividad. We thank Prof Michael Hynes for nkuAΔ::*bar*, Prof Berl Oakley for HhoA::mCherry, Prof Steve Osmani for gene tagging cassettes and the FGSC for *suA*1*palB*7 and *suD*2*palA*1 containing strains. We are grateful to Ade Akintade, Lily Stanton, Vicky Crome and Elena Reoyo for expert technical assistance. CS thanks Michel Flipphi for helpful discussion concerning the intron/exon organization of Fot1-like transposases.

References

Alkan, N., Meng, X., Friedlander, G., Reuveni, E., Sukno, S., Sherman, A. *et al.* (2013) Global aspects of *pacC* regulation of pathogenicity genes in *Colletotrichum gloeosporioides* as revealed by transcriptome analysis. *MPMI* **26**: 1345-1358.

Anisimova, M., and Gascuel, O. (2006) Approximate likelihood-ratio test for branches: A fast, accurate, and powerful alternative. *Syst Biol* **55**: 539-552.

Aréchiga-Carvajal, E.T., and Ruiz-Herrera, J. (2005) The *RIM101/pacC* homologue from the basidiomycete *Ustilago maydis* is functional in multiple pH-sensitive phenomena. *Eukaryotic Cell* **4**: 999-1008.

Arst, H.N., Jr., Bignell, E., and Tilburn, J. (1994) Two new genes involved in signalling ambient pH in *Aspergillus nidulans*. *Mol Gen Genet* **245**: 787-790.

Ashkenazy, H., Erez, E., Martz, E., Pupko, T., and Ben-Tal, N. (2010) ConSurf 2010: calculating evolutionary conservation in sequence and structure of proteins and nucleic acids. *Nucleic Acids Research* **38**: W529-W533.

Baek, Y.U., Martin, S.J., and Davis, D.A. (2006) Evidence for novel pH-dependent regulation of *Candida albicans* Rim101, a direct transcriptional repressor of the cell wall {beta}-glycosidase Phr2. *Eukaryot Cell* **5**: 1550-1559.

Barwell, K.J., Boysen, J.H., Xu, W., and Mitchell, A.P. (2005) Relationship of *DFG16* to the Rim101p pH response pathway in *Saccharomyces cerevisiae* and *Candida albicans*. *Eukaryot Cell* **4**: 890-899.

Beimforde, C., Feldberg, K., Nylinder, S., Rikkinen, J., Tuovila, H., Dörfelt,H. *et al.* (2014) Estimating the Phanerozoic history of the Ascomycota lineages: Combining fossil and molecular data. *Molecular Phylogenetics and Evolution* **78**: 386-398.

Bensen, E.S., Martin, S.J., Li, M., Berman, J., and Davis, D.A. (2004) Transcriptional profiling in *Candida albicans* reveals new adaptive responses to extracellular pH and functions for Rim101p. *Mol Microbiol* **54**: 1335-1351.

Bertuzzi, M., Schrettl, M., Alcazar-Fuoli, L., Cairns, T.C., Muñoz, A., Walker,L.A. *et al.* (2014) The pH-responsive PacC transcription factor of *Aspergillus fumigatus* governs epithelial entry and tissue invasion during pulmonary aspergillosis. *PLoS Pathog* **10**: e1004413.

Bignell, E., Negrete-Urtasun, S., Calcagno, A.M., Haynes, K., Arst, H.N., Jr., and Rogers, T. (2005) The *Aspergillus* pH-responsive transcription factor PacC regulates virulence. *Mol Microbiol* **55**: 1072-1084.

Blanchin-Roland, S. (2011) Identical domains of *Yarrowia lipolytica* Vps23 are required for both ESCRT and Rim pathways, but the latter needs an interaction between the Vps23 UEV domain and Rim8/PalF. *FEMS Yeast Research* **11**: 473-486.

Blanchin-Roland, S. (2013) Ambient pH signalling in *Yarrowia lipolytica*. In *Yarrowia lipolytica*, Microbiology Monographs 24. Barth, G. (ed) p. 121-144. Springer-Verlag Berlin Heidelberg.

Brody, H., Griffith, J., Cuticchia, A.J., Arnold, J., and Timberlake, W.E. (1991) Chromosome-specific recombinant DNA libraries from the fungus *Aspergillus nidulans*. *Nucleic Acids Res* **19**: 3105-3109.

Caddick, M.X., Brownlee, A.G., and Arst,H.N., Jr. (1986) Regulation of gene expression by pH of the growth medium in *Aspergillus nidulans*. *Mol Gen Genet* **203**: 346-353.

Calcagno-Pizarelli,A.M., Hervás-Aguilar, A., Galindo, A., Abenza, J.F., Peñalva, M.A., and Arst, H.N., Jr. (2011) Rescue of *Aspergillus nidulans* severely debilitating null mutations in ESCRT-0, I, II and III genes by inactivation of a salt-tolerance pathway allows examination of ESCRT gene roles in pH signalling. *J Cell Sci* **124**: 4064-4076.

Calcagno-Pizarelli, A.M., Negrete-Urtasun, S., Denison, S.H., Rudnicka, J.D., Bussink, H.J., Munéra-Huertas, T. *et al.* (2007) Establishment of the ambient pH signaling complex in *Aspergillus nidulans*: PalI assists plasma membrane localization of PalH. *Eukaryot Cell* **6**: 2365-2375.

Caracuel, Z., Roncero, M.I., Espeso, E.A., González-Verdejo, C.I., García-Maceira, F.I., and Di Pietro, P.A. (2003) The pH signalling transcription factor PacC controls virulence in the plant pathogen *Fusarium oxysporum*. *Mol Microbiol* **48**: 765-779.

Cecchetto, G., Amillis, S., Diallinas, G., Scazzocchio, C., and Drevet, C. (2004) The *AzgA* purine transporter of *Aspergillus nidulans*. Characterization of a protein belonging to a new phylogenetic cluster. *J Biol Chem* **279**: 3132-3141.

Celniker, G., Nimrod, G., Ashkenazy, H., Glaser, F., Martz, E., Mayrose, I. *et al.* (2013) ConSurf: using evolutionary data to raise testable hypotheses about protein function. *Isr J Chem* **53**: 199-206.

Cerqueira, G.C., Arnaud, M.B., Inglis, D.O., Skrzypek, M.S., Binkley, G., Simison, M. *et al.* (2014) The *Aspergillus* Genome Database: multispecies curation and incorporation of RNA-Seq data to improve structural gene annotations. *Nucleic Acids Research* **42 (Database issue)**: D705-D710.

Chinnici, J.L., Fu, C., Caccamise, L.M., Arnold, J.W., and Free, S.J. (2014) *Neurospora crassa* female development requires the PACC and other signal transduction pathways, transcription factors, chromatin remodeling, cell-to-cell fusion, and autophagy. *PLoS One* **9**: e110603.

Clutterbuck, A.J. (1993) *Aspergillus nidulans*. In Genetic Maps. Locus maps of complex genomes. O'Brien,S.J. (ed). 6th Ed., Vol. 3, p. 3.71-3.84. Cold Spring Harbor Laboratory Press, Cold Spring Harbor, NY.

Cornet, M., and Gaillardin, C. (2014a) pH signaling in human fungal pathogens: a new target for antifungal strategies. *Eukaryotic Cell* **13**: 342-352. Correction: *Eukaryotic Cell* **13:** 691.

Cove, D.J. (1966) The induction and repression of nitrate reductase in the fungus *Aspergillus nidulans*. *Biochim Biophys Acta* **113**: 51-56.

Cove, D.J. (1976) Chlorate toxicity in *Aspergillus nidulans*. Studies of mutants altered in nitrate assimilation. *Mol Gen Genet* **146**: 147-159.

Criscuolo, A., and Gribaldo, S. (2010) BMGE (Block Mapping and Gathering with Entropy): a new software for selection of phylogenetic informative regions from multiple sequence alignments. *BMC Evol Biol* **10**: 210.

Davis, D., Edwards, J.E., Jr., Mitchell, A.P., and Ibrahim, A.S. (2000a) *Candida albicans RIM101* pH response pathway is required for host-pathogen interactions. *Infect Immun* **68**: 5953-5959.

Davis, D., Wilson,R.B., and Mitchell,A.P. (2000b) *RIM101*-dependent and -independent pathways govern pH responses in *Candida albicans*. *Mol Cell Biol* **20**: 971-978.

Davis, D.A. (2009) How human pathogenic fungi sense and adapt to pH: the link to virulence. *Curr Opin Microbiol* **12**: 365-370.

Davis, D. (2003) Adaptation to environmental pH in *Candida albicans* and its relation to pathogenesis. *Curr Genet* **44**: 1-7. Erratum *Curr Genet* **44**:58.

Denison, S.H., Negrete-Urtasun, S., Mingot, J.M., Tilburn, J., Mayer, W.A., Goel, A. *et al.* (1998) Putative membrane components of signal transduction pathways for ambient pH regulation in *Aspergillus* and meiosis in *Saccharomyces* are homologous. *Mol Microbiol* **30**: 259-264.

Denison, S.H., Orejas, M., and Arst, H.N., Jr. (1995) Signaling of ambient pH in *Aspergillus* involves a cysteine protease. *J Biol Chem* **270**: 28519-28522.

Dereeper, A., Guignon, V., Blanc, G., Audic, S., Buffet, S., Chevenet, F. *et al.* (2008) Phylogeny.fr: robust phylogenetic analysis for the non-specialist. *Nucleic Acids Research* **36**: W465-W469.

Díez, E., Alvaro, J., Espeso, E.A., Rainbow, L., Suarez, T., Tilburn, J. *et al.* (2002) Activation of the *Aspergillus* PacC zinc finger transcription factor requires two proteolytic steps. *EMBO J* **21**: 1350-1359.

Dijkema, C., Rijcken, R.P., Kester, H.C.M., and Visser, J. (1986) 13C-NMR studies on the influence of pH and nitrogen source on polyol pool formation in *Aspergillus nidulans*. *FEMS Microbiology Letters* **33**: 125-131.

Dorn, G. (1965) Genetic analysis of the phosphatases in *Aspergillus nidulans*. *Genet Res* **10**: 13-26.

Eisendle, M., Oberegger, H., Buttinger, R., Illmer, P., and Haas, H. (2004) Biosynthesis and uptake of siderophores is controlled by the PacC-mediated ambient-pH regulatory system in *Aspergillus nidulans*. *Eukaryot Cell* **3**: 561-563.

Espeso, E.A., and Arst, H.N., Jr. (2000) On the mechanism by which alkaline pH prevents expression of an acid-expressed gene. *Mol Cell Biol* **20**: 3355-3363.

Espeso, E.A., and Peñalva, M.A. (1994) In vitro binding of the two-finger repressor CreA to several consensus and non-consensus sites at the *ipnA* upstream region is context dependent. *FEBS Lett* **342**: 43-48.

Espeso, E.A., and Peñalva, M.A. (1996) Three binding sites for the *Aspergillus nidulans* PacC zinc-finger transcription factor are necessary and sufficient for regulation by ambient pH of the isopenicillin N synthase gene promoter. *J Biol Chem* **271**: 28825-28830.

Espeso, E.A., Roncal, T., Díez, E., Rainbow, L., Bignell, E., Alvaro, J. *et al.* (2000) On how a transcription factor can avoid its proteolytic activation in the absence of signal transduction. *EMBO J* **19**: 719-728.

Fernández-Martínez, J., Brown, C.V., Díez, E., Tilburn, J., Arst, H.N., Jr., Peñalva, M. A., and Espeso, E.A. (2003) Overlap of nuclear localisation signal and specific DNA-binding residues within the zinc finger domain of PacC. *J Mol Biol* **334**: 667-684.

Fidel, S., Doonan, J.H., and Morris, N.R. (1988) *Aspergillus nidulans* contains a single actin gene which has unique intron locations and encodes a gamma-actin. *Gene* **70**: 283-293.

Galindo, A., Calcagno-Pizarelli, A.M., Arst, H.N., Jr., and Peñalva, M.A. (2012) An ordered pathway for the assembly of fungal ESCRT-containing ambient pH signalling complexes at the plasma membrane. *J Cell Sci* **125**: 1784-1795.

Galindo, A., Hervás-Aguilar, A., Rodríguez-Galán, O., Vincent, O., Arst, H.N., Jr., Tilburn, J., and Peñalva, M.A. (2007) PalC, one of two Bro1 domain proteins in the fungal pH signalling pathway, localizes to cortical structures and binds Vps32. *Traffic* **8**: 1346-1364.

Gomez-Raja, J., and Davis, D.A. (2012) The β-arrestin-like protein Rim8 is hyperphosphorylated and complexes with Rim21 and Rim101 to promote adaptation to neutral-alkaline pH. *Eukaryot Cell* **11**: 683-693.

Guindon, S., Dufayard, J.F., Lefort, V., Anisimova, M., Hordijk, W., and Gascuel, O. (2010) New algorithms and methods to estimate maximum-likelihood phylogenies: assessing the performance of PhyML 3.0. *Syst Biol* **59**: 307-321.

Herrador, A., Herranz, S., Lara, D., and Vincent, O. (2010) Recruitment of the ESCRT machinery to a putative seven-transmembrane-domain receptor is mediated by an arrestin-related protein. *Mol Cell Biol* **30**: 897-907.

Herrador, A., Livas, D., Soletto, L., Becuwe, M., Léon, S., and Vincent, O. (2015) Casein kinase 1 controls the activation threshold of an α-arrestin by multisite phosphorylation of the interdomain hinge. *Mol Biol Cell* **26**: 2128-2138.

Herranz, S., Rodríguez, J.M., Bussink, H.J., Sánchez-Ferrero, J.C., Arst, H.N., Jr., Peñalva, M.A., and Vincent, O. (2005) Arrestin-related proteins mediate pH signaling in fungi. *Proc Natl Acad Sci U S A* **102**: 12141-12146.

Hervás-Aguilar, A., Galindo, A., and Peñalva, M.A. (2010) Receptor-independent ambient pH signaling by ubiquitin attachment to fungal arrestin-like PalF. *J Biol Chem* **285**: 18095-18102.

Hervás-Aguilar, A., Rodríguez, J.M., Tilburn, J., Arst, H.N., Jr., and Peñalva, M.A. (2007) Evidence for the direct involvement of the proteasome in the proteolytic processing of the *Aspergillus nidulans* zinc finger transcription factor PacC. *J Biol Chem* **282**: 34735-34747.

Huang, W., Shang, Y., Chen, P., Gao, Q., and Wang, C. (2015) *MrpacC* regulates sporulation, insect cuticle penetration and immune evasion in *Metarhizium robertsii*. *Environ Microbiol* **17**: 994-1008.

Johnstone, I.L., Hughes, S.G., and Clutterbuck, A.J. (1985) Cloning an *Aspergillus nidulans* developmental gene by transformation. *EMBO J* **4**: 1307-1311.

Karlyshev, A.V., Pallen, M.J., and Wren, B.W. (2000) Single-primer PCR procedure for rapid identification of transposon insertion sites. *Biotechniques* **28**: 1078, 1080, 1082.

Katoh, K., and Standley, D.M. (2013) MAFFT multiple sequence alignment software version 7: improvements in performance and usability. *Mol Biol Evol* **30**: 772-780.

Ke, R., Haynes, K., and Stark, J. (2013) Modelling the activation of alkaline pH response transcription factor PacC in *Aspergillus nidulans*: involvement of a negative feedback loop. *J Theor Biol* **326**: 11-20.

King, B.R., and Guda, C. (2007) ngLOC: an n-gram-based Bayesian method for estimating the subcellular proteomes of eukaryotes. *Genome Biol* **8**: R68.

Kosugi, S., Hasebe, M., Tomita, M., and Yanagawa, H. (2009) Systematic identification of cell cycle-dependent yeast nucleocytoplasmic shuttling proteins by prediction of composite motifs. *Proc Natl Acad Sci U S A* **106**: 10171-10176.

La Cour, T., Kiemer, L., Mølgaard, A., Gupta, R., Skriver, K., and Brunak, S. (2004) Analysis and prediction of leucine-rich nuclear export signals. *Protein Eng Des Sel* **17**: 527-536.

Laemmli, U.K. (1970) Cleavage of structural proteins during the assembly of the head of bacteriophage T4. *Nature* **227**: 680-685.

Lamb, T.M., and Mitchell, A.P. (2003) The transcription factor Rim101p governs ion tolerance and cell differentiation by direct repression of the regulatory genes *NRG1* and *SMP1* in *Saccharomyces cerevisiae*. *Mol Cell Biol* **23**: 677-686.

Lamb, T.M., Xu, W., Diamond, A., and Mitchell, A.P. (2001) Alkaline response genes of *Saccharomyces cerevisiae* and their relationship to the *RIM101* pathway. *J Biol Chem* **276**: 1850-1856.

Lambert, M., Blanchin-Roland, S., Le,Louedec, F., Lepingle, A., and Gaillardin, C. (1997) Genetic analysis of regulatory mutants affecting synthesis of extracellular proteinases in the yeast *Yarrowia lipolytica*: identification of a *RIM101*/*pacC* homolog. *Mol Cell Biol* **17**: 3966-3976.

Landraud, P., Chuzeville, S., Billon-Grande, G., Poussereau,N., and Bruel, C. (2013) Adaptation to pH and role of PacC in the rice blast fungus *Magnaporthe oryzae*. *PLoS One* **8**: e69236.

Li Destri Nicosia, M.G., Brocard-Masson, C., Demais, S., Hua, V.A., Daboussi, M.J., and Scazzocchio, C. (2001) Heterologous transposition in *Aspergillus nidulans*. *Mol Microbiol* **39**: 1330-1344.

Li, M., Martin, S.J., Bruno, V.M., Mitchell, A.P., and Davis, D.A. (2004) *Candida albicans* Rim13p, a protease required for Rim101p processing at acidic and alkaline pHs. *Eukaryot Cell* **3**: 741-751.

Li, W., and Mitchell, A.P. (1997) Proteolytic activation of Rim1p, a positive regulator of yeast sporulation and invasive growth. *Genetics* **145**: 63-73.

Lucena-Agell, D., Galindo, A., Arst, H.N., Jr., and Peñalva, M.A. (2015) *Aspergillus nidulans* ambient pH signaling does not require endocytosis. *Eukaryot Cell* **14**: 545-553.

Lupas,A. (1996) Prediction and analysis of coiled-coil structures. *Methods Enzymol* **266**: 513-525.

Lupas,A., Van,D.M., and Stock,J. (1991) Predicting coiled coils from protein sequences. *Science* **252**: 1162-1164.

Maccheroni, W., Jr., May, G.S., Martinez-Rossi, N.M., and Rossi,A. (1997) The sequence of *palF*, an environmental pH response gene in *Aspergillus nidulans*. *Gene* **194**: 163-167.

MacPherson, S., Larochelle, M., and Turcotte, B. (2006) A fungal family of transcriptional regulators: the zinc cluster proteins. *Microbiol Mol Biol Rev* **70**: 583-604.

Marmorstein, R., Carey, M., Ptashne, M., and Harrison, S.C. (1992) DNA recognition by GAL4: structure of a protein-DNA complex. *Nature* **356**: 408-414.

Marmorstein, R., and Harrison, S.C. (1994) Crystal structure of a PPR1-DNA complex: DNA recognition by proteins containing a Zn2Cys6 binuclear cluster. *Genes Dev* **8**: 2504-2512.

Mingot, J.M., Espeso, E.A., Díez, E., and Peñalva, M.A. (2001) Ambient pH signaling regulates nuclear localization of the *Aspergillus nidulans* PacC transcription factor. *Mol Cell Biol* **21**: 1688-1699.

Mingot, J.M., Tilburn, J., Díez, E., Bignell, E., Orejas, M., Widdick, D.A. *et al.* (1999) Specificity determinants of proteolytic processing of *Aspergillus PacC* transcription factor are remote from the processing site, and processing occurs in yeast if pH signalling is bypassed. *Mol Cell Biol* **19**: 1390-1400.

Moreno-Mateos,M.A., Delgado-Jarana,J., Codón,A.C., and Benítez,T. (2007) pH and Pac1 control development and antifungal activity in *Trichoderma harzianum*. *Fungal Genet Biol* **44**: 1355-1367.

Nakao, N.C., and Nakai, K. (2002) Improvement of PSORT II Protein Sorting Prediction for Mammalian Proteins. *Genome Informatics* **13**: 441-442.

Negrete-Urtasun, S., Denison, S.H., and Arst, H.N., Jr. (1997) Characterization of the pH signal transduction pathway gene *palA* of *Aspergillus nidulans* and identification of possible homologs. *J Bacteriol* **179**: 1832-1835.

Negrete-Urtasun, S., Reiter, W., Díez, E., Denison, S.H., Tilburn, J., Espeso, E.A. *et al.* (1999) Ambient pH signal transduction in *Aspergillus*: completion of gene characterization. *Mol Microbiol* **33**: 994-1003.

Nierman, W.C., Pain, A., Anderson, M.J., Wortman, J.R., Kim, H.S., Arroyo, J. *et al.* (2005) Genomic sequence of the pathogenic and allergenic filamentous fungus *Aspergillus fumigatus*. *Nature* **438**: 1151-1156.

Nobile, C.J., Solis, N., Myers, C.L., Fay, A.J., Deneault, J.S., Nantel, A. *et al.* (2008) *Candida albicans* transcription factor Rim101 mediates pathogenic interactions through cell wall functions. *Cell Microbiol* **10**: 2180-2196.

O'Meara, T.R., Norton, D., Price, M.S., Hay, C., Clements, M.F., Nichols, C.B., and Alspaugh, J.A. (2010) Interaction of *Cryptococcus neoformans* Rim101 and protein kinase A regulates capsule. *PLoS Pathog* **6**: e1000776.

O'Meara, T.R., Xu, W., Selvig, K.M., O'Meara, M.J., Mitchell, A.P., and Alspaugh, J.A. (2014) The *Cryptococcus neoformans* Rim101 transcription factor directly regulates genes required for adaptation to the host. *Mol Cell Biol* **34**: 673-684.

Obara, K., and Kihara, A. (2014) Signaling events of the Rim101 pathway occur at the plasma membrane in a ubiquitination-dependent manner. *Mol Cell Biol* **34**: 3525-3534.

Olszewska, A., Krol, K., Weglenski, P., and Dzikowska, A. (2007) Arginine catabolism in *Aspergillus nidulans* is regulated by the *rrmA* gene coding for the RNA-binding protein. *Fungal Genet Biol* **44**: 1285-1297.

Orejas, M., Espeso, E.A., Tilburn, J., Sarkar, S., Arst, H.N., Jr., and Peñalva, M.A. (1995) Activation of the *Aspergillus* PacC transcription factor in response to alkaline ambient pH requires proteolysis of the carboxy-terminal moiety. *Genes Dev* **9**: 1622-1632.

Osmani, S.A., Pu, R.T., and Morris, N.R. (1988) Mitotic induction and maintenance by overexpression of a G2-specific gene that encodes a potential protein kinase. *Cell* **53**: 237-244.

Ost, K.S., O'Meara, T.R., Huda, N., Esher, S.K. and Alspaugh, J.A. (2015) *The Cryptococcus neoformans* alkaline response pathway: identification of a novel Rim pathway activator. *PLoS Genet* **11:** e1005159.

Pantazopoulou, A., and Peñalva, M.A. (2009) Organization and dynamics of the *Aspergillus nidulans* Golgi during apical extension and mitosis. *Mol Biol Cell* **20**: 4335-4347.

Pantazopoulou, A., and Peñalva, M.A. (2011) Characterization of *Aspergillus nidulans* RabC/Rab6. *Traffic* **12**: 386-406.

Parry, D.A. (1982) Coiled-coils in alpha-helix-containing proteins: analysis of the residue types within the heptad repeat and the use of these data in the prediction of coiled-coils in other proteins. *Biosci Rep* **2:** 1017-1024 .

Peñalva, M.A. (2005) Tracing the endocytic pathway of *Aspergillus nidulans* with FM4-64. *Fungal Genet Biol* **42**: 963-975.

Peñalva, M.A., and Arst, H.N., Jr. (2004) Recent advances in the characterization of ambient pH regulation of gene expression in filamentous fungi and yeasts. *Annu Rev Microbiol* **58**: 425-451.

Peñalva, M.A., Lucena-Agell, D., and Arst, H.N., Jr. (2014) Liaison alcaline: Pals entice non-endosomal ESCRTs to the plasma membrane for pH signaling. *Curr Opin Microbiol* **22**: 49-59.

Peñalva, M.A., Tilburn, J., Bignell, E., and Arst, H.N., Jr. (2008) Ambient pH gene regulation in fungi: making connections. *Trends Microbiol* **16**: 291-300.

Peñas, M.M., Hervás-Aguilar, A., Munéra-Huertas, T., Reoyo, E., Peñalva, M.A., Arst, H.N., Jr., and Tilburn, J. (2007) Further characterization of the signaling proteolysis step in the *Aspergillus nidulans* pH signal transduction pathway. *Eukaryot Cell* **6**: 960-970.

Perez-Esteban, B., Orejas, M., Gomez-Pardo, E., and Peñalva, M.A. (1993) Molecular characterization of a fungal secondary metabolism promoter: transcription of the *Aspergillus nidulans* isopenicillin N synthetase gene is modulated by upstream negative elements. *Mol Microbiol* **9**: 881-895.

Pokorska,A., Drevet,C., and Scazzocchio,C. (2000) The analysis of the transcriptional activator PrnA reveals a tripartite nuclear localisation sequence. *J Mol Biol* **298**: 585-596.

Porta, A., Ramon, A.M., and Fonzi, W.A. (1999) PRR1, a homolog of *Aspergillus nidulans palF*, controls pH-dependent gene expression and filamentation in *Candida albicans*. *J Bacteriol* **181**: 7516-7523.

Prieto, M., and Wedin, M. (2013) Dating the diversification of the major lineages of Ascomycota (Fungi). *PLoS One* **8**: e65576.

Ramon, A.M., Porta, A., and Fonzi, W.A. (1999) Effect of environmental pH on morphological development of *Candida albicans* is mediated via the PacC-related transcription factor encoded by *PRR2*. *J Bacteriol* **181**: 7524-7530.

Rodríguez-Galán, O., Galindo, A., Hervás-Aguilar, A., Arst, H.N., Jr., and Peñalva, M.A. (2009) Physiological involvement in pH signaling of Vps24-mediated recruitment of *Aspergillus* PalB cysteine protease to ESCRT-III. *J Biol Chem* **284**: 4404-4412.

Rothfels, K., Tanny, J.C., Molnar, E., Friesen, H., Commisso, C., and Segall, J. (2005) Components of the ESCRT pathway, DFG16, and YGR122w are required for Rim101 to act as a corepressor with Nrg1 at the negative regulatory element of the *DIT1* gene of *Saccharomyces cerevisiae*. *Mol Cell Biol* **25**: 6772-6788.

Ruiz, A., and Ariño, J. (2007) Function and regulation.of the *Saccharomyces cerevisiae* ENA sodium ATPase system: *Eukaryot Cell* **6**: 2175-2183.

Sambrook, J., Fritsch, E.F. and Maniatis, T. (1989) *Molecular Cloning: A Laboratory Manual.* 2nd edition. Cold Spring Harbour Laboratory Press. Cold Spring Harbor, NY.

Scazzocchio, C. (2015) Fungal biology in the post-genomic era. *Fungal Biology and Biotechnology* **1**: 7.

Schjerling, P., and Holmberg, S. (1996) Comparative amino acid sequence analysis of the C6 zinc cluster family of transcriptional regulators. *Nucleic Acids Res* **24**: 4599-4607.

Schoch, C.L., Sung, G.H., López-Giráldez, F., Townsend, J.P., Miadlikowska, J., Hofstetter, V. *et al.* (2009) The Ascomycota Tree of Life: A Phylum-wide Phylogeny Clarifies the Origin and Evolution of Fundamental Reproductive and Ecological Traits. *Systematic Biology* **58**: 224-239.

Selvig, K., and Alspaugh, J.A. (2011) pH Response Pathways in Fungi: Adapting to Host-derived and Environmental Signals. *Mycobiology* **39**: 249-256.

Serrano, R., Ruiz, A., Bernal, D., Chambers, J.R., and Ariño, J. (2002) The transcriptional response to alkaline pH in *Saccharomyces cerevisiae*: evidence for calcium-mediated signalling. *Mol Microbiol* **46**: 1319-1333.

Stimpson, H.E., Lewis, M.J., and Pelham, H.R. (2006) Transferrin receptor-like proteins control the degradation of a yeast metal transporter. *EMBO J* **25**: 662-672.

Strich, R., Surosky, R.T., Steber, C., Dubois, E., Messenguy, F., and Esposito, R.E. (1994) *UME6* is a key regulator of nitrogen repression and meiotic development. *Genes Dev* **8**: 796-810.

Su, S.S., and Mitchell, A.P. (1993a) Identification of functionally related genes that stimulate early meiotic gene expression in yeast. *Genetics* **133**: 67-77.

Su, S.S., and Mitchell, A.P. (1993b) Molecular characterization of the yeast meiotic regulatory gene *RIM1*. *Nucleic Acids Res* **21**: 3789-3797.

Suarez, T., de Queiroz, M.V., Oestreicher, N., and Scazzocchio, C. (1995) The sequence and binding specificity of UaY, the specific regulator of the purine utilization pathway in *Aspergillus nidulans*, suggest an evolutionary relationship with the PPR1 protein of *Saccharomyces cerevisiae*. *EMBO J* **14**: 1453-1467.

Tilburn, J., Sarkar, S., Widdick, D.A., Espeso, E.A., Orejas, M., Mungroo, J. *et al.* (1995) The *Aspergillus* PacC zinc finger transcription factor mediates regulation of both acid- and alkaline-expressed genes by ambient pH. *EMBO J* **14**: 779-790.

Todd, R.B., and Andrianopoulos, A. (1997) Evolution of a fungal regulatory gene family: the Zn(II)2Cys6 binuclear cluster DNA binding motif. *Fungal Genet Biol* **21**: 388-405.

Trushina, N., Levin, M.F., Mukherjee, P.K., and Horwitz,B.A. (2013) PacC and pH-dependent transcriptome of the mycotrophic fungus *Trichoderma virens*. *BMC Genomics* **14**: 138.

Viladevall, L., Serrano, R., Ruiz, A., Domenech, G., Giraldo, J., Barceló, A., and Ariño, J. (2004) Characterization of the calcium-mediated response to alkaline stress in *Saccharomyces cerevisiae*. *J Biol Chem* **279**: 43614-43624.

Vincent, O., Rainbow, L., Tilburn, J., Arst, H.N., Jr., and Peñalva, M.A. (2003) YPXL/I is a protein interaction motif recognized by *Aspergillus* PalA and its human homologue, AIP1/Alix. *Mol Cell Biol* **23**: 1647-1655.

Wang, Q., and Szaniszlo, P.J. (2009) Roles of the pH signaling transcription factor PacC in *Wangiella (Exophiala) dermatitidis*. *Fungal Genet Biol* **46**: 657-666.

Wheeler, K.A., Hurdman, B.F., and Pitt, J.I. (1991) Influence of pH on the growth of some toxigenic species of *Aspergillus*, *Penicillium* and *Fusarium*. *International Journal of Food Microbiology* **12**: 141-149.

Whiteway, M., Dignard, D., and Thomas, D.Y. (1992) Dominant negative selection of heterologous genes: isolation of *Candida albicans* genes that interfere with *Saccharomyces cerevisiae* mating factor-induced cell cycle arrest. *Proc Natl Acad Sci U S A* **89**: 9410-9414.

Xu,W., and Mitchell,A.P. (2001) Yeast PalA/AIP1/Alix homolog Rim20p associates with a PEST-like region and is required for its proteolytic cleavage. *J Bacteriol* **183**: 6917-6923.

Xu,W., Smith,F.J., Jr., Subaran,R., and Mitchell,A.P. (2004) Multivesicular body-ESCRT components function in pH response regulation in *Saccharomyces cerevisiae* and *Candida albicans*. *Mol Biol Cell* **15**: 5528-5537.

Yang,L., Ukil,L., Osmani,A., Nahm,F., Davies,J., De Souza,C.P. *et al.* (2004) Rapid production of gene replacement constructs and generation of a green fluorescent protein-tagged centromeric marker in *Aspergillus nidulans*. *Eukaryot Cell* **3**: 1359-1362.

Zhou, Y.H., Hou,L., Zhang,Y.J., Fan,Y.H., Luo,Z.B., Jin,D. *et al*. (2014) Expression and promoter characterization of BbPacC, a pH response transcription factor gene of the entomopathogenic fungus *Beauveria bassiana*. *Microbiology* **160**: 353-361.

Zou,C.G., Tu,H.H., Liu,X.Y., Tao,N., and Zhang,K.Q. (2010) PacC in the nematophagous fungus *Clonostachys rosea* controls virulence to nematodes. *Environ Microbiol* **12**: 1868-1877.

Table 1. *pacX* mutations isolated in this work.

ALLELE	NUCLEOTIDE CHANGE	PROTEIN CHANGE	MUTAGEN	SELECTION	REFERENCE
LARGE INSERTIONS OR DUPLICATION					
*pacX*12[a]	T-516*ins*Impala	PPI	none	growth at pH 7.5	This work
*pacX*18[a]	T667*ins*Fot1-like transposon	PSD	none	growth at pH 8.0	This work
*pacX*24[b]	T-297*ins*(C-296-T878)	N275fs, PPI	none	growth at pH 8.0	This work
TRUNCATING MUTATIONS					
*pacX*3503[i]	A35*ins*G25-A37	G12fs	none	growth at pH 8.0	This work
*pacX*20[a]	C133T	R44stop	none	growth at pH 8.0	This work
*pacX*28[a]	C180GG	P60fs	none	growth at pH 7.5	This work
*pacX*8[a]	ΔC190	I63fs	UV	growth at pH 8.0	This work
*pacX*13[a]	ΔG(241-243)	G81fs	none	growth at pH 8.0	This work
*pacX*26[a]	G314-316*ins*G	R105fs	none	growth at pH 8.0	This work
*pacX*34[c]	G331T	H110stop	none	growth at pH 8.0	This work
*pacX*19[b]	(T359-G364)A	W199fs	none	growth at pH 8.0	This work
*pacX*33[a]	A379-A385*ins*A	K127fs	none	growth at pH 7.5	This work
*pacX*3501[i]	ΔA445-A449	Y148fs	none	growth at pH 8.0	This work
*pacX*3502[i]	ΔC505	M168fs	none	growth at pH 8.0	This work
*pacX*27[a]	G554T	D181stop	none	growth at pH 7.5	This work
*pacX*31[a]	C687T	R211stop	none	growth at pH 7.5	This work
*pacX*4[d]	(C942-944)*ins*C	P297fs	NQO	growth at pH 8.0	Denison and Arst, unpublished
*pacX*2[e] (*su*A1*pal*B7)	ΔG945	G299fs	none	alkaline phosphatase	(Dorn, 1965)
*pacX*15[a]	(G945-951)*ins*G	G299fs	none	growth at pH 8.0	This work
*pacX*3511[i]	(G945-951)*ins*G	G299fs	none	growth at pH 8.0	This work
*pacX*3506[i]	A951*ins*GGAGAAG	G299GKfs	none	growth at pH 8.0	This work
*pacX*1[a]	ΔC957, ΔC958	A301fs	UV	growth at pH 8.0	This work
*pacX*3512[i]	ΔT(108 -1090)	F345fs	none	growth at pH 8.0	This work
*pacX*3513[i]	G1128*ins*C1121-G1128	Y347fs	none	growth at pH 8.0	This work
*pacX*5[d]	ΔG1250	A399fs	NQO	growth at pH 8.0	Denison and Arst, unpublished
*pacX*6[d]	ΔCG (1340,- 1345)	A430fs	NQO	growth at pH 8.0	Denison and Arst, unpublished
*pacX*25[a]	ΔT1391	D246fs	none	growth at pH 8.0	This work
*pacX*14[a]	ΔG1393	R447fs	none	growth at pH 8.0	This work
*pacX*32[a]	ΔC(1526-1529)	P492fs	none	growth at pH 7.5	This work
*pacX*3508[i]	ΔC(1526-1529)	P492fs	none	growth at pH 8.0	This work
*pacX*3509[i]	G1530insA	P492Sfs	none	growth at pH 8.0	This work
*pacX*3507[i]	ΔC1571, ΔA1572	S506fs	none	growth at pH 8.0	This work
MISSENSE MUTATIONS					
*pacX*3[f] (*suD*2*palA*1)	C130T	R44W (ef)	none	alkaline phosphatase	Dorn*
*pacX*16[a]	T248C	L83P (bs)	none	growth at pH 8.0	This work

*pacX*21[a]	C310A	P104T (ef)	none	growth at pH 8.0	This work
*pacX*23[a]	G357T	W119C (bs)	none	growth at pH 8.0	This work
*pacX*17[a]	ΔG458-G460	(R153, (ef) V154L)(bs)	none	growth at pH 8.0	This work
*pacX*3505[i]	G679C	R209P (ef)	none	growth at pH 8.0	This work
*pacX*22[a]	G700C	R216P (ef)	none	growth at pH 8.0	This work
*pacX*9[g]	G715C	R221P (ef)	NQO	growth at pH 8.0	Denison and Arst, unpublished
*pacX*11[h]	C721G	A223G (ef)	none	none	This work
*pacX*7[a]	C1384T	P444L (ef)	none	molybdate resistance	This work
*pacX*30[a]	G1396T	C448F (bs)	none	growth at pH 7.5	This work
*pacX*29[a]	G1468T	C472F (bs)	none	growth at pH 7.5	This work
*pacX*10[h]	P1470C	S473P (ef)	UV	molybdate resistance	Akintade and Tilburn, unpublished

Mutation isolated as suppressor of: [a] *pacC*$^{+/-}$20205, (Díez *et al.*, 2002), [b] *pacC*$^{+/-}$ 207 (Vincent *et al.*, 2003), [c] *palF*58 (Arst *et al.*, 1994), [d] *palI*30 (Denison *et al.*, 1998c), [e] *palB*7 (Dorn, 1965; Peñas *et al.*, 2007), [f] *palA*1 (Dorn, 1965), [g] *palI*49 (Arst *et al.*, 1994; Denison *et al.*, 1998b), [h] *pacC*209 (Díez *et al.*, 2002), [I] *pacC*900^{L498S} (Peñas *et al.*, 2007). [i] mutations were isolated in *pacX*35 which is an S-tagged *pacX*$^{+}$ allele (PacX::4GA::S-tag, see **Experimental Procedures**). PPI, predicted promoter insertion; PSD, predicted splicing defect. The ConSurf (http://consurf.tau.ac.il/) predictions for substituted residues are given in parentheses: ef, exposed and functional; bs, buried and structural. See **Experimental Procedures** for media. *pacX*11 arose spontaneously in strain *pacC*$^{+/-}$209 *pantoB*100 (L186) on storage. Dorn*, Dorn http://fgsc.net/Archive/nid.html

Table 2. Modified and unmodified *pacC* allele phenotypes

pacC allele	Phenotype	PacC mutant protein (unprocessed form)	Effect of *pacX*⁻ in double mutant
MODIFIED PHENOTYPE			
pacC$^{+/-}$207 [b]	acidity mimicry	Y455N	Suppression
pacC$^{+/-}$209 [b]	acidity mimicry	L498S	Suppression
pacC$^{+/-}$210 [b]	acidity mimicry	L498F	Suppression
pacC$^{+/-}$20205 [b,*]	acidity mimicry	5 - 464 IDRPGSPL 541 - 678	Suppression
pacC^{c}39 [b]	weak alkalinity mimicry	L266F	Additivity
pacC^{c}234 [b]	weak alkalinity mimicry	L340F	Additivity
pacC^{c}20042 [b]	weak alkalinity mimicry	R579T	Additivity
pacC$^{+/-}$20002 [b]	acidity mimicry	Q155K	Enhanced loss-of -function phenotype
pacC$^{c/-}$20000 [c]	neutrality mimicry	5 - 251 + 5	Additivity
alcA^{p}::PacC5-252 [a]	alkalinity mimicry	5 - 252	Increased toxicity
NO MODIFICATION OF PHENOTYPE			
pacC⁻Δ::*Ncpyr4* [a]	null		
pacC⁻6310 [c]	null	5 - 163	
pacC$^{+/-}$7604 [b]	acidity mimicry	5 - 173 + 9	
pacC$^{+/-}$230 [c]	acidity mimicry	5 - 238	
pacC^{c}700 *pacC*$^{+/-}$70001 [c]	acidity mimicry	GFP::5-250 K159M	
pacC$^{c/-}$20601 [c]	neutrality mimicry	5 - 260	
pacC^{c}50 [c]	alkalinity mimicry	5 - 266	
pacC$^{+/-}$206 [c]	acidity mimicry	5 – 310	
pacC^{c}69 [b]	alkalinity mimicry	L340S	
pacC$^{+/-}$7601 [c]	acidity mimicry	5 - 379	
pacC^{c}504, *pacC*5 [b]	weak neutrality mimicking	1 - 523	

The *pacX* allele is indicated after the *pacC* allele number: [a] *pacX*20, [b] *pacX*1, [c] *pacX*3.
[*]The *pacC*$^{+/-}$20205 allele also includes *pacC*^{c}202.

Legends

Fig. 1. *pacC* is an alkaline-expressed gene due to derepression resulting from depletion of PacC^{72} rather than activation by PacC^{27} upon alkalinization. (A and B) Northern blots of total RNA probed with P^{32}-(A)and DIG- (B) labelled *pacC* specific probes prepared with primers TILREV and 1217FF (A) and 850U and 1217FF (B) and methylene blue stained rRNA as loading controls. The mycelia were grown overnight in acidic medium and transferred to alkaline medium for the times indicated. 'Drop out' medium and MFA were used in (A) and (B), respectively. *pacC*$^{-}$6309 is a null allele which can specify only residues 1-4 (Fernández-Martínez *et al.*, 2003). The wild type *pacC* allele used in (A) was *pacC*900 which encodes a 3 x MYC tag at the amino-terminus (Peñas *et al.*, 2007), hence the reduced mobility of the transcripts relative to those of *pacC*$^{-}$6309, which differ from wild type in only a few nucleotides. Comparing the 90 min time points for the two strains suggests that *pacC*$^{-}$6309 transcript levels are not fully derepressed; however, this might be due to reduced transcript stability of *pacC*$^{-}$6309 mRNA, for instance, through nonsense-mediated decay. (B) *pacC*$^{-}$6309 transcript is used as a reporter of *pacC* gene expression to observe the effects of PacC^{72} (*gpdA*^{mini}::GFP::PacC5-678 in acidic medium (H^{+})) and PacC^{27} (*gpdA*^{mini}::GFP::PacC5-251) on *pacC* gene expression. The *gpdA*^{mini}::GFP::PacC strains contain the *trans* genes at *pyroA*. *gpdA*^{mini} is a moderate strength, constitutive promoter derived from the glyceraldehyde 3-phosphate dehydrogenase (*gpdA*) promoter as described by Pantazopoulou and Peñalva (2009). Strains J2402 *pabaA*1 *pyroA*4 *pacC*$^{-}$6309, J2422 and J2427 (**Experimental Procedures**) were used.

Fig. 2. Western blots illustrating PacC processing. (A) pH signalling proteolysis occurs rapidly after alkalinization and, (B) becomes rate limiting in PacC processing after one and a half to two hours. (A) and (B) Mycelia were grown in acidic media and transferred to alkaline media for the times shown. A *pacC*900 [MYC3-PacC, (Peñas *et al.*, 2007)] strain MAD2352 *wA*4 *pyroA*4 *inoB*2 *palF*500 *pyrG*89 *nkuA*Δ::bar *pacC*900 was used. [*palF*500 is *palF*::HA3::*pyrGfum*, a *palF*$^{+}$ tagged allele (Hervás-Aguilar *et al.*, 2010)

Fig. 3. *palF* is an acid expressed gene and its over-expression results in alkalinity mimicry. (A and B) Northern blots of total RNA probed with P^{32} labelled *palF*-specific probe. Methylene blue stained rRNA is a loading control. Strains were grown in MFA derived media either in steady-state conditions at the pH values shown (A) or shifted from pH 4.3 (H^{+}) to pH 8.3 (OH^{-}) for up to six hours (B). Northerns show that *palF* is preferentially expressed under acidic growth conditions and in the acidity mimicking strains carrying *pacC*$^{-}$6309, *palB*38 and *pacC*$^{+/-}$209 as compared with in the wild type and the alkalinity mimicking *pacC*^{c}14strains (A) and that *palF* transcript levels quickly fall on shifting from acidic to alkaline growth conditions (B). In (C) progeny from a cross of an *argB*2 (arginine requiring) strain carrying *pacC*900 [MYC_3-tagged *pacC*$^{+}$ (Peñas *et al.*, 2007)] [*pabaA*1 *yA*2 *pyrG*89 *argB*2 *pacC*900 (MP12)] and a strain carrying *alcA*^{p}::*palF*::*argB*$^{+}$ containing the *palF* over-expressing cassette driven by the alcohol-inducible alcohol dehydrogenase promoter and integrated at *argB* to restore arginine prototrophy [*alcA*^{p}::*palF*::*argB*$^{+}$ *pantoB*100 (JR110)] are shown. Position 21 *argB*2 *pacC*900 (MP12), position 25 *alcA*^{p}::*palF*::*argB*$^{+}$(JR110), position 26 *biA*1 wildtype strain. (Ci) acid phosphatase stain (Acid phos) on minus phosphate medium containing 1% glucose pH 6.5, (Cii) acid phosphatase stain on minus phosphate medium containing 1% ethanol as carbon source pH 6.5 and (Ciii) synthetic complete

glucose medium minus arginine. *pacC*^{c}14 and *pacC*^{c}50, which are strong and moderate *pacC* constitutive alleles, respectively, are shown below the acid phosphatase plates. Comparison of panels ii and iii demonstrates co-segregation of arginine prototrophy and reduced acid phosphatase levels under *alcA*^{p} inducing (*palF* over-expression) conditions. (D) Suppression of *palB*524 by *palF* over-expression. Acid phosphatase stained colonies are shown after growth on minus phosphate medium containing 1% glucose (G) or 1% ethanol (E). Repressed levels of acid phosphatase are restored in the *palB*524 *argB*$^{+}$::*alcA*^{p}::*palF* progeny after growth on ethanol. *palB*524 is a leaky loss of function allele described by Peñas *et al*,(2007). The genotype of the *palB*524 *argB*$^{+}$::*alcA*^{p}::*palF* progeny was checked by sequencing to confirm the *palB*524 mutation and southern blot analysis to confirm the presence of the over-expression cassette. (E) Western blot comparing PalF levels and PacC processing in shifted strains containing endogenously or constitutively (*gpdA*^{mini}) expressed *palF* shows that elevated PalF levels correlate with increased PacC processing and that attenuation of the pH signal, manifest by accumulation of PacC^{72} with time after shifting, is almost completely removed when *palF* is over-expressed from the heterologous (*gpdA*^{mini}) promoter. Strains MAD2352 and MAD4500 were used. (F) Petri dish assays show the alkalinity mimicking phenotype of *gpdA*^{mini}::GFP::PalF (TM280) as compared to a wild-type (*biA*1) strain with respect to molybdate resistance and reduced acid phosphatase staining. The *pyroA*4 *palF*15 recipient strain (TM261) is also shown. The full genotypes of the strains are described in **Experimental Procedures**.

Fig. 4. Suppression of *pal*$^{-}$ and *pacC*$^{+/-}$20205 mutations by *pacX*1. Petri dish assays of typical strains following 48 hours' growth on synthetic complete medium containing 25 mM sodium molybdate

($MoO_4^{=}$), 1 mg ml^{-1} neomycin sulphate (Neomycin), pH 8.0 medium (pH 8.0) and phosphatase staining following 24 hours' growth on minus phosphate medium at the pH values shown, followed by staining for alkaline or acid phosphatase (Alk phos or Acid phos), are shown.

Fig. 5. *pacX*$^{-}$ mutations result in derepressed expression of *pacC*. (A and B) Northern blots of total RNA are shown. (A) The *pac*C transcript was detected amongst RNA from a variety of strains grown at neutral pH, pH ~6.5, using a ^{32}P-labelled 1041 bp *pacC* specific fragment which had been generated by PCR using the primers BIGFF and TILREV (Table S1). Mycelia were grown for 14 hours in shaken minimal medium, containing 1% glucose as sole carbon source and 10 mM 2-(*N*-morpholino)ethanesulphonic acid, at 30ºC. Loading controls were established using a 650 bp *Nco*I-*Nco*I fragment from the *Aspergillus nidulans* actin gene (Fidel *et al.*, 1988). (B) Strains were grown overnight (~14 h) at 37^{o}C with shaking in acidic MFA and transferred to alkaline MFA for the times shown. Methylene blue stained 18S rRNAs are included as loading controls. *pacX*$^{+}$, *yA*2 *pabaA*1 *pacC*900 (J2153) and *pacX*20, *yA*2 *pabaA*1 *pacC*900 *pacX*20 (X900A) strains were used. (C) Western blots of cell lysates. The 3 x MYC tagged *pacC*$^{+}$ allele (*pacC*900) was carried by all strains (Peñas *et al*., 2007). The strains were pre-grown in acidic media and transferred to alkaline media for the times indicated. *pacX*$^{+}$, *pyroA*4 *pacC*900 (MAD3877); *pacX*20, *yA*2 *pabaA*1 *pacX*20 *pacC*900 (MAD1652); *palB*38, *inoB*2 *palB*38 *pacC*900 (MAD1362) and *palB*38 *pacX*20, *pacC*900 *pantoB*100 *pacX*20 *palB*38 (MAD4777) strains were used.

Fig. 6. Features of PacX and its homologues**.** A. A scheme illustrates features of *A. nidulans* PacX. Portions of an alignment containing the coiled-coil and zinc binuclear cluster regions are shown. The

alignment features selected homologues with different degrees of divergence from *A. nidulans* PacX, *Aspergillus fumigatus, Cochliobolus heterostrophus, Mycosphaerella graminicola* (now designated *Zymoseptoria tritici*), *Botrytis cinerea* and *Neurospora crassa*. The accession numbers are shown in Fig. S6. Arrows indicate the positions of the coiled-coil regions above the alignment for *A. nidulans* and below the alignment for *N. crassa*. The line indicates a putative nuclear export signal (NES) in the *A. nidulans* PacX. NLS indicates a bipartite nuclear localization signal, which contains a shorter monopartite NLS. A putative NES is indicated within the coiled-coil in white. Putative zinc chelating residues of the zinc binuclear cluster are indicated with boxes. B. Fungal phyla which contain PacX homologues are indicated with black lettering: those which apparently do not are indicated in grey.

Fig. 7. Sub-nuclear localization of PacX. (A) Image of a hyphal tip cell co-expressing PacX-GFP and HhoA::mCherry (histone 1) to label chromatin. DIC, Nomarski optics. (B) Top, individual planes of a z-stack of images, acquired with the indicated Z-distance. Bottom, maximal intensity projection (MIP) of the above stack and orthogonal [(X, Z) and (Y, Z)] views across the indicated lines. All images were captured from cells cultured in acidic medium. Exposure to alkaline media for 60 min did not alter this PacX sub-nuclear localization pattern.

Fig. 8. Model summarising currently available data on regulation of the pH response. The fine lines indicate that it is a minor proportion of $PacC^{72}$ that exists in an open conformation and is therefore susceptible to Pal independent processing. The dotted lines indicate that it is unclear whether

transcriptional repression of *palF* is mediated by PacC[53] or PacC[27] and whether such repression is direct or indirect.

Fig. 9. *pacX*20 suppresses *palA*1 when *pacC* is expressed from a heterologous promoter. The *trans* gene expressing PacC residues 5 to 678, corresponding to the wild type allele, from the ethanol-inducible alcohol dehydrogenase promoter, *alcA*^{p}::PacC5-678 is integrated at *argB* in a *pacC*Δ*Ncpyr4* background (Mingot *et al.*, 1999). Strains are wild type HB81 *pantoB*100, *alcA*^{p}::PacC5-678 *palA*1 *pacC*Δ (9-1), *alcA*^{p}::PacC5-678 *palA*1 *pacX*20 *pacC*Δ (9-21), *alcA*^{p}::PacC5-678 *pacC*Δ (9-17) and full geneotypes of the *trans* gene strains are given in **Experimental Procedures**. Lithium chloride was added to 300 mM.

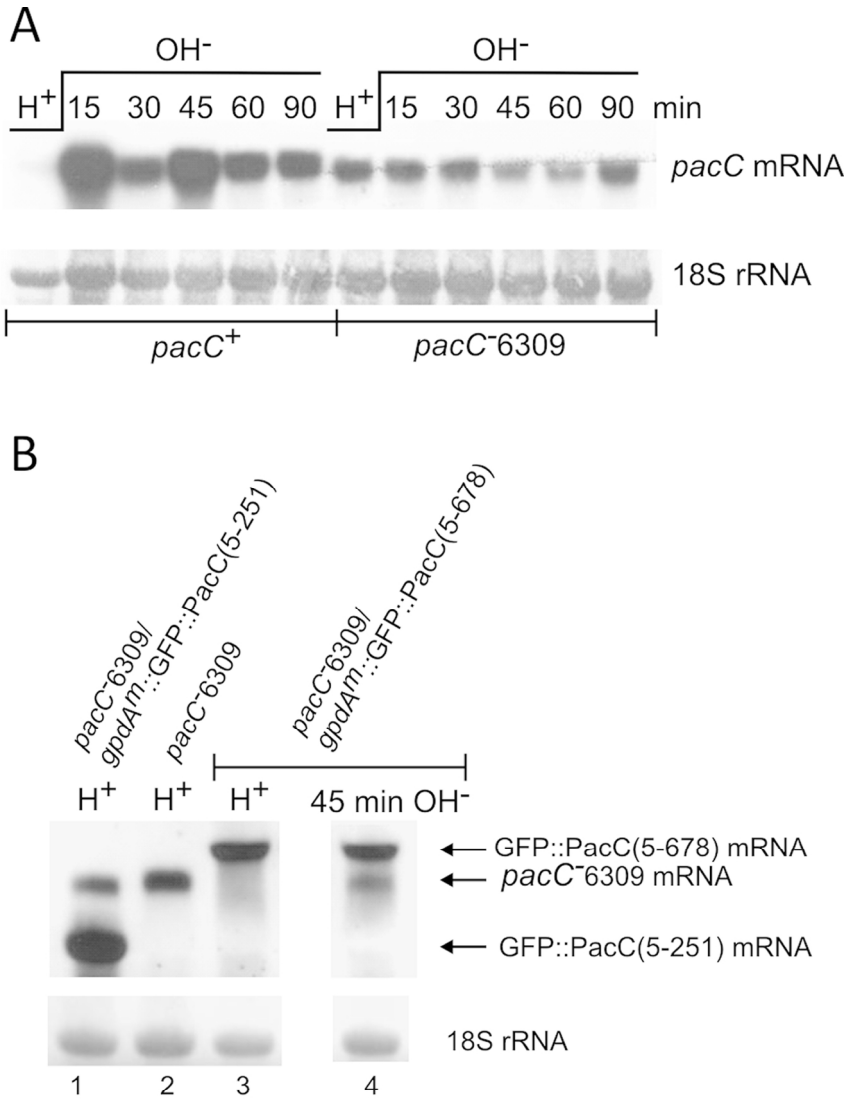

Figure 1, *pacX*

113x161mm (300 x 300 DPI)

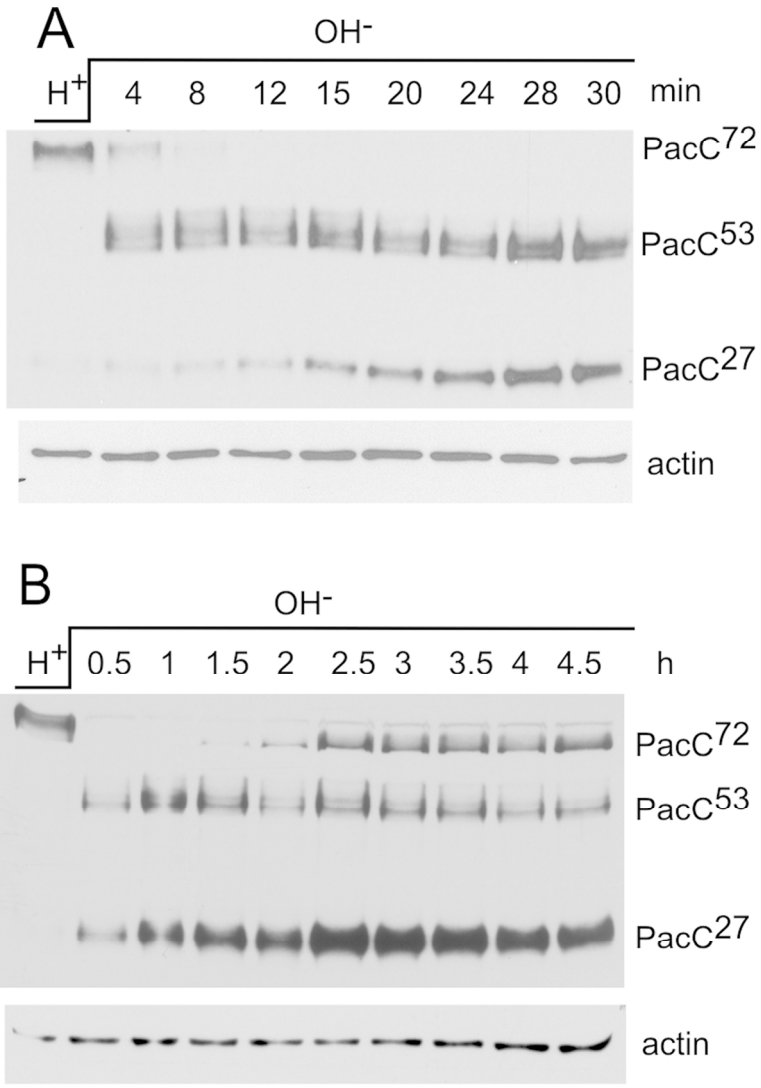

Figure 2, pacX

127x202mm (300 x 300 DPI)

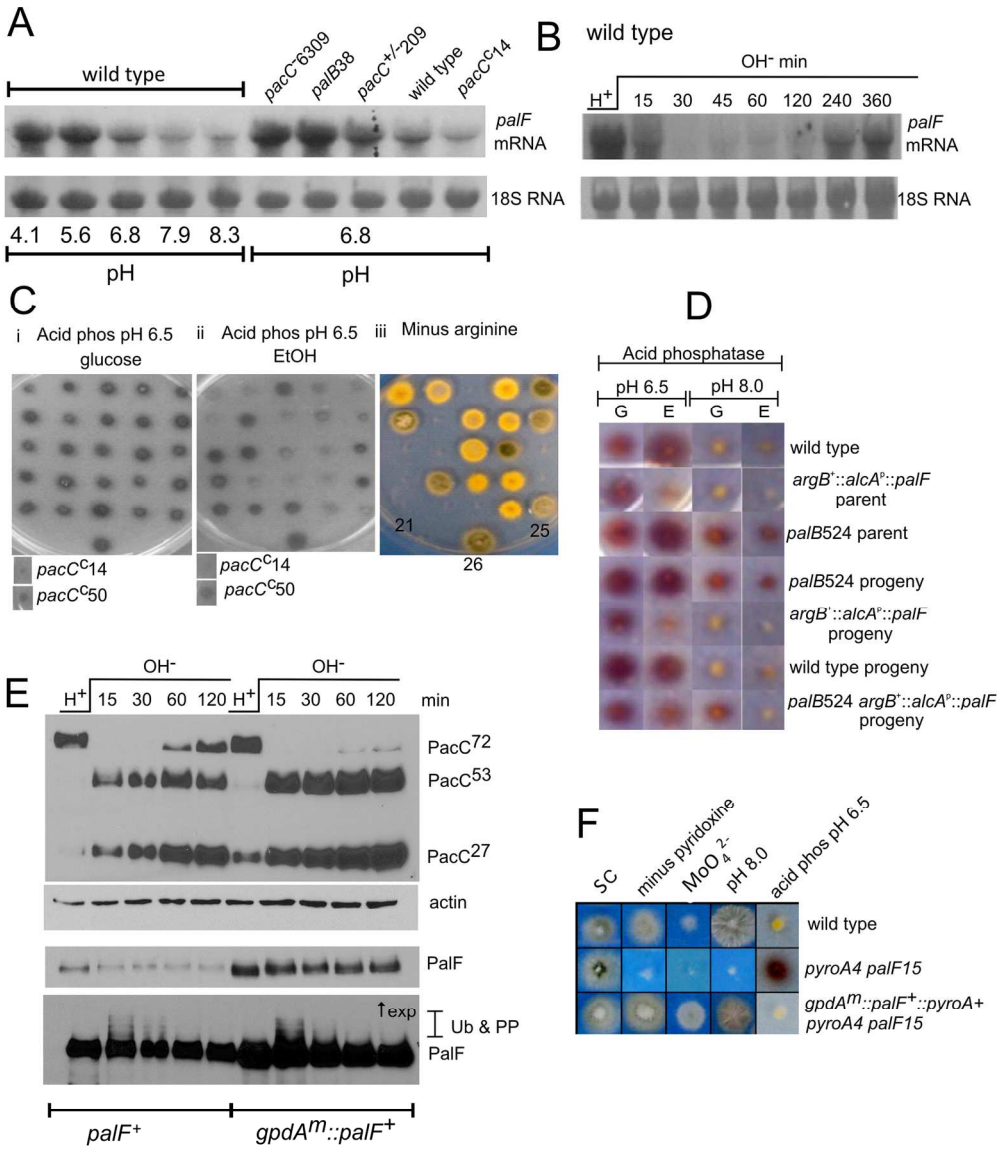

Fig. 3, pacX

204x247mm (300 x 300 DPI)

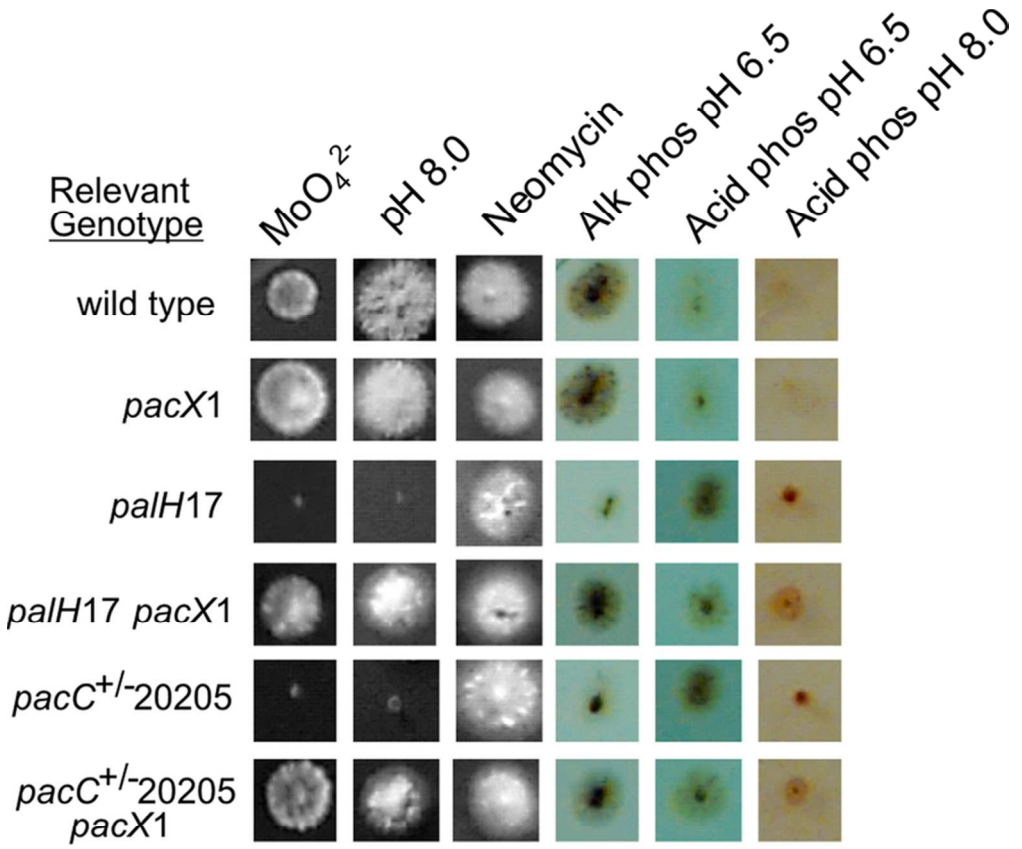

Fig. 4, pacX

73x67mm (300 x 300 DPI)

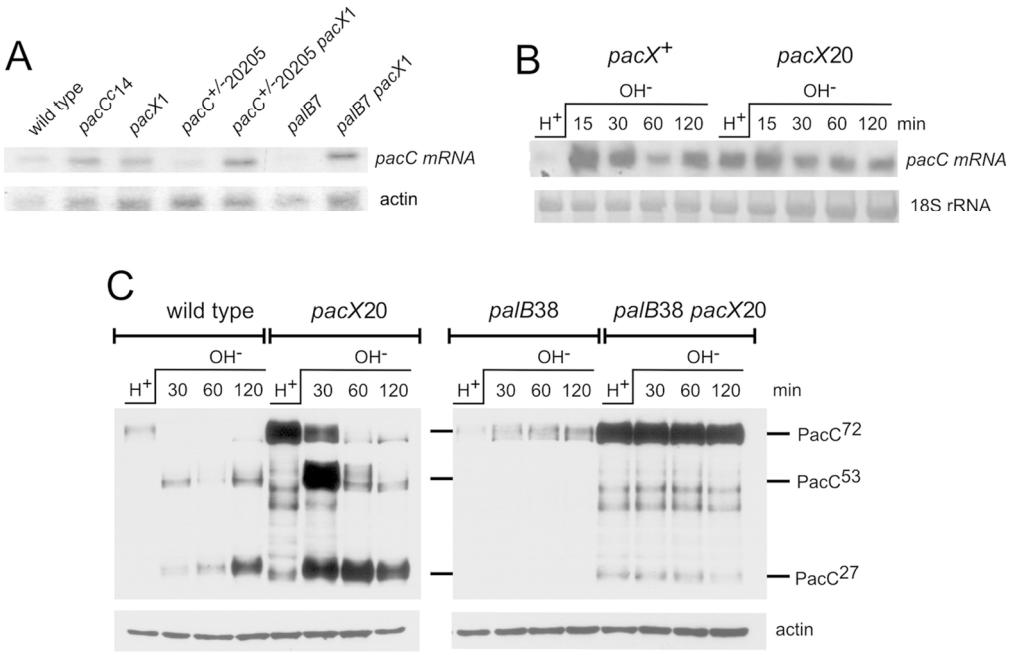

Fig. 5, pacX

120x85mm (300 x 300 DPI)

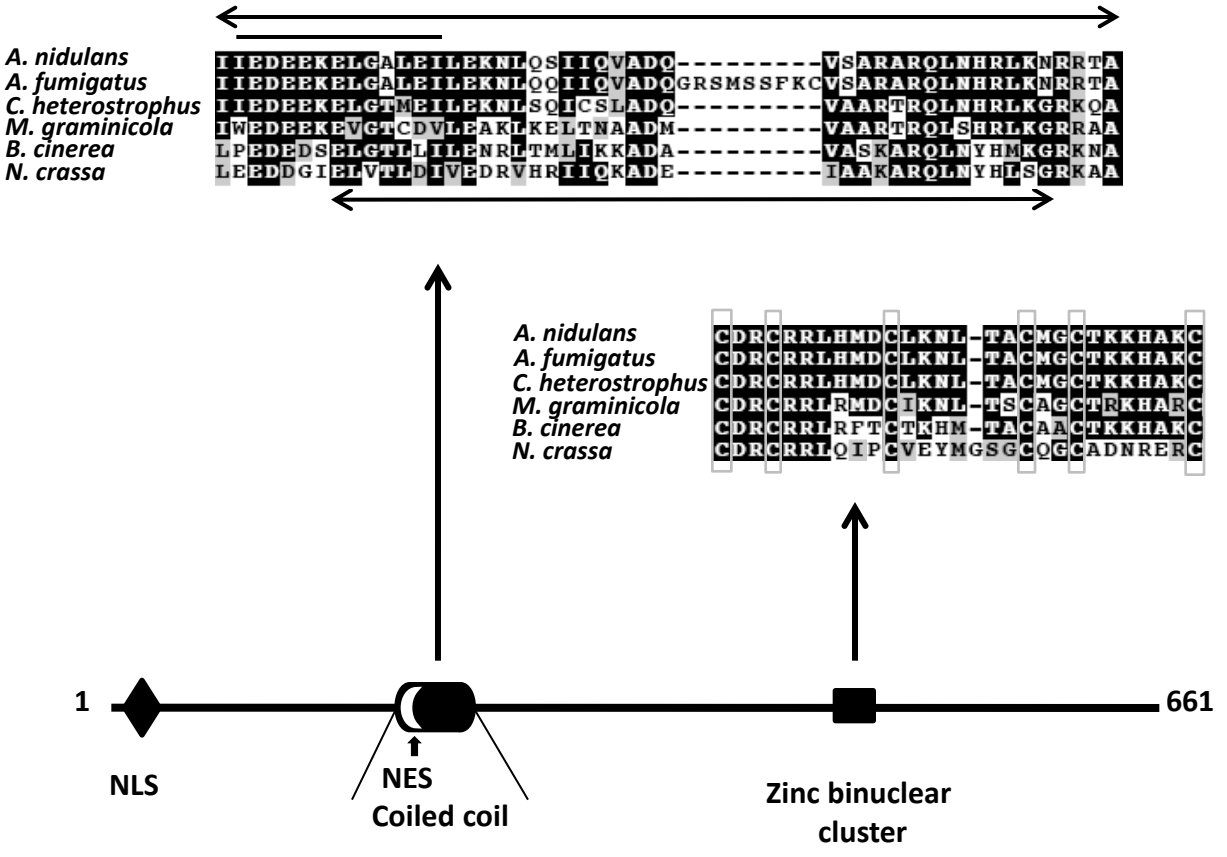

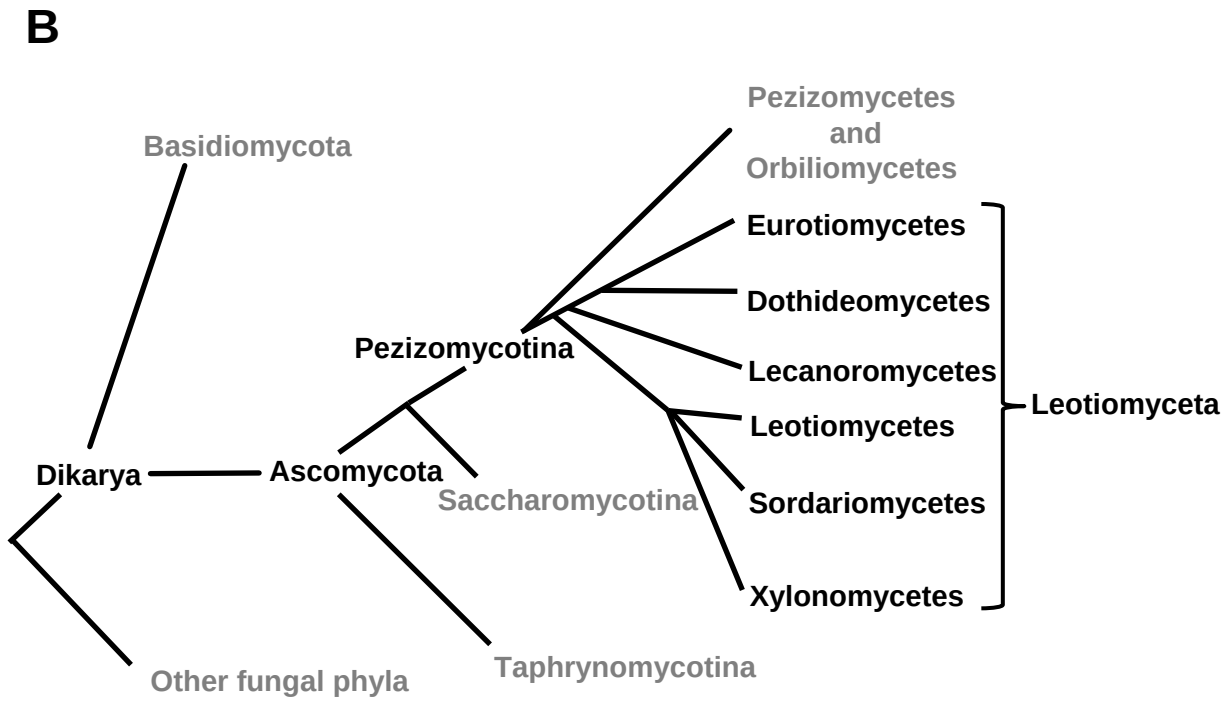

Figure 6, pacX

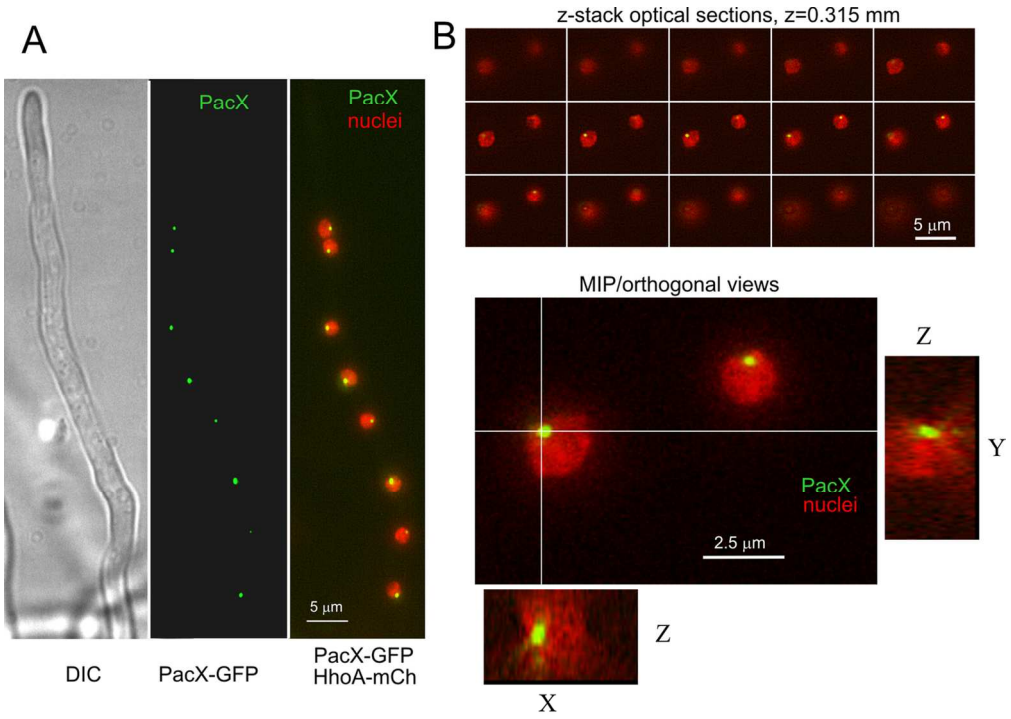

Fig 7, pacX

131x101mm (300 x 300 DPI)

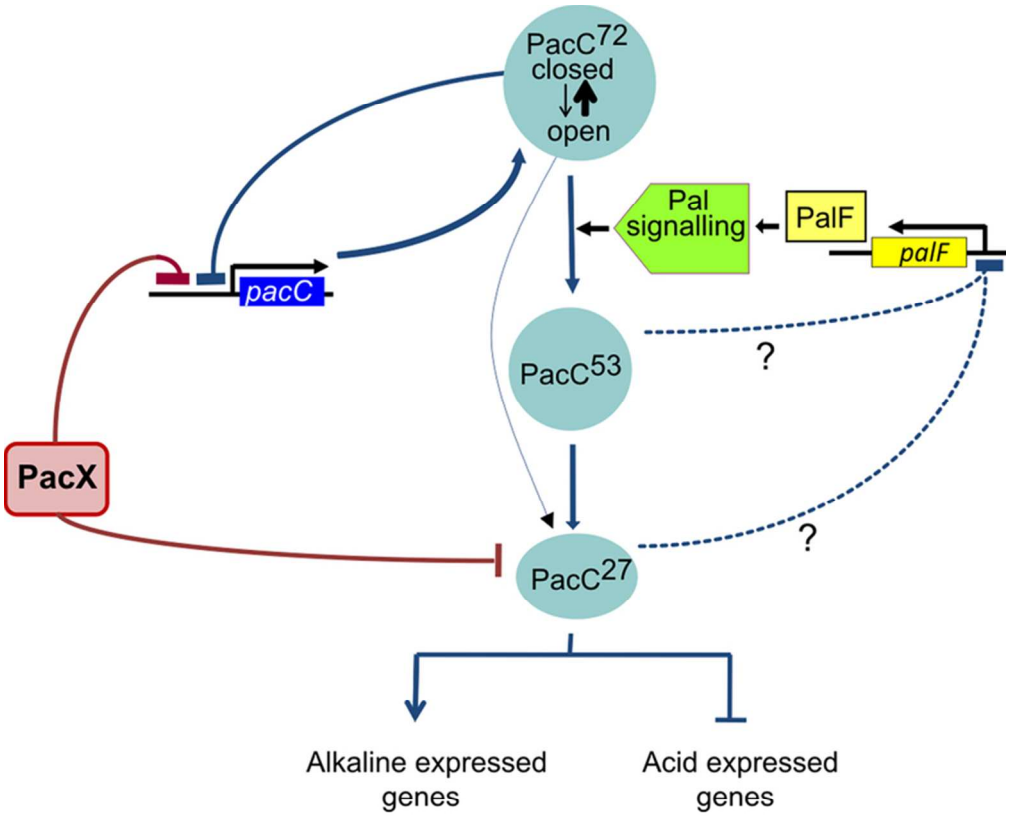

Fig. 8, pacX

71x63mm (300 x 300 DPI)

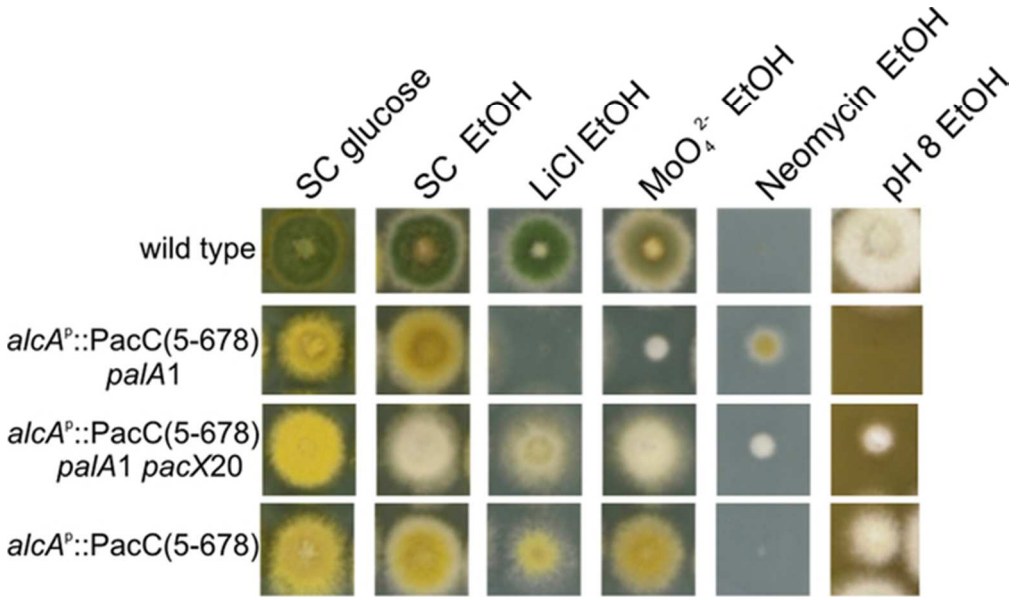

Fig. 9, pacX

55x37mm (300 x 300 DPI)

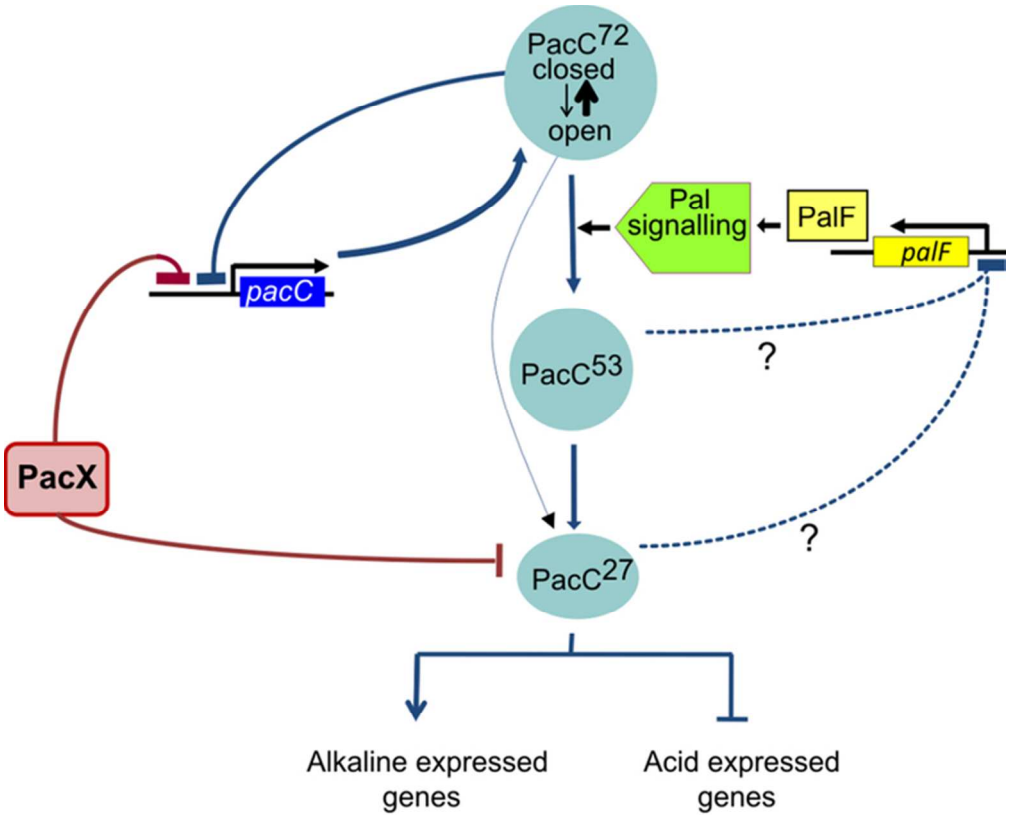

64x52mm (300 x 300 DPI)

The *Aspergillus nidulans* pH response, mediated by PacC which is proteolytically activated in response to Pal mediated alkaline pH signalling, moderates itself. *pacC* is negatively autoregulated by the acid prevalent form $PacC^{72}$ and a runaway pH response is prevented by negative feedback at signalling gene *palF*. PacX, a zinc binuclear cluster protein with unusual architecture and restricted taxonomic distribution, tempers PacC activity and is required to tether the pH response to the ambient pH signal.

Supplementary Information

Refining the pH response in *Aspergillus nidulans*: a modulatory triad involving PacX, a novel zinc binuclear cluster protein

Henk-Jan Bussink[1], Elaine M. Bignell[1,2], Tatiana Múnera-Huertas[1], Daniel Lucena-Agell[3], Claudio Scazzocchio[1,4], Eduardo A. Espeso[3], Margherita Bertuzzi[2], Joanna Rudnicka[1], Susana Negrete-Urtasun[1], Maria M. Peñas-Parilla[1], Lynne Rainbow[1], Miguel Á. Peñalva[3], Herbert N. Arst Jr.[1] and Joan Tilburn[1*]

[1] *Section of Microbiology, Imperial College London, Flowers Building, Armstrong Road, London SW7 2AZ, UK.*

[2] *Manchester Fungal Infection Group, Institute for Inflammation and Repair, University of Manchester, 46 Grafton Street, Manchester M13 9NT, UK.*

[3] *Department of Cellular and Molecular Biology, Centro de Investigaciones Biológicas CSIC, Ramiro de Maeztu 9, Madrid 28040, Spain.*

[4] *Institute for Integrative Biology of the Cell (I2BC), CEA, CNRS, Université Paris-Sud, Orsay, France.*

*Corresponding author

Joan Tilburn

Email j.tilburn@imperial.ac.uk

Telephone +1 240 271 4557

Running title: PacX and pH regulation refinement in *A. nidulans*

Key words: pH regulation, transcription, PacX, *Aspergillus nidulans*, zinc binuclear cluster, *palF* regulation.

Contents

Table S1. List of primers used in this work

Primer name	primer sequence (5’ to 3’)
850U	GTCGCTCCTGTAGCTGTG
1217FF	GTTCGTGCTCTTTCGGCCA
AN0826F	CATGGTTTGCAGCCGCCA
AN0826R	GAAACTCAGATGCGGCCT
BIGFF	GCCGTTAAAACAGGCAGG
p1673-EcoRI-Fw	CGAGCTGTACAAGGAATTCCCCATGGCCGAAG
p1673-EcoRI-Rv	CTTCGGCCATGGGGAATTCCTTGTACAGCTCG
TILREV	CATTTCTCGTCCGCTCAT
XF2	CCGGGGGATTCAAGAAC
XF5	CAAAACAGAGTCGCGTGGAGAT
XR1	AAGGAGCAGAAAAGAGTCATGG
XR5	GTTCACCTCGCTGCAGTTC
XR6	CCAATGCGGGTTTAGATTCGG
XR8	GCGGAGTAGGATGTTGATTG
yA1	GGGAACCTGTCAACGCAAATC
yA2	GCCATACCCAGATCCCTTGAC
ZNF2	GGGGTACCKRCANCKRTCRCANGG

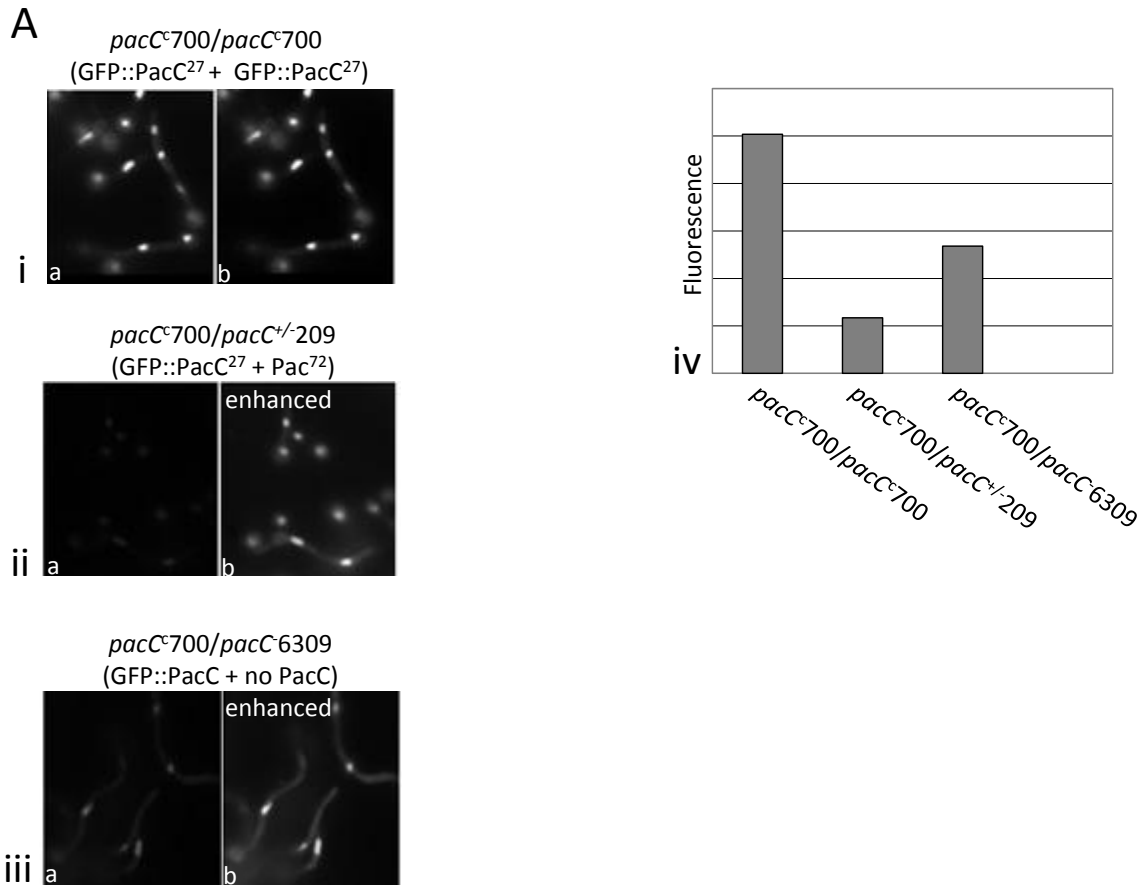
A
pacC^c700/pacC^c700
(GFP::PacC^27 + GFP::PacC^27)
i
a
b
pacC^c700/pacC^+/-209
(GFP::PacC^27 + Pac^72)
enhanced
ii
a
b
pacC^c700/pacC^-6309
(GFP::PacC + no PacC)
enhanced
iii
a
b
Fluorescence
iv
pacC^c700/pacC^c700
pacC^c700/pacC^+/-209
pacC^c700/pacC^-6309

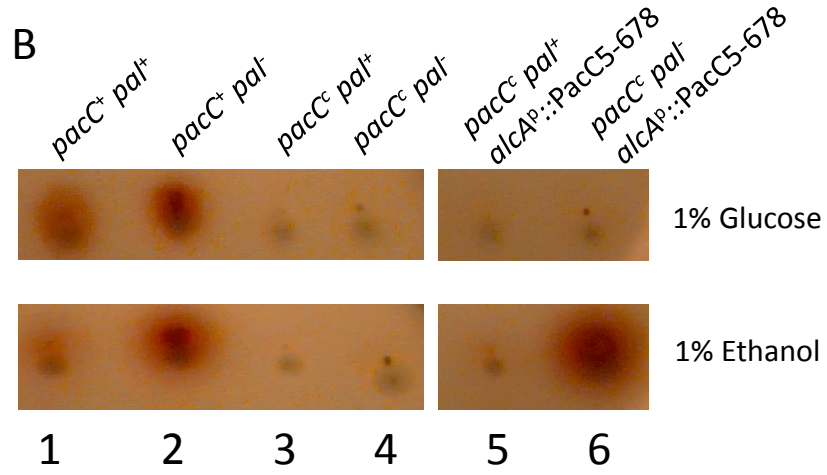
B
pacC^+ pal^+
pacC^+ pal^-
pacC^c pal^+
pacC^c pal^-
pacC^c pal^+ alcA^p::PacC5-678
pacC^c pal^- alcA^p::PacC5-678
1% Glucose
1% Ethanol
1
2
3
4
5
6

Figure S 1

Fig. S1 (A). Epifluorescence microscopy of preferentially nuclear localized GFP-tagged PacC^{27} reveals that PacC^{27} levels are greatly reduced when co-expressed with PacC^{72} in a diploid strain. The *pacC*^{c}700 GFP tagged *pacC* constitutive allele (GFP::PacC5-250) corresponding to PacC^{27} is integrated at the *pacC* resident locus and expressed from the *pacC* promoter. The *pacC*$^{-}$6309 null mutation [specifying PacC(1-4)] reduced the fluorescence intensity of GFP::PacC5-250 to ~50% (ia or b, iiia and iv), which would be the expected dilution effect. The *pacC*$^{+/-}$209 processing recalcitrant mutation (specifying PacC^{72}) had a greater effect resulting in a reduction of fluorescence intensity to less than 25% of that found in the diploid *pacC*^{c}700 strain (Ia or b, iia and iv) or a haploid *pacC*^{c}700 strain (results not shown). These results are consistent with our proposal that PacC^{72} is a repressor of *pacC* expression. Enhanced images for diploids *pacC*^{c}700/*pacC*$^{+/-}$209 and *pacC*^{c}700/*pacC*$^{-}$6309 (iib and iiib, respectively) were obtained by modifying brightness and contrast to improve visualisation of the GFP::PacC5-250 protein to a level comparable to that in the *pacC*^{c}700 homozygous diploid (unenhanced, ia and b). Fluorescence images of haploid and diploid *pacC*^{c}700 cells (Fig. S1A) were taken using a DMI6000b microscope equipped with a 63x objective 1.4 N.A. and an Orca-ERII camera. Strains were cultivated in WMM [watch minimal medium (Peñalva, 2005)], containing the required supplements and glucose 1% and 5 mM ammonium tartrate as carbon and nitrogen sources, respectively. Cells were grown at 25^{o}C for 18 hours before epifluorescence analyses. To compare nuclear fluorescence intensities, all images were obtained in the same conditions with an exposure time of 2 seconds. Nuclear fluorescence intensities were estimated using Metamorph 6.3r software by measuring selected areas of 80 pixels into 10 nuclei per strain. The mean of accumulative pixel intensities for areas of 80 pixels are shown in the chart (n=10 nuclei). The diploid strains are *pacC*^{c}700/*pacC*^{c}700, *pabaA*1 *yA*2 *glrA*1 *pacC*^{c}700 / *lysA*2 *pacC*^{c}700 (J2000); *pacC*^{c}700/*pacC*$^{+/-}$209, *lysA*2 *pacC*^{c}700 / *biA*1 *sB*3 *pacC*$^{+/-}$209 (J1977) and *pacC*^{c}700/*pacC*$^{-}$6309, *pabaA*1 *yA*2 *glrA*1 *pacC*^{c}700 / *pacC*$^{-}$6309 (*pacC*^{c}63) *pantoB*100 (J1999).

(B). Reversal of epistasis relationships by over-expression of *alcA*p::PacC5-678 in a *pacC*^{c}14 *palA*1 strain. Acid phosphatase staining after growth on minus phosphate medium pH 6.5 is shown. The *pacC*^{c}14 and *palA*1 alleles were used. The *alcA*^{p}::PacC5-678 cassette was integrated at the *argB* locus. In haploid strains *pacC*^{c} mutations are epistatic to *pal*$^{-}$ mutations (Caddick *et al*., 1986; Denison *et al*., 1995; Orejas *et al*., 1995), as shown by reduced acid phosphatase staining in positions 3 and 4. However, in a merodiploid strain containing *alcA*^{p}::PacC5-678 integrated in *argB* in addition to *pacC*^{c}14, *pal*A1 which is hypostatic to *pacC*^{c}14 on glucose medium becomes epistatic to *pacC*^{c}14 when PacC5-678 is over expressed under *alcA*^{p} inducing conditions (1% ethanol) lane 5. The strains containing the transgene were obtained by transformation (Tilburn *et al*., 1983) of a strain *pabaA*1 *yA*2 *argB*2 *pacC*^{c}14 or *yA*2 *argB*2 *palA*1 *pacC*Δ::*Ncpyr4 pantoB*100 with plasmid p[*alcA*^{p}::PacC5-678] (Mingot *et al*., 1999) and crossing. Strains in lanes (1) wildtype *biA*1 (J734 or 2167A), (2) *biA*1 *palA*1 (BXS), (3) *pabaA*1 *pacC*^{c}14 (J542), (4) *biA*1 *pabaA*1 *argB*::*alcA*^{p}::PacC5-678) *pacC*^{c}14 (J601), (5) *yA*2 *pabaA*1 *palA*1 *argB*::*alcA*^{p}::PacC5-678 *pacC*^{c}14 *pantoB*100 (J776).

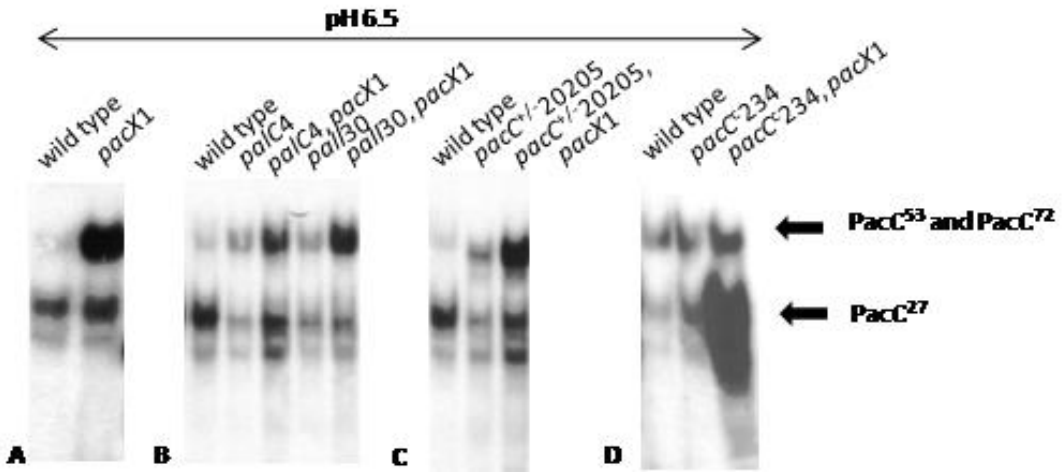

Fig. S2

Electrophoretic Mobility Shift Assays (EMSAs) showing the effects of *pac*X1 on complexes formed by PacC in *pac*C^{+} (i), *pal*$^{-}$ (ii), *pacC*$^{+/-}$20205 (iii), and *pacC*^{c}234 backgrounds. PacC was detected using a ^{32}P-labelled oligonucleotide containing *ipn*A2 (Tilburn *et al*., 1995). The positions of the PacC forms are indicated. Each binding reaction contained 5 μg of crude protein. Strains were grown from conidial inocula of 1 - 2 x 10^{6} ml^{-1} in 200 ml of appropriately supplemented *Aspergillus* complete media (Cove, 1966), containing 3% ($^{w}/_{v}$) sucrose, 20 mM MES pH 6.5, at 37°C for 16 hours with shaking at 120 rev min^{-1}. Mycelia were harvested on sterile Miracloth™ (Calbiochem) and samples of mycelia were cut into small strips of approximately 300 mg and frozen in liquid nitrogen. Cell lysates were prepared essentially as described by Peñas *et al.* (2007) except that the samples were centrifuged immediately after cell disruption. Double stranded oligonucleotide probes were prepared and binding reactions and electrophoresis were carried out following Perez-Esteban *et al.* (1993) and Espeso and Peñalva (1994).

Aspergillus nidulans pacX

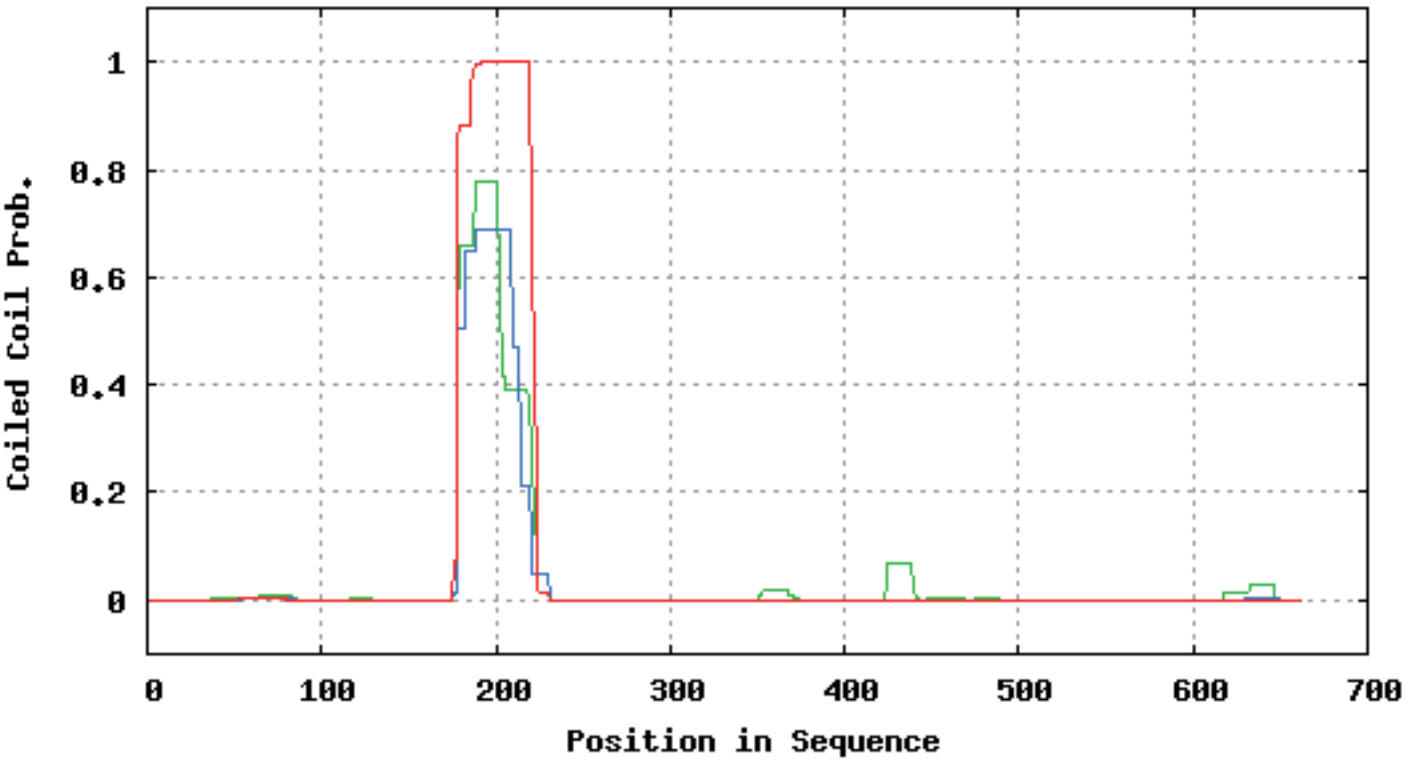

Alignment

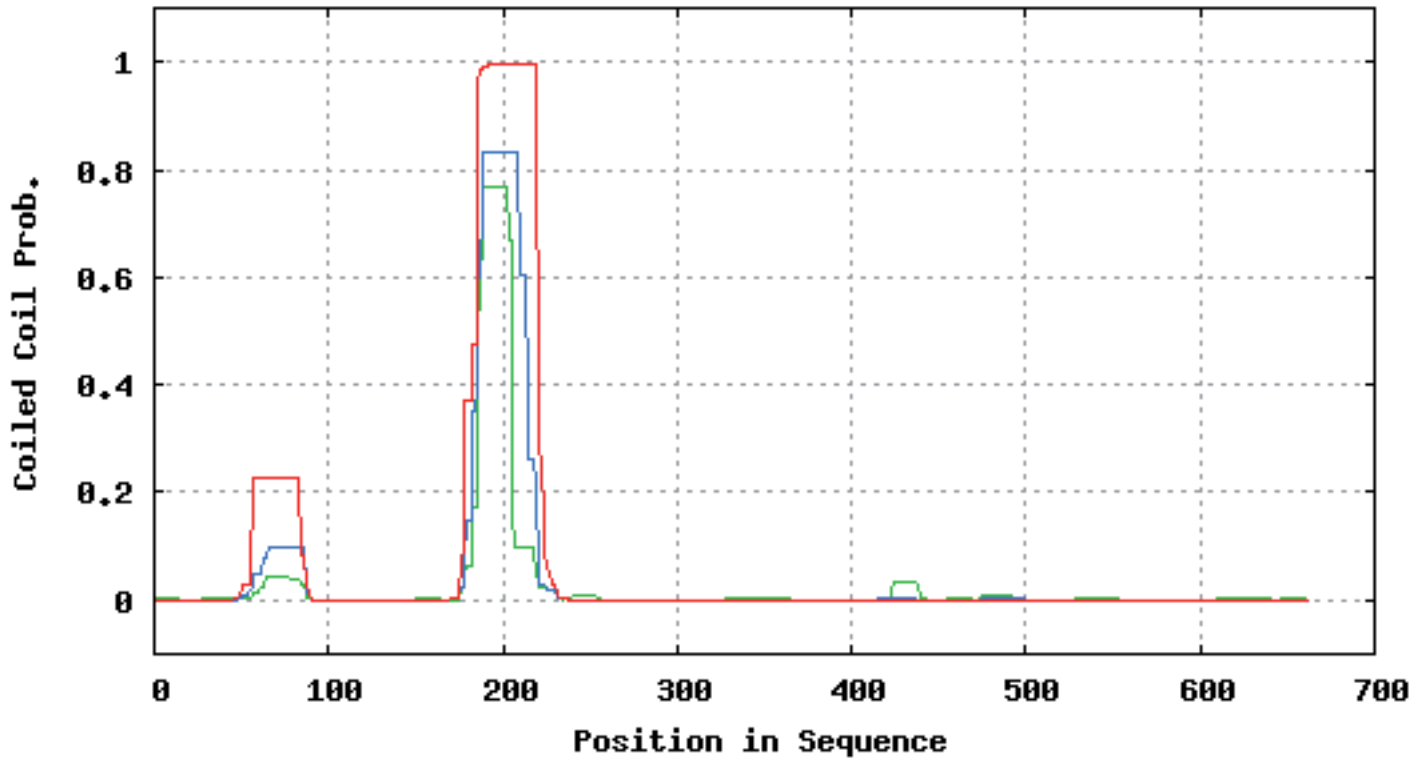

window = 14 window = 21 window = 28

Fig. S3. Coiled-coil predictions for PacX and the consensus derived from a 177-membered alignment of PacX homologues were obtained at http://toolkit.tuebingen.mpg.de/pcoils. The same alignment used to generate the phylogeny shown in Fig.S6 was used to obtain the coiled-coil prediction.

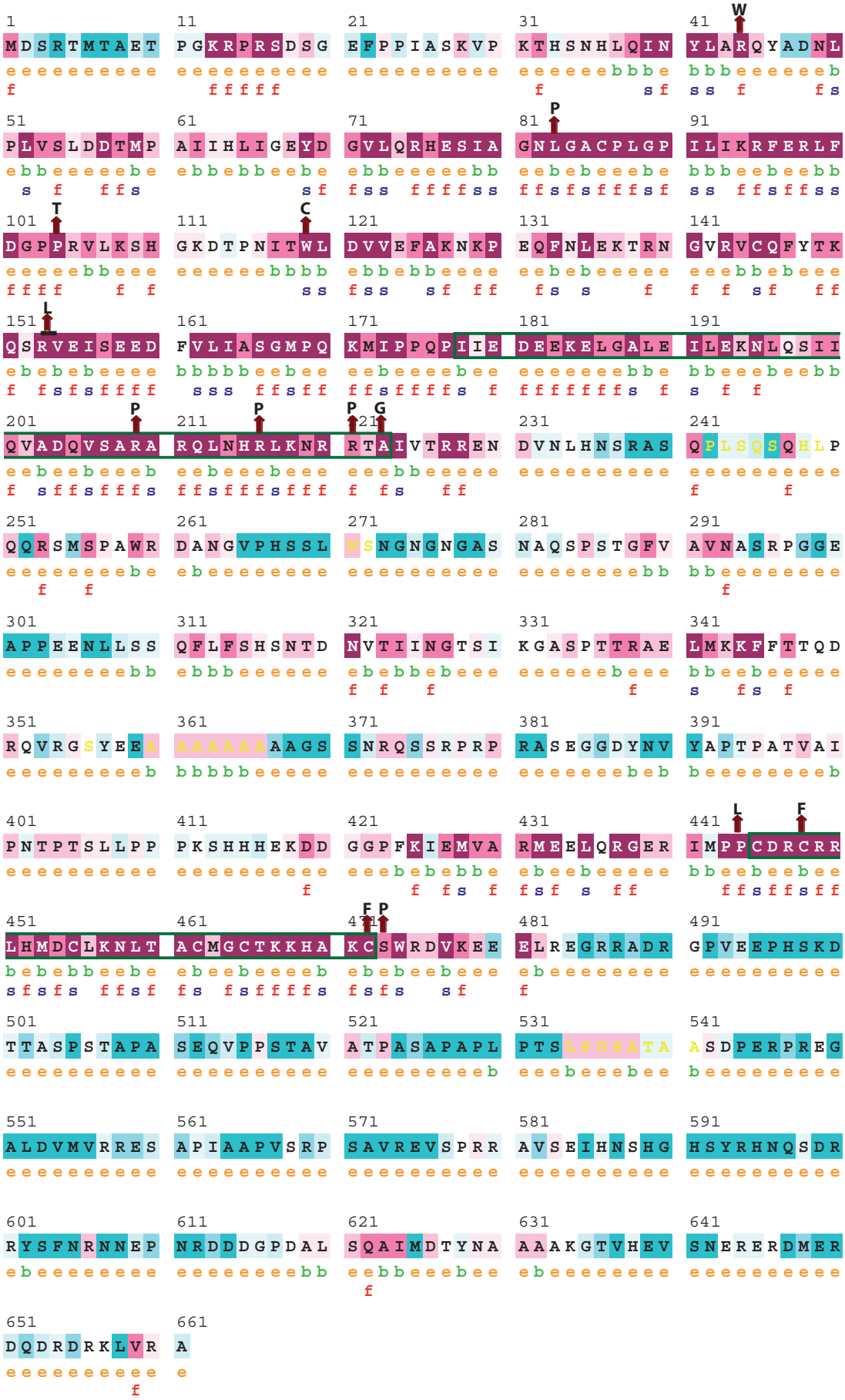

The conservation scale:

1	2	3	4	5	6	7	8	9

Variable **Average** **Conserved**

e - An exposed residue according to the neural-network algorithm.

b - A buried residue according to the neural-network algorithm.

f - A predicted functional residue (highly conserved and exposed).

s - A predicted structural residue (highly conserved and buried).

X - Insufficient data - the calculation for this site was performed on less than 10% of the sequences.

Fig. S4. ConSurf (http://consurf.tau.ac.il) results for PacX based on the 177-membered alignment used to generate the phylogeny in Fig. S6. Residues where point mutations map are indicated with dark arrows and residue changes are shown. The coiled-coil region and zinc binuclear cluster are outlined in green.

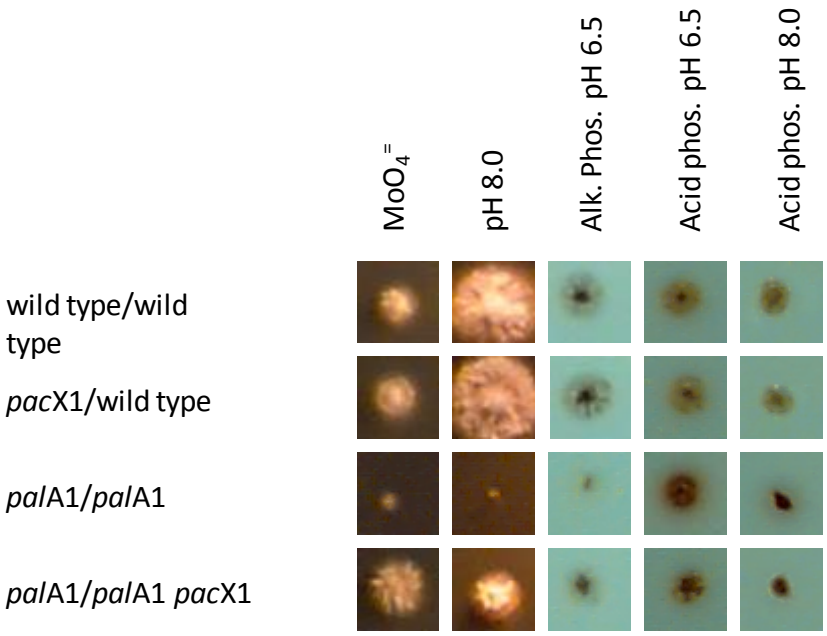

Fig. S5. Partial dominance of *pacX*1 to the wild type allele in a homozygous *palA*1 diploid. Diploids of relevant partial genotype are indicated. Growth on 25 mM molybdate and pH 8.0 medium are shown. Alkaline and acid phosphatase staining was carried out after growth on minus phosphate medium, buffered at the pH values shown, for ~24h at 37^{o}C.

Cordyceps_militaris_6447
Beauveria_bassiana_6668
Trichoderma_virens_71258
Trichoderma_reesei_476357
Trichoderma_reesei_109177
Trichoderma_atroviride_300895
Trichoderma_asperellum_54212
Metarhizium_robertsii_9306
Metarhizium_acridum_7851
Acremonium_strictum_132095
Myrothecium_inundatum_477476
Niesslia_exilis_824864
Ilyonectria_sp_302194
Nectria_haematococca_25109
Fusarium_graminearum_9256
Fusarium_verticillioides_7295
Fusarium_oxysporum_11330
Fusarium_fujikuroi_8319
Valetoniellopsis_laxa_446166
Apiospora_montagnei_61894
Apiospora_montagnei_389327
Hypoxylon_C-4A_249974
Anthostoma_avocetta_450004
Daldinia_eschscholzii_65630
Hypoxylon_EC38_49203
Hypoxolon_CO275_20279
Verticillium_dahliae_7372_
Acremonium_alcalophilum_1074992
Sodiomyces_alkalinus_322741
Colletotrichum_graminicola_1979
Colletotrichum_higginsianum_1604
Glomerella_acutata_1563521
Glomerella_cingulata_1833803
Coniochaeta_sp_967471
Thozetella_sp._707142
Neurospora_tetrasperma_70900
Neurospora_discreta_91808
Neurospora_crassa_515
1
0.82
Corynespora_cassiicola_606263
Amniculicola_lignicola_251083
Verruculina_enalia_474271
Pleomassaria_siparia_457933
Melanomma_pulvis-pyrius_261845
Karstenula_rhodostoma_487107
Trematosphaeria_pertusa_520355
Lentithecium_fluviatile_389658
Ophiobolus_disseminans_320628
Cucurbitaria_berberidis_288735
Leptosphaeria_maculans_1933
Phoma_tracheiphila_140591
Dothidotthia_symphoricarpi_350253
Stagonospora_nodorum_737
Stagonospora_sp_242455
Macroventuria_anomochaeta_209078
Didymella_exigua_104558
Clathrospora_elynae_440328
Alternaria_alternata_939505
Alternaria_brassicicola_5468
Setosphaeria_turcica_42485
Cochliobolus_lunatus_46287
Cochliobolus_heterostrophus_105256
Cochliobolus_sativus_103244
Cochliobolus_carbonum_110584
Cochliobolus_miyabeanus_98240
Cochliobolus_victoriae_111985
Pyrenophora_teres-teres_3684
Pyrenophora_tritici-repentis_156073
Byssothecium_circinans_183654
Massarina_eburnea_397300
Lindgomyces_ingoldianus_326039
Cenococcum_geophilum_571263
Zopfia_rhizophila_546509
Lophium_mytilinum_52630
Lepidopterella_palustris_363517
Rhytidhysteron_rufulum_2683
Hysterium_pulicare_118396
Aaosphaeria_arxii_355420
Sporormia_fimetaria_450147
Westerdykella_ornata_314014
Delitschia_confertaspora_367674
Pseudovirgaria_hyperparasitica_539098
Phyllosticta_citricarpa_435776
Macrophomina_phaseolina_10039
Saccharata_proteae_42850
0.8
0.99
Zasmidium_cellare_69841
Cladosporium_fulvum_192270
Dothistroma_septosporum_69494
Mycosphaerella_graminicola_68877
Zymoseptoria_pseudotritici_795922
Zymoseptoria_ardabiliae_773786
Cercospora_zeae-maydis_34037
Septoria_musiva_162042
Septoria_populicola_43891
Dissoconium_aciculare_383333
Piedraia_hortae_258161
Teratosphaeria_nubilosa_272282
Acidomyces_richmondensis_67993
Polychaeton_citri_213878
Aureobasidium_subglaciale_5673
Aureobasidium_namibiae_58227
Aureobasidium_pullulans_358482
Myriangium_duriaei_232598
Trypethelium_eluteriae_537871
0.89
0.21
Venturia_inaequalis_20653
Tothia_fuscella_61920
Trichodelitschia_bisporula_585285
Aulographum_hederae_421159
Xanthoria_parietina_39399
0.66
Cladonia_grayi_1444
0.99
Talaromyces_marneffei_2827
Talaromyces_aculeatus_469058
Talaromyces_stipitatus_6936
Arthroderma_benhamiae_3838
Trichophyton_verrucosum_5014
Trycophyton_rubrum_8344
Microsporum_canis_6773
Thermoascus_aurantiacus_38763
Monascus_ruber_495689
Monascus_purpureus_494146
Aspergillus_zonatus_118698
Penicillium_canescens_370245
Penicillium_lanosocoeruleum_379096
Penicillium_rubens_142075
Penicillium_chrysogenum_36868
Penicillium_expansum_381492
Penicillium_digitatum_5320
Penicillium_raistrickii_381685
Penicillium_brevicompactum_40391
Penicillium_fellutanum_379850
Penicillium_glabrum_137101
Penicillium_janthinellum_419275
Penicillium_oxalicum_289
Penicillium_bilaiae_369599
Aspergillus_wentii_27688
Aspergillus_ochraceoroseus_515001
Aspergillus_sydowii_145096
Aspergillus_versicolor_78681
Aspergillus_nidulans_5967_AN0766_pacX
Aspergillus_steynii_476964
Aspergillus_carbonarius_207850
Aspergillus_kawachii_16265
Aspergillus_acidus_503896
Aspergillus_tubingensis_54716
Aspergillus_niger_1150021
Aspergillus_brasiliensis_120152
Aspergillus_campestris_308532
Aspergillus_novofumigatus_460037
Aspergillus_fumigatus_1295
Neosartoria_fischeri_2495
Aspergillus_terreus_630
Aspergillus_clavatus_7112
Aspergillus_flavus_30493
Aspergillus_oryzae_10327
Eurotium_rubrum_399384
Aspergillus_glaucus_119317
Coccidioides_immitis_8834
Uncinocarpus_reesii_6922
Gymnascella_aurantiaca_70239
Gymnascella_citrina_350598
Histoplasma_capsulatum_3581
Paracoccidioides_brasiliensis_1145
Symbiotaphrina_kochii_776176
Xylona_hevea_271009
Trinosporium_guianense_528296
0.35
0.99
0.86
1
Chalara_longipesis_325002
Meliniomyces_bicolor_560497
Rhizoscyphus_ericae_518240
Meliniomyces_variabilis_560832
Ascocoryne_sarcoides_9207
Philocephala_scopiformis_680350
Glarea_lozoyensis_9817
Marssonina_brunnea_7210
Cadophora_sp_512117
Botrytis_cinerea_10956
Sclerotinia_sclerotiorum_9696
Oidiodendron_maius_101421
Amorphotheca_resinae_49121
0.65
0.98
1
0.3

Fig. S6. Maximum likelihood phylogeny of 177 putative PacX orthologues. The tree is shown in a cartoon, circular form. The name of each species is indicated, followed by the protein accession number in the JGI data base. The classes and orders within the Pezizomycotina are colour coded as follows: Blue, Dothideomycetes, Pleosporales; LIght blue, Dothideomycetes, Capnodiales; Very light blue; Dothideomycetes, *Incerta sedis*; Grey, Leotiomycetes; Green, Eurotiomycetes; Purple, Xylonomycetes;Yellow, Leotiomycetes; Pink Sordariomycetes, Hypocreales, Red, Sordariomycetes, other orders. Names in purple indicate species that map outside their taxonomic order (but within its class); e.g. *Acremonium alcalophilum* does not map together with other Hypocreales, such as *Acremonium strictum, Trichodelitschia bisporula* does not map with other Pleosporales. Species in red are those used in Fig. 6. Alignment carried out with MAFFT E-INS-i, (recommended for sequences with multiple conserved domains and long gaps) with a Blosum 30 matrix, alignment refinement carried out with BMGE with a Blosum 30 similarity matrix. Tree generated with PhyML and re-drawn with Figtree. Support values in the nodes are aLRT (approximate likelihood ratio tests, see **Experimental Procedures**).

Supplementary Data

Inactivation of the *pacX* gene by an endogenous *Fot1*-like transposon

PCR amplification of *pacX*18, using primers XF2 and XR8, showed this mutation to result from an insertion of ~1.7 kb. Complete sequencing showed the insert to be 1860 bp (not including the characteristic TA duplication) with an open reading frame identical to that of AN0826, which is annotated in the http://www.aspergillusgenome.org data base as "Uncharacterised transposable element gene". The open reading frame of 1622 nt is bounded by 44 nt inverted repeats, the 5' terminating 50 nt upstream of the ATG, the 3' initiating 57 nt downstream from a double ochre chain termination signal. These features are identical to those flanking AN0826. The element is integrated in an orientation opposite to that of the open reading frame of *pacX* between the T and A of the acceptor site of the intron of *pacX*, and it generated a typical TA duplication. The open reading frame shows an obvious similarity with that of transposons of the *Fot1*/*pogo* family (Supplementary Fig. S7) shows the similarity of the peptidic sequences.

There are sixteen sequences in the *A. nidulans* genome which show high similarity with AN0826, with complete or incomplete open reading frames, all bounded by identical (in one case incomplete, AN7516) inverted repeats. These are namely, in order of similarity: AN4391, AN6559, AN3478, AN11091, AN4877, AN5334, AN0669, AN7516, AN2732, AN0975, AN8788, AN11044, AN3047, AN2291, AN5863, AN9046 (Cerqueira *et al*., 2014). Even the most similar sequences show sufficient nucleotide differences with AN0826 to make the identification of the inserted element certain. Southern blots had already revealed a minimum of eleven copies in the standard Glasgow laboratory strain (Li Destri Nicosia *et al.*, 2001) The most conserved open reading frames (AN0826 to AN3478, also AN11044) are not predicted to be interrupted by introns. In other ORFS introns are predicted. While we have not checked manually all putative ORFs, these introns are probably spurious, and are derived by automatic annotation from the presence of chain termination codons inactivating some of the ORFs. The variability in the position of

the putative intron within the different ORFs supports this contention. The case of AN8788 is glaring, a 472 nt putative intron results in an overlap of the proposed ORF with convergently transcribed AN8789 and would place the putative C-terminal exon beyond the inverted repeat. In this case a -2 frame shift has resulted in a truncated protein at residue 595, automated intron recognition process "fabricating", in fact, two introns.

It is striking that among the hundreds of loss-of-function mutations obtained by classical genetics and now sequenced, *pacX*18 is the first and only one due to the insertion of an endogenous transposon. Attempts to select specifically such events were never successful in *A. nidulans*. This contrasts with the ready mobility of heterologous *Fot1*, *impala* and *Minos* transposons inserted in the genome of *A. nidulans* (Li Destri Nicosia *et al.*, 2001; Carr *et al.*, 2010; Evangelinos *et al*., 2015)

An explanation for the extreme rarity of endogenous transposition in *A. nidulans* may derive from the absence of active transposase in the cell. Caddick and co-workers have carried out global RNAseq of the *A. nidulans* transcriptome under 5 different conditions (Sibthorp *et al.*, 2013). These data are accessible on line (http://www.aspgd.org/, JBrowse). A search for each one of the paralogues indicated above showed virtually (and in some cases absolutely) no transcripts. Some transcripts are seen for AN9604, the most divergent of the homologues, which cannot encode an active transposase. In contrast with this data, a signal for a transcript of the correct length was detected in early experiments by conventional Northern blots (Li Destri Nicosia *et al.*, 2001) in culture conditions similar to one of those used by (Sibthorp *et al.*, 2013). The probe used was derived from the only *A. nidulans Fot*-like element known at the time, whose position within a sequenced cosmid, F2P08, (Kupfer *et al.*, 1997) identifies it unequivocally as AN0975. The high similarity between all *Fot1*-like paralogues implies that cumulative transcription of all Fot-1 like elements in the genome were detected in this experiment.

The different homologues are spread throughout the genome, are not methylated (Li Destri Nicosia *et al.*, 2001), and active transcription of neighbouring genes show that they are not located in silent regions of the genome. It would be interesting to know if the absence of transcripts derives from very infrequent transcription or from selective degradation of the cognate RNAs though the dicer/argonaute system (Hammond *et al.*, 2008a and b). The strain in which *pacX18* was isolated carries an autonomous copy of an *impala* element from *F. oxysporum,* belonging to the *Tc1*/*mariner* family. While the cognate transposase cannot mobilise a *Fot1*-like element, the possibility remains that its presence may affect the regulation of its expression. In addition, possible effects of the *pacC*$^{+/-}$20205 mutation and the stressful alkaline growth conditions under which the *pacX*18 mutation was selected may ,have contributed to the activation of the AN 0826 *Fot-1-like* element

Transposons of the *Fot1*/*Pogo* family operate through a mechanism of cut and paste, rather than the copy and paste characteristic of retroposons, and among the eukaryotic DNA transposons, of helitrons. We thus tested the presence of the resident copy of AN0826 in the strain where transposition to *pacX* had occurred. Fig S7 shows clearly that AN0826 is conserved at its locus in the strain carrying the *pacX*18 mutation, thus demonstrating a copy/paste mechanism, however, the precise insertion of the inverted repeats and the TA duplication implies that this event was catalysed by the specific transposase.

That copy and paste expansion of eukaryotic type II transposons must occur is indicated by the multiple copies of these elements in genomes where they are present (Daboussi and Capy, 2003; Dufresne *et al.*, 2011, specifically for *Fot1* elements), and in the specific case of the *Fot1*-like transposons of *A. nidulans* by their polymorphism in different strains of this species (Li Destri Nicosia *et al.*, 2001). A class II "cut and paste" DNA transposon can replicate by transposing from a position behind a replication fork to an un-replicated sequence or by double-stranded gap repair at the donor site by an intact sister chromatid (Rubin and Levy, 1997; Bessereau, 2006; Wicker *et al.*, 2007; Izsvak *et al.*, 2009; Skipper *et al.*,

2013 and refs therein). Both mechanisms imply a temporal coupling of replicative transposition and the S phase of the cell cycle. AN0826 and *pacX* are both on chromosome VIII at ~180 kb from each other, which is not incompatible with these genes being within the same replicon. This proximity may have facilitated a local transposition event [local hopping, (Tower *et al.*, 1993; Timakov *et al.*, 2002; Carlson and Largaespada, 2005; Muñoz-Lopez and García-Pérez, 2010)] and allowed us to detect this very rare occurrence.

```
AN0826     1 MPRVRVSSSQNCHEKEGRLLLAVQAIKKKEITSIREAARRFNVPESTLRTRLRGTTNRAESRA-NGHKLTEIEEEVLKQW
Tan1       1 MPPKASIPSKSQVEQEGRILLAIEAIQKGQITSIREAARVVDVARTTLQARLSGRVFAKNMTN-ARQKLSNNEEESLVKW
Fot1       1 MPVYSADDLEN----------AIADFKNG--VSLKTAAKKNGLPPSTLRGRLTGAQSRQVARQ-EQLRLTTDQEDDLERW
Aft1       1 MPKSSKI-------NESYLLEACEAAQAQKKPNISKIAREYGVPYATLRDRVKKHVHPRLANKPVNRALKGYQEEALIQW

AN0826    80 ILSLDLRGAAPTKAHVREMANILLAKRGSTPIQTVGQKWVYNYTQRHPE---LESRLSRQYDCQRAKQENPKVIQAWFNT
Tan1      80 ILSLDKRGASPRPLDIRDMANLIISKRGYSTVEQVGINWAYSFVKRHES---LRTRFARRLNYQRAKMEDPEVIKDWFKR
Fot1      68 ILRQEKLGHAPTHAQVRTIVRSVLARHGDH--APLGRKWTTRFVERHPA---LKTKLGRRTDWERVNAATPANIKRLFDV
Aft1      74 IVCMRDRNMPVTPKLLEEYANQALRRAGES--RQVSKMWAYRFEKRLPEHLNLGPAKQKIKESKRIQAEDAGLLTHWYNQ

AN0826   157 VRATHEQYGILPDDIYNFDETGFAMGLCAHQKVITKSE-SCGRRPVLQPGNR-EWVTAIESISASGWAL-PILIFKGKQ-
Tan1     157 VQEVIQEYGISSDDIYNFDETGFAMGMIATYKVVTSSQ-RAGRPSLVQPGNR-EWVTAIECIRSNGEVLPSTLIFKGKT-
Fot1     143 YETVD---WIPPERRYNADEGGIMEGQGVNGLVIGSSQESPNAVPVKTATVR-TWTSIIECISAVGVVLHPLVIFKAKT-
Aft1     152 LAGVVKK-DTPARLVYNFDECGFQPGEGKSRKVISS---KGSKVPDLAESERGENITAIECVAADGWQMDPWFIFKGNGI

AN0826   233 YNQAWF-TG--LPP--DWRFEISTNGWTTNEISLRWLQKQFIPSTEHRTRGRYQLLVLDGHGSHLTPEFDQICTDHNIIP
Tan1     234 HLKAWY-EGQSIPP--TWRFEVSDNGWTTDKIGLRWLQKHFIPLIRGKSVGKYSLLVLDGHGSHLTPEFDQSCAENEVIP
Fot1     218 IQEQWF-RREFLQKHLGWQVTFSKNGWTSNSIALEWLEKVFLPQTAPADPADARLLIVDGHGSHATEQFMAKCYLNNVYL
Aft1     228 FMESWFNNESEALPP--DTTIATSPNGWISDELAVQWLQSFINATNERTKKGEKRILIFDGHGSHLTVEFLQLCEDNGVIP

AN0826   308 LCMPAHSSHLLQPLDIGCFAVLKRSYASLVDQKMRLG-ISHIDKLDFLAAYPQARISTFKLDTIRNSFRAAGLVPLNPEP
Tan1     311 ICMPAHSSHLLQPLDVGCFSVLKRTYGGMVQKQMQYG-RNHIDKLDFLEVYPKAHQCALSKSNILSGFRATGLVPLDPDQ
Fot1     297 LFLPAHCSHVLQPLDLGCFSSLKAAYRTLVGEHTALTDSTRVGKQRFLDFYARAREIGFRKVNIRSGWRAAGLWPVNINK
Aft1     306 FGFLPHTTHLCQPLDGKPFLSYKQHFRRMNNELSYWA-GEPVGKSEFLHMIGPVREKAFNQRIIREAFKDRGIWPVN-SK

AN0826   387 VLSKLSIQA--------------CTPTPPG----SRGSQASTFCPHTPANVDELLKQASLLRDFLKQRSKSPPSPSHNAL
Tan1     390 VLSRLHIRL--------------KTPPTPD-------SQSSGSVLQTPHNIKHLLKHQKSVERLLRKRQASPTSPTNSTL
Fot1     377 PLASRWVMVL-------------TKSALPP----------SETLDIATPKRGGDVVK-------LFSAKSSSPSSRL--SI
Aft1     384 IADDLAILLWEGIPDIYAPDLDKMTPSTPPSQPPSRPPSSSSIDISPPRTIQALKKNQAK----LSKHADLLLTPKLQRNL

AN0826   449 NQLIKGGQIAMQKGILLEQENRALRAENAIQRRK-RARTHRW----IAHDNGLSVQEA----TE--LEEAHNASF-QAIP
Tan1     449 RQLLKGGELAITNSILLAKENAELRASHEKQLQK-RKRSRKQ----VIYTEGTIVEEAQRAIQE--VEEVQNDED-IEVE
Fot1     426 RKAAAALDKVAIELAMKDREIERLRAQLEAAQPK-KKRKIRQDPNECFISLAQILAEANREPDQRVIQSQKGDLDCIVVD
Aft1     460 ERIFEHNRIAAEHLAIANETIGRIRAAQAPLRRQYTKRQVKP----LSQSGILTLRDANRSIAS----------------

AN0826   517 GPCGPPAEGAQTPKARALPT-CSTCHRIGHRRNAC---PNK
Tan1     521 ----PQSQYTETP-SRAPPR-CSNCFNIGHRRTQCSKPPTN
Fot1     505 GKSSSESEEDPAPVRRSTRVRRATKMYIRQDLSSE---ESD
Aft1     520 -----RKAKDAAAQERRLQT---QWEKVHGKPPPL---AST
```

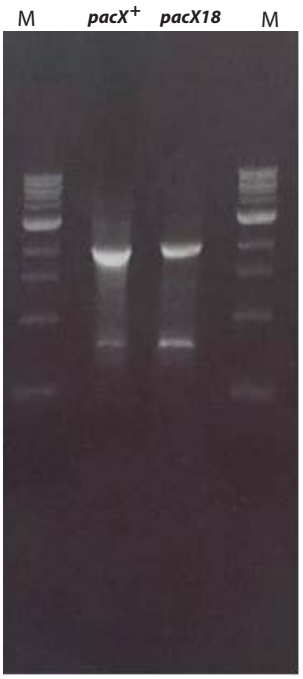


```
acgtggttggtaagcgagctgcgcatgtaagcgagctgcgcacc
||||||||||||||||||||||||||||||||||||||||||||
tgcaccaaccattcgctcgacgcgtacattcgctcgacgcgtgg
```

Fig. S7. Protein alignment: AN0826 ORF compared with known active fungal transposons of the *Fot1*/*Pogo* family, *Tan1* from *A. niger* (Nyyssönen *et al.*, 1996), *Aft1* from *A. fumigatus* (Hey *et al.*, 2008) and *Fot1* from *Fusarium oxysporum* (Daboussi *et al.*, 1992). Alignment carried out with MAFT, G-INS-i, visualised with Box-Shade (http://www.ch.embnet.org/software/BOX_form.html). Nucleotide alignment: inverted repeat (without the TA duplication) of AN0826 at its genomic locus and within the *pacX* gene in the *pacX*18 mutation. Inverted repeats detected with einverted: (http://emboss.bioinformatics.nl/cgibin/emboss/einverted). Right panel, PCR amplification with primers external to the AN0826 inverted repeats at its chromosomal location. M, molecular size markers. *pacX*$^{+}$ is the parent strain XC34 (*yA*Δ::*Ncpyr4 pabaA*1 *pacC*^{C}202 *pacC*$^{+/-}$20205 *pantoB*100 *niaD*Δ*::impala::yA*$^{+}$) for the *pacX*18 derivative (strain A869). The expected size of the amplified sequence would be 2118 bp in the *pacX*$^{+}$ strain and 456 bp if the *pacX*18 mutation resulted from a Cut and Paste mechanism. In the event amplified bands in both strains are of identical size, showing a Copy and Paste mechanism to be operating. Primers used for amplification, AN0826F and AN0826R.

Supplementary References

Bessereau, J.L. Transposons in *C. elegans*.(January 18, 2006) *WormBook*, ed. The *C. elegans* Research Community, WormBook, doi/iv.1895/wormbook.1.70.1, http://www.wormbook.org.

Caddick, M.X., Brownlee, A.G., and Arst,H.N., Jr. (1986) Regulation of gene expression by pH of the growth medium in *Aspergillus nidulans*. *Mol Gen Genet* **203**: 346-353.

Carlson, C.M., and Largaespada, D.A. (2005) Insertional mutagenesis in mice: new perspectives and tools. *Nat Rev Genet* **6**: 568-580.

Carr, P.D., Tuckwell, D. Hey, P.M. Simon, L., D'Enfert, C., Birch, M. *et al.* (2010) The transposon impala is activated by low temperatures: use of a controlled transposition system to identify genes critical for viability of *Aspergillus fumigatus*. *Eukaryot Cell* **9**: 438-448.

Cerqueira, G.C., Arnaud, M.B., Inglis, D.O., Skrzypek, M.S., Binkley, G., Simison, M. *et al.* (2014) The *Aspergillus* Genome Database: multispecies curation and incorporation of RNA-Seq data to improve structural gene annotations. *Nucleic Acids Research* **42 (Database issue)**: D705-D710.

Cove, D.J. (1966) The induction and repression of nitrate reductase in the fungus *Aspergillus nidulans*. *Biochim Biophys Acta* **113**: 51-56.

Daboussi, M.J., and Capy, P. (2003) Transposable elements in filamentous fungi. *Annu Rev Microbiol* **57**: 275-299.

Daboussi, M.J., Langin, T., and Brygoo, Y. (1992) Fot1, a new family of fungal transposable elements. *Mol Gen Genet* **232**: 12-16.

Denison, S.H., Orejas, M., and Arst, H.N., Jr. (1995) Signaling of ambient pH in *Aspergillus* involves a cysteine protease. *J Biol Chem* **270**: 28519-28522.

Díez, E., Alvaro, J., Espeso, E.A., Rainbow, L., Suarez, T., Tilburn, J. *et al.* (2002) Activation of the *Aspergillus* PacC zinc finger transcription factor requires two proteolytic steps. *EMBO J* **21**: 1350-1359.

Dufresne, M., Lespinet, O., Daboussi, M.J., and Hua-Van, A. (2011) Genome-wide comparative analysis of pogo-like transposable elements in different *Fusarium* species. *J Mol Evol* **73**: 230-243.

Espeso, E.A., and Peñalva, M.A. (1994) In vitro binding of the two-finger repressor CreA to several consensus and non-consensus sites at the *ipnA* upstream region is context dependent. *FEBS Lett* **342**: 43-48.

Evangelinos M, Anagnostopoulos G, Karvela-Kalogeraki I, Stathopoulou PM, Scazzocchio C, Diallinas G. (2015) Minos as a novel Tc1/mariner-type transposable element for functional genomic analysis in *Aspergillus nidulans*. *Fungal Genet Biol* **81**:1-11.

Fernández-Martínez, J., Brown, C.V., Díez, E., Tilburn, J., Arst, H.N., Jr., Peñalva,M. A., and Espeso, E.A. (2003) Overlap of nuclear localisation signal and specific DNA-binding residues within the zinc finger domain of PacC. *J Mol Biol* **334**: 667-684.

Hammond, T.M., Andrewski, M.D., Roossinck, M.J., Keller,N.P. (2008a) *Aspergillus* mycoviruses are targets and suppressors of RNA silencing. *Eukaryot Cell* **7:** 350-357

Hammond, T.M., Bok, J.W., Andrewski, M.D., Reyes-Dominguez, Y., Scazzocchio, C., and Keller,N.P. (2008b) RNA silencing gene truncation in the filamentous fungus *Aspergillus nidulans*. *Eukaryot Cell* **7**: 339-349.

Hey, P., Robson,G., Birch, M., and Bromley, M. (2008) Characterisation of Aft1 a Fot1/Pogo type transposon of *Aspergillus fumigatus*. *Fungal Genet Biol* **45**: 117-126.

Izsvak, Z., Chuah, M.K., Vandendriessche, T., and Ivics, Z. (2009) Efficient stable gene transfer into human cells by the Sleeping Beauty transposon vectors. *Methods* **49**: 287-297.

Kupfer, D.M., Reece, C.A., Clifton, S.W., Roe, B.A., and Prade, R.A. (1997) Multicellular ascomycetous fungal genomes contain more than 8000 genes. *Fungal Genet Biol* **21**: 364-372.

Li Destri Nicosia, M.G., Brocard-Masson, C., Demais, S., Hua, V.A., Daboussi, M.J., and Scazzocchio, C. (2001) Heterologous transposition in *Aspergillus nidulans*. *Mol Microbiol* **39**: 1330-1344.

Muñoz-Lopez, M., and García-Pérez, J.L. (2010) DNA transposons: nature and applications in genomics. *Curr Genomics* **11**: 115-128.

Nyyssönen, E., Amutan, M., Enfield, L., Stubbs, J., and Dunn-Coleman, N.S. (1996) The transposable element Tan1 of *Aspergillus niger* var. *awamori*, a new member of the Fot1 family. *Mol Gen Genet* **253**: 50-56.

Orejas, M., Espeso, E.A., Tilburn, J., Sarkar, S., Arst, H.N., Jr., and Peñalva, M.A. (1995) Activation of the *Aspergillus* PacC transcription factor in response to alkaline ambient pH requires proteolysis of the carboxy-terminal moiety. *Genes Dev* **9**: 1622-1632.

Peñalva, M.A. (2005) Tracing the endocytic pathway of *Aspergillus nidulans* with FM4-64. *Fungal Genet Biol* **42**: 963-975.

Peñas, M.M., Hervás-Aguilar, A., Munéra-Huertas, T., Reoyo, E., Peñalva, M.A., Arst, H.N., Jr., and Tilburn, J. (2007) Further characterization of the signaling proteolysis step in the *Aspergillus nidulans* pH signal transduction pathway. *Eukaryot Cell* **6**: 960-970.

Perez-Esteban, B., Orejas, M., Gomez-Pardo, E., and Peñalva, M.A. (1993) Molecular characterization of a fungal secondary metabolism promoter: transcription of the *Aspergillus nidulans* isopenicillin N synthetase gene is modulated by upstream negative elements. *Mol Microbiol* **9**: 881-895.

Rubin, E., and Levy, A.A. (1997) Abortive gap repair: underlying mechanism for Ds element formation. *Mol Cell Biol* **17**: 6294-6302.

Sibthorp, C., Wu, H., Cowley, G., Wong, P.W., Palaima, P., Morozov, I.Y. *et al.* (2013) Transcriptome analysis of the filamentous fungus *Aspergillus nidulans* directed to the global identification of promoters. *BMC Genomics* **14**: 847.

Skipper, K.A., Andersen, P.R., Sharma, N., and Mikkelsen, J.G. (2013) DNA transposon-based gene vehicles - scenes from an evolutionary drive. *J Biomed Sci* **20**: 92.

Tilburn,J.; Scazzocchio,C.; Taylor,G.G.; Zabicky-Zissman,J.H.; Lockington,R.A.; Davies,R.W.(1983) Transformation by integration in *Aspergillus nidulans*. *Gene* **26**: 205-221.

Tilburn, J., Sarkar, S., Widdick, D.A., Espeso, E.A., Orejas, M., Mungroo, J. *et al.* (1995) The *Aspergillus* PacC zinc finger transcription factor mediates regulation of both acid- and alkaline-expressed genes by ambient pH. *EMBO J* **14**: 779-790.

Timakov, B., Liu, X., Turgut, I., and Zhang, P. (2002) Timing and targeting of P-element local transposition in the male germline cells of *Drosophila melanogaster*. *Genetics* **160**: 1011-1022.

Tower, J., Karpen, G.H., Craig, N., and Spradling, A.C. (1993) Preferential transposition of *Drosophila* P elements to nearby chromosomal sites. *Genetics* **133**: 347-359.

Wicker, T., Yahiaoui, N., and Keller, B. (2007) Illegitimate recombination is a major evolutionary mechanism for initiating size variation in plant resistance genes. *Plant J* **51**: 631-641.